Jean Françoais Van Huele
- BYU AUG 91 -

The Behavior of Electromagnetic Precursors in Dielectric Media

by
Eric W. Hirschmann

Submitted to Brigham Young University
in partial fulfillment of the requirements for
University Honors

June 1991

Advisor: Jean-François Van Huele Jean Françoais Van Huele

Honors Dean: S. Neil Rasband S. Neil Rasband

Contents

Preface

Although these are much more feelings in hindsight and perhaps belong in here as a sort of epilogue, it seems appropriate to comment on my experience with this honors thesis in general. It has certainly not been without its frustrations and headaches, having been drawn out over a rather long period of time. But when I say that it took me much longer than I had originally thought or intended, I would have to say that I am grateful for that because of what I have learned in that time. For one thing, I have come to realize how unprepared I was to undertake this research. By that, I am referring not merely to my understanding of the subject matter but to my knowledge of even the background necessary to approach the problem. It took me several months of study and reading to get to the point where I felt that I understood what the main articles that I was working with were saying. In fact, I didn't feel that I was even asking the right questions until about two or three months ago. I give a lot of credit and thanks to my advisor, Dr. Jean-François Van Huele, who very patiently helped me along. He recognized the gaps in my understanding when I did not and kindly helped me address them and then point me in the direction I needed to go. I have appreciated the relationship I have had with him and the mentor he has been to me.

I would also like to thank Dr. William E. Dibble, Dr. William E. Evenson, and Dr. S. Neil Rasband for having read the manuscript and provided helpful comments and suggestions.

Whether this thesis will have served as the capstone and highlight of my undergraduate experience remains to be seen. I believe time will be the best determiner of that. But it certainly has been a rich and varied learning experience, similar, I

hope, to what future research may hold for me.

1 Introduction

The separation of white light into its constituent colors by a glass prism is one of the oldest and more dramatic examples of the effects on light of material substances. This phenomenon is known as dispersion and is usually explained by the spreading out and slowing down of light, or any other kind of electromagnetic signal, on going from air (or vacuum) into a material. Dispersion is a consequence of the fact that the index of refraction of most materials, far from being constant, is dependent on the frequency of the incoming signal. Thus a complete description of the development of a wave or signal in a dispersive medium must take into account this complexity.

By the beginning of the twentieth century, it was recognized that there are at least two types of velocities which can be associated with light, or any other type of electromagnetic signal. These are the phase and the group velocities. The phase velocity gives the speed at which the wavelets within the profile of the wave move. It is given as

$$v_p = \frac{\omega}{k} = \frac{c}{n}$$

where ω and k are the angular frequency and the propagation number of the wave, respectively. c is the speed of light in vacuum, and n is the index of refraction. The other motion to be considered in connection with the signal is the speed of any modulation of the wave. This modulation appears as a change in amplitude of the wave train. The rate at which this amplitude change travels is known as the group velocity and is defined in general as

$$v_g = \frac{d\omega}{dk}.$$

A "dispersion relation" relates ω and k such that v_p and v_g can be determined. For

example, for a monochromatic wave in vacuum

$$\omega = kc.$$

It is easy to show that when the phase velocity is a constant, as in the above example, phase and group velocity will be identical. However, for dispersive media this will no longer be the case as the index of refraction and hence the phase velocity will be frequency dependent.

Further, in certain frequency regions for many materials, regions of so-called anomalous dispersion, both the phase and group velocities may be greater than c, seemingly in contradiction to special relativity. In the first few years after 1905 when Einstein's work on special relativity was published, this fact was used to argue against the speed of light in vacuum being an upper limit at which signals could travel. In an effort to resolve the debate, Arnold Sommerfeld and Léon Brillouin investigated the velocities associated with a signal in a dispersive dielectric and the shape of the signal for all times. They proved that no signal could travel faster than c although the wavefront itself (which we identify with the beginning of any kind of signal at a point z in the medium due to the input signal) traveled at the velocity c in all media. In addition, they showed that the main part of the signal arrives after the wavefront and that there are very weak signals present at a given point in the medium between the arrival of the wavefront and the beginning of the main signal. These weak signals they called forerunners or precursors. For a medium with a single resonance frequency, they were able to identify two precursors. The first to arrive after the wavefront (the Sommerfeld precursor) is of very high frequency and is followed by a low frequency precursor (the Brillouin precursor). After these two precursors, the main portion of the signal arrives. This work enabled them also to define a third velocity, the signal velocity, that at which the main portion of the signal travels.

To evaluate the integrals which describe the time evolution of the signal, and in particular the precursors, requires asymptotic approximations. In recent work, Kurt Oughstun, George Sherman, and others have made improvements to the approximations in the original theory. They have verified many of these improvements numerically and have been able to use them in more precisely defining the signal velocity.

Our work has been an investigation into the structure and development of these precursors. Thus a more formal and rigorous development of their form and time evolution is left to the text. The attempts we have made to extend this work have centered partly in confirming numerically the improvements to the approximations involved. In addition, we have examined some of the parameters of the dispersive medium and attempted to generalize what can be said about the time evolution of the precursors for a broader range of materials. We have also begun to examine the implications of media that possess more than a single resonant frequency to the development of the precursors. By no means have all our questions been answered, and in a real sense, we now have more questions than when we began our research.

More work could still be done, and several additional questions could be addressed. For example, the dispersion with which we deal here is entirely temporal dispersion. What complications arise in the theory when a spatially dispersive medium is considered? We could try to determine what adjustments must be made for non-normal incidence. We could continue our investigations of a multiple resonance medium and consider more closely the effect of the medium parameters on the precursors which develop in such a material. A number of related numerical problems could also be pursued. We could attempt a numerical integration of the integrals involved and compare these with the results of both sets of researchers. Some of this has

been done by Oughstun and Sherman, but they have not solved for all the precursors in this way. In addition, it would be nice to simply iron out a few minor numerical problems that we encountered.

What follows in the remainder of this thesis is a background on the dispersive model we have used, the Lorentz model, brief summaries of the work and results of the two sets of researchers whom we have considered, and a description of the work we have done. The appendices contain a section on complex analysis and the asymptotic integration method used as well as graphs, tables, and programs referred to in the text.

2 The Lorentz Model

An analytic expression for the complex index of refraction of a dielectric material, $n(\omega)$, can be derived by modeling the atoms in the dielectric as classical harmonic oscillators, as was first done by H.A. Lorentz. We consider a material as a collection of a very large number of atoms. Each atom consists of a small, positive center with a symmetric "cloud" of electrons surrounding it. The center, or nucleus, is very massive compared to the electrons. An electromagnetic wave impinging on such an atom will cause the electron cloud to vibrate or oscillate with respect to the nucleus. A displacement of the electron cloud will cause the atom to be polarized. The wave (partly an oscillating electric field) will force this polarization to oscillate similarly.

Two possiblities arise as to the behavior of the atom when an electromagnetic wave impinges on it. In addition to the behavior just described, where the oscillating atom will reradiate the energy of the wave which is "absorbed" to cause the vibration of the atom, the energy of the incoming wave may exactly match the energy needed to raise an electron to a higher energy level. This excitation energy given to the atom is not radiated away but transferred through collisions into thermal energy within the material. Hecht calls this *dissipative absorption*, whereas the first he terms *nonresonant scattering* (Hecht 1987, 57).

Modeled thus, the atom is envisioned as a driven classical harmonic oscillator. The external electric field arising from the electromagnetic wave becomes the forcing function. There is assumed to be a linear restoring force on the electron cloud which tends to pull the oscillating electrons back towards equilibrium. We include a damping term proportional to velocity to account for energy loss within the atom due to "frictional" forces and energy loss when the atoms reradiate at the frequency of the

total electric field. That this term is linear in velocity is a result of the fact that we linearize the general damping problem in order that we can put it into a form which we can solve. The equation of motion for a driven classical harmonic oscillator is:

$$\ddot{x} + \frac{a}{m}\dot{x} + \frac{k}{m}x = \frac{qE_T(t)}{m} \tag{1}$$

In this equation m and q are the mass and charge of the particle, a and k are the proportionality constants for the damping term and the linear restoring force respectively and $E_T(t)$ is the total electric field felt by the particle. (In general, E_T will include not only the external driving force of the incoming wave but also the electric fields of neighboring atoms.) The form of E_T will be assumed to be a uniform harmonic wave of frequency ω:

$$E_T(t) = E_0 e^{-i\omega t}.$$

This can be considered a general solution since a superposition of these solutions with different freuquencies can give any driving function.

With this as the form of the driving function, a solution to eq. (1) can be found which is of the form:

$$x(t) = x_0 e^{-i\omega t}$$

On substitution of this into eq. (1) and solving for x_0, one obtains:

$$x(t) = \frac{qE_0/m}{\omega_0^2 - \omega^2 - 2\delta i\omega} e^{-i\omega t} \tag{2}$$

In eq. (2) we have set $\delta = a/2m$, the phenomenological damping constant and $\omega_0^2 = k/m$, the square of the natural frequency of oscillation. This relationship for $x(t)$ then enables us to find the polarization density $P(t)$ which is given by:

$$P(t) = x(t)Nq$$

Here, N is the density of particles of charge q. We assume a linear, isotropic dielectric such that the polarization and the external electric field are proportional:

$$P(t) = \chi E(t)$$

where χ is known as the electric susceptibility and is given in terms of the permittivity of the material, ϵ, and the permittivity of free space, ϵ_0 (which in turn allows us to define the dielectric constant, K):

$$\chi = \epsilon - \epsilon_0 \quad \text{and} \quad K = \frac{\epsilon}{\epsilon_0} = 1 + \frac{\chi}{\epsilon_0}.$$

Thus,

$$\chi E(t) = \frac{Nq^2}{m} \frac{1}{\omega_0^2 - \omega^2 - 2\delta i\omega} E_T(t) \tag{3}$$

For an isotropic medium the total electric field can be shown to be (Reitz et al, 493):

$$E_T(t) = E(t) + \frac{\nu}{\epsilon_0} P(t) \tag{4}$$

where ν is a local correction factor which is introduced to account for the fields and mutual interactions of the surrounding particles. For an isotropic, nonpolar dielectric, a good approximation for ν is $\nu \approx \frac{1}{3}$. For a metal, $\nu = 0$. Substituting the relation for the polarization density, we get

$$E_T(t) = E(t)(1 + \frac{\nu}{\epsilon_0}\chi) \tag{5}$$

On substitution of this into eq. (3), we get

$$\frac{\chi}{1+\frac{\nu\chi}{\epsilon_0}} = \frac{Nq^2}{m}\frac{1}{\omega_0^2-\omega^2-2\delta i\omega}$$

Since $\chi = \epsilon_0(K-1)$, this can be expressed in terms of K:

$$\frac{K-1}{1+\nu(K-1)} = \frac{Nq^2}{\epsilon_0 m}\frac{1}{\omega_0^2-\omega^2-2\delta i\omega} \tag{6}$$

It should be noted that this equation holds for a material with only one resonant frequency, namely ω_0. A material may easily be composed of a number of different particles each having different properties (i.e. different charge or mass) but which will individually still obey the above relation. Thus, it is seldom the case that in physical situations a material will have a single resonant frequency. In the more general case where the material has i resonances, eq. (6) becomes:

$$\frac{K-1}{1+\nu(K-1)} = \sum_i \frac{N_i q_i^2}{\epsilon_0 m_i}\cdot\frac{1}{\omega_{0_i}^2-\omega^2-2\delta_i i\omega} \tag{7}$$

In this paper we will mostly consider materials with only one resonant frequency and so we will use eq. (6). However, a problem arises in Shen and Oughstun's 1989 paper which considers a multiple resonance medium. Because they leave out ν, the local field correction factor, we believe they get a result which is not applicable to most dense media (Hecht, 61). This will be seen later, however. For now, solving for K in eq. (6) yields:

$$K = 1+\frac{\omega_p^2}{\omega_0^2-\omega_p^2\nu-\omega^2-2\delta i\omega} \tag{8}$$

where $\omega_p^2 = Nq^2/m\epsilon_0$ is the square of the so-called plasma frequency. The index of refraction can now be found. It is defined as:

$$n^2(\omega) = \left(\frac{c}{v}\right)^2 = \frac{\epsilon\mu}{\epsilon_0\mu_0} = K_e K_m$$

We have taken c as the speed of light in vacuum and v as the speed of light in the medium being modelled. K_e and K_m are the relative permittivity and relative permeability respectively. For the vast majority of non-ferromagnetic materials, K_m differs only a very small amount from 1. We therefore make the approximation that $n^2(\omega) = K_e$ which is the K we found above in eq. (8). Combining these relationships, we find that the complex index of refraction for a dielectric according to the Lorentz model is given by:

$$n(\omega) = \left(1 - \frac{\omega_p^2}{\omega^2 - (\omega_0^2 - \omega_p^2\nu) + 2\delta i\omega}\right)^{1/2} \tag{9}$$

Note that Oughstun and Sherman do not consider the local field correction factor, ν in their 1988 paper when considering a single resonance medium. For a single resonance medium this is no real problem since the term in eq. (9), $\omega_0^2 - \omega_p^2\nu$ will behave as a natural frequency $\omega_0'^2$ and can be considered as such. Oughstun and Sherman, however allow ν to be zero and so they simply use the square of the natural frequency, ω_0^2. Thus their expression for the complex index of refraction for a Lorentz medium is

$$n(\omega) = \left(1 - \frac{b^2}{\omega^2 - \omega_0^2 + 2\delta i\omega}\right)^{1/2} \tag{10}$$

where they set $b^2 = \omega_p^2$. This is also the expression we will use in considering a single resonance medium in most of what follows.

3 The Theory of Sommerfeld and Brillouin

In order to derive an analytic expression which would describe the behavior of an electromagnetic wave in a dispersive medium, Sommerfeld assumed the following (Brillouin 1960, 23-24). A uniform, isotropic, single resonance, dispersive medium extends from $z = 0$ to $z = \infty$. A monochromatic wave is incident normally on the medium at $z = 0$ at time $t = 0$. To insure convergence in the Fourier integrals used in the theory, Sommerfeld further assumed a finite wave. The signal was a superposition of two semi-infinite waves, one beginning at $t = 0$ and the other beginning at $t = T$ (where $T > 0$). The wave which starts at $t = T$ is assumed to have a phase opposite to that of the wave which begins at $t = 0$. In this way, the two superposed waves cancel for $t > T$.

Thus, on the boundary (at $z = 0^+$), the wave is given mathematically as

$$f(t) = \begin{cases} 0 & \text{for } t < 0, \\ \sin \omega_c t & \text{for } 0 < t < T \\ 0 & \text{for } t > T \end{cases} \tag{11}$$

where ω_c is the frequency of the incoming wave. The Fourier transform of $f(t)$,

$$g(\omega) = \frac{1}{2\pi} \int_{-\infty}^{\infty} f(t) e^{i\omega t} dt$$

can then be used to express $f(t)$ as

$$\begin{aligned} f(t) &= \frac{1}{2\pi} \int_{-\infty}^{\infty} \left(\int_{-\infty}^{\infty} f(t') e^{i\omega t'} dt' \right) e^{-i\omega t} d\omega \\ &= \frac{1}{\pi} \int_0^{\infty} \int_0^{T} \sin \omega_c t' e^{-i\omega(t-t')} dt' d\omega. \end{aligned} \tag{12}$$

If T is taken to be an integral multiple of the period $T = 2\pi m/\omega_c$, where m is an integer, on integrating with respect to t', $f(t)$ becomes

$$f(t) = \frac{\omega_c}{\pi} \int_0^\infty \frac{d\omega}{\omega^2 - \omega_c^2} \left(e^{-i\omega(t-T)} - e^{-i\omega t} \right).$$

By using the residue theorem from complex analysis, this can be shown to be equal to

$$f(t) = \frac{1}{2} \left(\sin \omega_c t + \sin \omega_c (t - T) \right). \tag{13}$$

By recalling that $T = 2\pi m/\omega_c$ we can see that this is the original function $f(t) = \sin \omega_c t$ as defined at $z = 0^+$ between $t = 0$ and $t = T$. Again, by using the calculus of residues, eq. (13) can be shown to be identical to

$$f(t) = \frac{1}{2\pi} \Re \left\{ \int_{-\infty}^{\infty} \frac{1}{\omega - \omega_c} \left(e^{-i\omega(t-T)} - e^{-i\omega t} \right) d\omega \right\} \tag{14}$$

where $\Re$ tells us that we should take the real part.

If ω is taken as purely real, there is a singularity in each individual term in the integrand of eq. (14) as $\omega \to \omega_c$. At this point in each term, both the numerator and the denominator individually go to zero. However, the integrand in this limit is finite and nonzero so long as the two exponentials are not evaluated separately. Sommerfeld remedies the problems caused by the singularity by moving the path of integration (Brillouin 1960, 26). As the above equation indicates, the path of integration is originally the real axis extending from negative infinity to positive infinity. To avoid the singularity, the path is deformed off the real axis into the upper half of the complex plane. In this way, we can separate $f(t)$ into two separate integrals each of which represents a semi-infinite wave:

$$f(t) = \frac{1}{2\pi} \Re \int_C \frac{1}{\omega - \omega_c} e^{-i\omega t} d\omega - \frac{1}{2\pi} \Re \int_C \frac{1}{\omega - \omega_c} e^{-i\omega(t-T)} d\omega$$

where we take the contour C to extend from $+\infty + ia$ to $-\infty + ia$. Since the original contour (the real axis) extended from $-\infty$ to $+\infty$, this explains the change in signs of the two integrals. The positive constant a is the distance above the real axis the contour is deformed. Since both our integrals now converge independent of the other, the second, which represents a semi-infinite wave beginning at $t = T$, can be discarded. We are then left with a signal beginning at $t = 0$ and extending to infinity.

One might ask why we added the second wave if we were only going to get rid of it in the end. The answer is that we did not have to begin with such a formulation. Had we begun with a signal which began at $t = 0$ and extended to infinity, in eq. (12) we would have had to replace the T in the limit of the integral over dt' with ∞. With these limits, the integral would not have converged for t' under the assumption that ω was real. We could then have assumed that ω was complex in order to insure the convergence of the Fourier integral. As it turned out, by using the method presented here, that is what we were forced to accept to regain our semi-infinite signal. Either way, the results would have been the same.

Our signal on the boundary $z = 0^+$ is then expressed as a contour integral of the form

$$f(t) = -\frac{1}{2\pi}\Re\int_{-\infty+ia}^{+\infty+ia}\frac{1}{\omega-\omega_c}e^{-i\omega t}d\omega. \tag{15}$$

Now that we have the signal on the boundary, we want an expression for the signal for all time and for all points in the medium. It is known that a wave traveling through a medium will have the form

$$e^{-i\omega t+ikz}$$

where z is the distance into the medium which the signal has propagated, and k is the wave number given by

$$k = \frac{\omega}{c} n(\omega).$$

Here, c is the speed of light in vacuum and $n(\omega)$ is the complex index of refraction characteristic of the dispersive medium.

It is therefore reasonable to assume that our signal in the medium, $f(z,t)$, will be of this same form. Hence, we construct our signal to be

$$\begin{aligned} f(z,t) &= -\frac{1}{2\pi} \Re \int_{-\infty+ia}^{+\infty+ia} \frac{1}{\omega - \omega_c} e^{-i\omega t + ikz} d\omega \\ &= -\frac{1}{2\pi} \Re \int_{-\infty+ia}^{+\infty+ia} \frac{1}{\omega - \omega_c} e^{\frac{z}{c}\phi(\omega,\theta)} d\omega \end{aligned} \tag{16}$$

where

$$\phi(\omega, \theta) = i\omega[n(\omega) - \theta]$$

and θ is a dimensionless parameter given as $\theta = ct/z$. As it will be important in our later discussions, it would be well to discuss this parameter. For a fixed z, θ is a scaled time variable. If $\theta = 0$, the signal has arrived at the boundary. $\theta = 1$ corresponds to the amount of time needed for light in vacuum to travel the distance z. On the other hand, for fixed t, θ is proportional to the inverse distance from the boundary. For $\theta = 0$, z is at infinity and at $\theta = \infty$, $z = 0$ or at the boundary. The distance traveled by light in time t is given by $\theta = 1$. Returning to our equations, we note that for large values of z, eq. (16) is in such a form as can be evaluated asymptotically by using the method of steepest descent. "Large" values of z can be on the order of 1×10^{-4} cm since this is large in comparison to the absorption depth, c/δ, of the medium (Oughstun and Sherman 1988, 840).

In the original papers by Sommerfeld and Brillouin, Sommerfeld obtains an expression for $f(z,t)$ in a medium given by an $n(\omega)$ as we calculated in the section on the Lorentz Model. However, Sommerfeld makes the simplifying assumption that damping is negligible and hence he sets the damping coefficient in $n(\omega)$ equal to zero (Brillouin 1960, 40). This assumes a nonabsorbing medium which is, at best, an approximation to a physical situation. It is left to Brillouin, using the method of steepest descent, to find analytic expressions for the more general case of a dispersive and absorptive medium.

To use the method of steepest descent, it is necessary to know the behavior of the real part of the phase function in the complex ω plane. In particular, we must know the location of any branch points or saddle points of this complex phase function. To evaluate the integrals, it is assumed that the major contribution to the integral comes at these saddle points. Thus, in addition to knowing the location of any branch points, it becomes imperative to find the location and behavior of the saddle points.

To begin, we rewrite the complex index of refraction which we found in the section on the Lorentz Model:

$$n(\omega) = \left(1 - \frac{b^2}{\omega^2 - \omega_0^2 + 2\delta i\omega}\right)^{1/2} \tag{17}$$

$$= \left(\frac{\omega^2 - \omega_1^2 + 2\delta i\omega}{\omega^2 - \omega_0^2 + 2\delta i\omega}\right)^{1/2} \tag{18}$$

$$= \left[\frac{(\omega - \omega'_+)(\omega - \omega'_-)}{(\omega - \omega_+)(\omega - \omega_-)}\right]^{1/2} \tag{19}$$

where $\omega_1^2 = \omega_0^2 + b^2$ and the four points, $\omega'_\pm$ and $\omega_\pm$, are the locations of the branch points and are given by

$$\omega'_{\pm} = \pm(\omega_1^2 - \delta^2)^{1/2} - i\delta$$

$$\omega_{\pm} = \pm(\omega_0^2 - \delta^2)^{1/2} - i\delta.$$

At $\omega'_{\pm}$, the real part of the phase function, $\phi(\omega, \theta)$ is zero. At $\omega_{\pm}$, the real part of ϕ goes to infinity. We note at this point that Brillouin's analysis as well as that done by Oughstun and Sherman consider only the case where $\delta < \omega_0$ (Oughstun and Sherman 1988, 847).

To find the location of the saddle points of the phase function for values of ω near the origin, Brillouin expands $n(\omega)$ (Brillouin 1960, 51). Setting, $\alpha = \omega^2 + i2\delta\omega$, and assuming that the relevant frequencies are much less than the resonance frequency: $|\alpha| \ll \omega_0^2 (< \omega_1^2)$, we find

$$\begin{aligned} n^2(\omega) &= 1 + \frac{b^2}{\omega_0^2 - \omega^2 - i2\delta\omega} \\ &= \frac{\omega_1^2 - \alpha}{\omega_0^2 - \alpha} \\ &= \frac{\omega_1^2}{\omega_0^2}\left(1 - \frac{\alpha}{\omega_1^2}\right)\left(1 + \frac{\alpha}{\omega_0^2} + \frac{\alpha^2}{\omega_0^4} + \cdots\right). \end{aligned}$$

On multiplying this series expansion through, taking the square root (by using the binomial expansion), and neglecting terms in ω of third order and higher, the approximation for $n(\omega)$ gives

$$n(\omega) \approx \frac{\omega_1}{\omega_0} + \frac{b^2}{2\omega_0^3\omega_1}\omega(\omega + i2\delta). \tag{20}$$

Oughstun and Sherman correctly point out that this approximation does not actually contain all the second order terms which come out of the series expansion for $n(\omega)$ (Oughstun and Sherman 1988, 821). We were able to verify that an extra second

order term should appear in the above equation if all are to be taken into account. The approximation for $n(\omega)$ then becomes

$$n(\omega) \approx \frac{\omega_1}{\omega_0} + \frac{b^2}{2\omega_0^3\omega_1}\omega(\omega + i2\delta) - \frac{\delta^2 b^2(4\omega_1^2 - b^2)}{2\omega_1^3\omega_0^5}\omega^2.$$

However, we performed a further calculation of the order of this term and found that using the parameter values which Brillouin considers, this additional second order term is only 1/60 of the next larger term. Thus, it can be reasonably neglected.

Using eq. (20), we are still able to approximate the location of the saddle points. Taking the derivative of the phase function ϕ with respect to ω,

$$\frac{\partial\phi(\omega,\theta)}{\partial\omega} = in(\omega) - i\theta + i\omega n'(\omega) \tag{21}$$

substituting the approximation for $n(\omega)$ into this equation, and setting it to zero (the condition for a saddle point) yields a quadratic equation in ω

$$3\omega^2 + 4i\delta\omega + (\frac{\omega_1}{\omega_0} - \theta)\frac{2\omega_0^3\omega_1}{b^2} = 0$$

which has roots

$$\omega_{sp_n} = -i\frac{2}{3}\delta \pm \frac{1}{3}\left((\theta - \frac{\omega_1}{\omega_0})\frac{6\omega_0^3\omega_1}{b^2} - 4\delta^2\right)^{1/2}. \tag{22}$$

Three possible cases result, depending on the sign under the radical in eq. (22). If the expression under the radical is negative, the two saddle points in the region about the origin are located on the imaginary axis. They are situated symmetrically about the line $\omega'' = -\frac{2}{3}\delta$ and the lines of steepest descent run through the saddle points parallel to the imaginary axis.

For values of θ which make the expression under the radical positive, the saddle points are off the imaginary axis, although they remain on the line $\omega'' = -\frac{2}{3}\delta$ and

are symmetric with respect to the imaginary axis. For the saddle point which leaves the imaginary axis moving towards the branch cut on the right, the path of steepest descent makes an angle of $\frac{\pi}{4}$ with the real axis. For the saddle point which leaves the imaginary axis moving towards the branch cut on the left, its path of steepest descent makes an angle of $\frac{3\pi}{4}$ with the real axis.

For the single value of θ which makes the radical zero,

$$\theta = \frac{2\delta^2 b^2}{3\omega_0^3 \omega_1} + \frac{\omega_1}{\omega_0}$$

there is only one saddle point found. It is on the imaginary axis at

$$\omega_{sp_n} = -\frac{2}{3}\delta.$$

This is a second order saddle point since both the first and second derivatives of the phase function are zero.

In general, the saddle points near the origin are located at first on the imaginary axis. As time increases, they move towards each other coalescing into a single saddle point of higher order. They then separate, moving into the complex frequency plane, perpendicular to the imaginary axis.

To find the location of any saddle points for large values of ω, Brillouin assumed $\omega^2 \gg \omega_0^2$, or in other words, that for these saddle points, the frequencies of interest are much larger than the resonant frequency. Doing this, we can then approximate $n^2(\omega)$ as

$$\begin{aligned} n^2(\omega) &= 1 - \frac{b^2}{\omega^2 - \omega_0^2 + i2\delta\omega} \\ &\approx 1 - \frac{b^2}{\omega(\omega + i2\delta)}. \end{aligned} \tag{23}$$

Assuming the denominator in eq. (23) is large compared to b^2, one can further approximate $n(\omega)$ as

$$n(\omega) \approx 1 - \frac{b^2}{2}\frac{1}{\omega(\omega + i2\delta)}.$$

On substitution of this approximation for $n(\omega)$ into the equation for the first derivative of the phase function, eq. (21), and setting that equal to zero, after some rearranging, we get the following quadratic equation in ω

$$\omega^2 + i4\delta\omega - 4\delta^2 - \frac{b^2}{2}\frac{1}{\theta - 1} = 0.$$

On solving this for the distant saddle points, we find

$$\omega_{spd}^{\pm} = -2\delta i \pm b\sqrt{\frac{1}{2(\theta - 1)}}$$

which tells us that there are two saddle points which begin at a distance from the origin and approach each other symmetrically with respect to the imaginary axis. Though the equation would indicate that these saddle points remain on the line $\omega'' = -2\delta$, Brillouin acknowledges that as the saddle points approach the region about the origin, the approximations made above are no longer valid (Brillouin 1960, 55). In actuality, these saddle points move off this line and approach the ends of the branch cuts farthest away from the origin, $\omega'_{\pm}$.

Now that we have the expressions for the approximations of the locations of the saddle points, we can evaluate the integral which we derived in eq. (16):

$$f(z,t) = \frac{1}{2\pi}\int_C \frac{1}{\omega_c - \omega} e^{\frac{z}{c}\phi(\omega,\theta)} d\omega \tag{24}$$

where C is the contour of integration. It is given a general label in anticipation that we will further deform the contour. Again, we define the complex phase function as

$$\phi(\omega, \theta) = i\omega[n(\omega) - \theta].$$

We will consider the contributions of the saddle points to the integral in reverse order to the way we calculated their location. This is because, as we shall discover, the distant saddle points will contribute to the first, or Sommerfeld precursor and the near saddle points will be the predominant contribution to the second precursor, the Brillouin precursor. Using the approximations for the locations of the distant saddle points, the complex phase function and its second derivative become

$$\phi(\omega^{\pm}_{sp_d}, \theta) = i\omega^{\pm}_{sp_d}(1 - \theta) - \frac{ib^2/2}{\omega^{\pm}_{sp_d} + i2\delta} \tag{25}$$

$$\left.\frac{\partial^2 \phi}{\partial \omega^2}\right|_{\omega=\omega^{\pm}_{sp_d}} = \frac{-ib^2}{(\omega + i2\delta)^3}$$

$\omega^{+}_{sp_d}$ is found in the right half of the plane, $\omega^{-}_{sp_d}$ is in the left half of the plane and the two are located symmetrically about the imaginary axis and are given as

$$\omega^{\pm}_{sp_d} = -2i\delta \pm b\sqrt{\frac{1}{2(\theta - 1)}}. \tag{26}$$

We can now use the result from the method of steepest descent where we assume that the integrand rapidly goes to zero as we move along C away from the saddle point in either direction. For the distant saddle points, in the asymptotic limit as z gets large, our integral becomes (see the appendix on dealing with the method of steepest descent)

$$f(z,t) \approx \frac{1}{2\pi}\Re\left\{\frac{\sqrt{2\pi}}{\omega_c - \omega^{\pm}_{sp_d}} \exp\left[\frac{iz}{c}\omega^{\pm}_{sp_d}[n(\omega^{\pm}_{sp_d}) - \theta] \mp \frac{i\pi}{4}\right] \cdot \left|\frac{z}{c}\frac{-ib^2}{(\omega^{\pm}_{sp_d} + i2\delta)^3}\right|^{-1/2}\right\}. \tag{27}$$

The total contribution to the integral from the distant saddle points is given by adding the two parts together and taking the real part of the sum. The result is

$$f(z,t) \approx -\frac{\omega_c}{b}\left(\frac{2c\sqrt{2(\theta-1)}}{\pi b z}\right)^{1/2} e^{-2\delta(\theta-1)\frac{z}{c}} \cos\left(2b(\theta-1)\frac{z}{c}+\frac{\pi}{4}\right). \qquad (28)$$

This is the expression describing the first, or Sommerfeld precursor and immediately follows the arrival of the wavefront which travels at c, the velocity of light in vacuum.

We do a similar thing for the near saddle points using the appropriate approximations for both the complex index of refraction and the complex phase function. Using these, the phase function and its second derivative at the values for the near saddle points are given as

$$\phi(\omega^{\pm}_{sp_n},\theta) = \frac{i\omega^{\pm}_{sp_n}\omega_1}{\omega_0} + \frac{ib^2}{2\omega_0^3\omega_1}\omega^{\pm^2}_{sp_n}(\omega^{\pm}_{sp_n}+i2\delta) - i\omega^{\pm}_{sp_n}\theta \qquad (29)$$

$$\frac{\partial^2\phi}{\partial\omega^2}\,|_{\omega=\omega^{\pm}_{sp_d}} = \frac{ib^2}{\omega_0^3\omega_1}(3\omega^{\pm}_{sp_n}+i2\delta) \qquad (30)$$

where the near saddle points are found in eq. (22)

$$\omega^{\pm}_{sp_n} = -i\frac{2}{3}\delta \pm \frac{1}{3}\left((\theta-\frac{\omega_1}{\omega_0})\frac{6\omega_0^3\omega_1}{b^2} - 4\delta^2\right)^{1/2}. \qquad (31)$$

As mentioned before, this equation for the near saddle points indicates that these saddle points begin on the imaginary axis at $\theta = 1$ and symmetrically approach each other about the line $\omega'' = -i\frac{2}{3}\delta$. They then coalesce into a single saddle point after which they separate and move off the axis into the complex plane. During the time the saddle points are on the imaginary axis, the lower saddle point is not

included in the calculation and the path of integration (the path of steepest descent) through the upper saddle point is parallel to the real axis.

Thus, using our expression for the asymptotic expansion of $f(z,t)$ for the interval that the upper saddle point remains on the imaginary axis, we get

$$f(z,t) \approx \frac{1}{2\pi}\Re\left\{\frac{\sqrt{2\pi}}{\omega_c - \omega^+_{spn}}\exp\left[\frac{iz}{c}\omega^+_{spn}(n(\omega^+_{spn}) - \theta)\right]\cdot\left|\frac{z}{c}\frac{-ib^2}{\omega_0^3\omega_1}(3\omega^+_{spn} + i2\delta)\right|^{-1/2}\right\} \tag{32}$$

On simplification, this becomes

$$f(z,t) \approx \frac{\omega_c}{2(\omega_c^2 + \eta_p^2)}\sqrt{\frac{2\omega_0^3\omega_1 c}{\pi x b^2(3\eta_p + 2\delta)}}\exp\left(\frac{x}{c}\left[\eta_p(\theta - \frac{\omega_1}{\omega_0}) + \frac{b^2}{2\omega_0^3\omega_1}\eta_p^2(\eta_p + 2\delta)\right]\right) \tag{33}$$

where η_p is

$$\eta_p = -\frac{2}{3}\delta + \frac{1}{3}\left(4\delta^2 - (\theta - \frac{\omega_1}{\omega_0})\frac{6\omega_0^3\omega_1}{b^2}\right)^{1/2}$$

Once the saddle points have coalesced and moved off the imaginary axis, both saddle points are considered in the evaluation of the integral, and we get an oscillatory solution which we present in its final form:

$$f(z,t) \approx \frac{\omega_c}{\omega_c^2 - \xi_p^2}\left(\frac{2\omega_0^3\omega_1 c}{3\pi\xi_p x b^2}\right)^{1/2}\exp\left[\frac{2\delta x}{3c}(\frac{\omega_1}{\omega_0} - \theta + \frac{9b^2\delta^2}{16\omega_0^3\omega_1})\right](\cos\psi + \frac{4\delta\xi_p}{3(\omega_c^2 - \xi_p^2)}\sin\psi) \tag{34}$$

where ξ_p is

$$\xi_p = \frac{1}{3}\left[(\theta - \frac{\omega_1}{\omega_0})\frac{6\omega_0^3\omega_1}{b^2} - 4\delta^2\right]^{1/2}$$

and we have given ψ as

$$\psi = \frac{\pi}{4} + \frac{x}{c}\xi_p \left[\frac{\omega_1}{\omega_0} - \theta + \frac{b^2}{2\omega_0^3\omega_1}(\xi_p^2 + \frac{4}{3}\delta^2)\right].$$

These final equations thus describe the form of the second precursor, or the Brillouin precursor as derived by Brillouin using the method of steepest descent. We have plotted $f(z,t)$ in these equations versus the parameter θ for a fixed distance into the medium. This graph (figure 2) is located in the graph appendix and given the title "Precursors for a modified sine wave - B." It should help give an idea of the general field structure of these precursors.

4 The Developments of Oughstun and Sherman

In their reexamination and development of the original theory of precursors, Oughstun and Sherman begin by making a slight generalization in formulating the problem of an electromagnetic signal in a dispersive dielectric (Oughstun and Sherman 1988, 818). Considering the medium to be in the region $z > 0$, any scalar component of the electric field can be given in the form

$$A(z,t) = \int_c A(z,\omega)e^{-i\omega t}d\omega \tag{35}$$

where $A(z,\omega)$ is the spectral amplitude and satisfies the Helmholtz equation

$$\nabla^2 A(z,\omega) + k^2(\omega)A(z,\omega) = 0 \tag{36}$$

and where $k(\omega)$ is the complex wave number and is given in terms of the complex index of refraction $n(\omega)$ and the speed of light in vacuum

$$k(\omega) = \frac{\omega}{c}n(\omega).$$

As before, we assume a knowledge of the field at $z = 0$ for all time and that the field is nonzero for $t > 0$ and is identically zero for $t < 0$. This behavior at $z = 0$ we call $f(t)$. As in our previous derivation of the shape of the signal in a dielectric, to insure convergence of eq. (35), we take the frequency to be complex. Thus, the contour of integration, c is taken off the real axis and into the upper half of the complex plane. Solution of eq. (36) gives

$$A(z,\omega) = A_+e^{ikz} + A_-e^{-ikz}$$

which is the superposition of two traveling waves, one of which (A_+) is traveling in the positive z direction and the the other in the negative z direction. Since we are

only interested in the waveform within the medium, we ignore any reflection from the surface at $z = 0$ and set $A_- = 0$. Thus the scalar field is

$$A(z,t) = \int_c A_+(\omega) e^{i(kz-\omega t)} d\omega. \tag{37}$$

Knowing the initial behavior, we find that

$$A(0,t) = f(t) = \int_c A_+(\omega) e^{-i\omega t} d\omega.$$

The inverse transform gives

$$A_+(\omega) = \frac{1}{2\pi} \int_0^\infty f(t) e^{i\omega t} dt = \frac{1}{2\pi} \tilde{f}(\omega) \tag{38}$$

which, on substitution into eq. (37), gives the integral form of the propagation of a plane wave through a dispersive dielectric with index of refraction $n(\omega)$

$$A(z,t) = \frac{1}{2\pi} \int_c \tilde{f}(\omega) \exp\left(\frac{z}{c}\phi(\omega,\theta)\right) d\omega \tag{39}$$

where we have reintroduced the complex phase function $\phi(\omega,\theta)$

$$\phi(\omega,\theta) = i\omega\left(n(\omega) - \theta\right)$$

and the dimensionless parameter θ

$$\theta = \frac{ct}{z}.$$

The complex index of refraction must obey

$$n(-\omega) = n^*(\omega^*)$$

and the inverse transform of the signal at $z = 0$ satisfies a similar equation

$$\tilde{f}(-\omega) = \tilde{f}^*(\omega^*).$$

Using these relations one can show that the field for all $z \geq 0$ is given by

$$A(z,t) = \frac{1}{2\pi}\Re\left\{\int_{-\infty+ia}^{\infty+ia} \tilde{f}(\omega)\exp\left(\frac{z}{c}\phi(\omega,\theta)\right)d\omega\right\} \tag{40}$$

which, like eq. (39), is in a form which can be evaluated asymptotically.

In their analysis, Oughstun and Sherman consider two forms for the initial time behavior (Oughstun and Sherman 1988, 819). These are the delta pulse at a time $t = t_0 > 0$

$$f(t) = \delta(t - t_0) \tag{41}$$

and the semi-infinite sine wave with carrier frequency ω_c which is the unit step-modulated signal

$$f(t) = \begin{cases} 0 & t < 0 \\ \sin\omega_c t & t > 0 \end{cases} \tag{42}$$

To be able to evaluate the integrals, the locations of the saddle points of this complex phase function $\phi(\omega,\theta)$ must be found for all $\theta > 1$. Thus, all the theory in the Sommerfeld and Brillouin section preceding the approximations for the location of the saddle points is applicable. This requires that we differentiate the phase function with respect to ω and set it equal to zero:

$$n(\omega) + \omega n'(\omega) - \theta = 0.$$

The roots of this equation will yield the location of the saddle points as functions of θ. Using the expression for the complex index of refraction given in eq. (10) in Section 2, we get the following

$$\left[\omega^2 - \omega_1^2 + 2\delta i\omega + \frac{b^2\omega(\omega+i\delta)}{\omega^2-\omega_0^2+2\delta i\omega}\right]^2 - \theta^2(\omega^2-\omega_1^2+2\delta i\omega)(\omega^2-\omega_0^2+2\delta i\omega) = 0 \tag{43}$$

where $\omega_1^2 = \omega_0^2 + b^2$. On expanding, this becomes an eighth order polynomial in the complex variable ω. An approximate solution of this equation must be found. As found by Brillouin, there are four saddle points (Brillouin 1960, 50-54). Two of these are distant saddle points which lie in the lower half of the complex frequency plane and which begin at infinity and symmetrically approach the far branch points as θ increases. The other two are near saddle points (located about the origin) which begin on the imaginary axis, approach each other as θ increases, coalescing into a single saddle point (at a θ value which is defined as $\theta = \theta_1$) and then move off the imaginary axis into the complex plane. The derivations of the locations of these saddle points in Oughstun and Sherman's analysis involve a considerable amount of algebra. For this reason we will only present the final expressions for the approximations of the saddle points.

For $\omega^2 \gg \omega_1^2$, the distant saddle points are given as

$$\omega_{sp_d}^{\pm}(\theta) \approx \pm\xi(\theta) - i\delta(1 + \eta(\theta)) \tag{44}$$

where we have

$$\xi(\theta) = \left(\omega_0^2 - \delta^2 + \frac{b^2\theta^2}{\theta^2 - 1}\right)^{1/2},$$

$$\eta(\theta) = \frac{\delta^2/27 + b^2/(\theta^2 - 1)}{\xi^2(\theta)}.$$

For the region $\omega^2 \ll \omega_0^2$, the near saddle points are approximated to be

$$\omega_{sp_n}^{\pm} \approx \pm\psi(\theta) - i\frac{2}{3}\delta\zeta(\theta) \tag{45}$$

where we have

$$\psi(\theta) = \left[\frac{\omega_0^2(\theta^2 - \theta_0^2)}{\theta^2 - \theta_0^2 + \frac{3b^2}{\omega_0^2}\alpha} - \delta^2\left(\frac{\theta^2 - \theta_0^2 + \frac{2b^2}{\omega_0^2}}{\theta^2 - \theta_0^2 + \frac{3b^2}{\omega_0^2}\alpha}\right)^2\right]^{1/2},$$

$$\zeta(\theta) = \frac{3}{2}\frac{\theta^2 - \theta_0^2 + \frac{2b^2}{\omega_0^2}}{\theta^2 - \theta_0^2 + \frac{3b^2}{\omega_0^2}\alpha}.$$

and α is a constant defined as (different from the α which we used in the Brillouin section to expand the index of refraction)

$$\alpha = 1 - \frac{\delta^2}{3\omega_0^2\omega_1^2}(4\omega_1^2 + b^2).$$

With approximations for the locations of the saddle points, the asymptotic expansion of the field can be given. The original contour, c in eq. (9) which is in the upper half of the complex frequency plane at the value $\omega'' = a$ must be deformed to a new contour we call $P(\theta)$ so as to pass through the saddle points. Because Oughstun and Sherman use the asymptotic method of Olver which does not require that we know the path of steepest descent through the saddle points, the chosen paths become a bit less rigid. These paths must still satisfy certain, albeit less restrictive, conditions given by Olver (Olver 1970, 229). Any poles of the spectral function $\tilde{f}(\omega)$ which are crossed by the deforming of c will, by the Cauchy residue theorem, contribute to the integral in eq. (40)

$$A(z,t) = I(z,\theta) - \Re\left[2\pi i \sum(\text{residues of poles crossed by } P(\theta)\right]$$

where the integral $I(\theta)$ has the same form as before, only the contour has been changed from c to $P(\theta)$. The minus sign before the sum is a result of the fact that all the poles which are crossed will be encircled in a clockwise direction as the contour is deformed from the upper half of the complex plane to the lower half plane.

The integral $I(z,\theta)$ is composed of the contributions from the saddle points which $P(\theta)$ crosses. For $\theta < \theta_1$, there are three of these, the two distant saddle points and the upper near saddle point. The lower near saddle point for $\theta < \theta_1$ cannot be reached by an appropriately deformed contour and is thus neglected. For all $\theta > \theta_1$

the saddle points originally on the imaginary axis have moved into the complex plane and all four saddle points contribute to the integral $I(z,\theta)$. This can be expressed as

$$A(z,t) = A_S(z,t) + A_B(z,t) + A_c + R(z,t).$$

Here, A_S is the field component known as the Sommerfeld precursor and arises from the contributions from the distant saddle points. A_B is the Brillouin precursor and comes about from the saddle points near the origin. For $\theta \leq \theta_1$, only the upper near saddle point on the imaginary axis contributes to this term while for $\theta > \theta_1$, both near saddle points will contribute. A_c is the sum of the value of the poles as given above and $R(z,t)$ is the remainder in the asymptotic approximation.

That these saddle points contribute to the various precursor fields in the way that we have said can perhaps be seen by considering the value of the real part of the phase function, $X(\omega,\theta)$, at each of these saddle points as θ varies. We do this because it is $X(\omega,\theta)$ that makes the largest contribution to the asymptotic expression of the integral in the method of steepest descent. For $\theta \leq \theta_1$, only the upper near saddle point For θ just barely larger than one, $X(\omega,\theta)$ is largest at the lower near saddle point, but since this saddle point is never crossed by the contour, we ignore it. At the distant saddle points, $X(\omega,\theta)$ has its next largest value and is the same for both saddle points. As θ increases, the value of $X(\omega,\theta)$ at the distant saddle points decreases in a steady manner while the value of X at the upper near saddle point, which was originally the least, *increases* until $\theta = \theta_1$ when the two near saddle points coalesce. For $\theta > \theta_1$, the value of $X(\omega,\theta)$ at the two near saddle points is the same for the two and decreases in a continuous manner. What all this means is that for a short time, the distant saddle points contribute predominantly to the integral describing the field after which the near saddle points are the most important contributions. We

therefore associate the first, or Sommerfeld precursor with the earliest contributions to the field which happen to made by the distant saddle points. Similarly, the next contributions to the field are given by the near saddle points and are associated with the Brillouin precursor. Depending on the strength and location of the poles in the transform of the initial time behavior, these precursors will likely be followed by the arrival of the main signal.

We will show in general terms how to get the form of the Sommerfeld precursor from what we now know. For the Sommerfeld precursor, we have the following expression

$$A_S(z) = \frac{1}{2\pi}\Re\left\{\int_{b_1}^{\omega_{sp_d}^+} \tilde{f}(\omega)e^{\frac{z}{c}\phi(\omega,\theta)}d\omega + \int_{b_2}^{\omega_{sp_d}^-} \tilde{f}(\omega)e^{\frac{z}{c}\phi(\omega,\theta)}d\omega\right\} \tag{46}$$

where b_1 and b_2 are points along the path which satisfy Olver's conditions (see the section on Olver's method in the appendix on complex analysis). Using the method of Olver, we can express the first term in the asymptotic expansion as

$$A_S(z) \sim \frac{1}{2\pi}\Re\left\{e^{\frac{z}{c}\phi(\omega_{sp_d}^+,\theta)}\Gamma(\frac{1}{2})\frac{1}{z^{1/2}}\frac{\tilde{f}(\omega_{sp_d}^+,\theta)}{2[-\frac{1}{2}\phi''(\omega_{sp_d}^+)]^{\frac{1}{2}}} + e^{\frac{z}{c}\phi(\omega_{sp_d}^-,\theta)}\Gamma(\frac{1}{2})\frac{1}{z^{1/2}}\frac{\tilde{f}(\omega_{sp_d}^-,\theta)}{2[-\frac{1}{2}\phi''(\omega_{sp_d}^-)]^{\frac{1}{2}}}\right\}. \tag{47}$$

To write out the general solution then requires us to calculate the second derivative of the phase function, $\phi(\omega,\theta)$, with respect to ω and to evaluate it along with the phase function itself at the two distant saddle points using the approximations found earlier in this section. Since $\tilde{f}(\omega)$, and the phase function will be complex, we will have some kind of oscillatory behavior in θ.

The above expression is practically general for both the Brillouin and Sommerfeld precursors since we have calculated the field contribution from two saddle points.

A few changes, however, will apply to the Brillouin precursor since we must account for the changes in the number of appropriate saddle points as θ increases. For $\theta < \theta_1$, there is a single first order saddle point so that the second term above is zero and the first term applies so long as the approximation for the upper near saddle point, ω_{sp_n} is used everywhere. At $\theta = \theta_1$, we have a second order saddle point. This will require that the third derivative of the phase function with respect to ω be taken, evaluated at the point where the saddle points have coalesced, multiplied by $-\frac{1}{3!}$, and its cube root taken instead of the term involving the second derivative which we now have in the denominator above. In addition, we will have a gamma function of $\frac{1}{3}$ and we will have z to the $-\frac{1}{3}$ instead of to the $-\frac{1}{2}$. Of course the point at which we evaluate everything is the ω value at which the two saddle points have come together. Finally, for $\theta > \theta_1$ we have two saddle points and two contributions as in the Sommerfeld precursor and our equation is as given above where the approximations for the near saddle points, $\omega^{\pm}_{sp_n}$ are used everywhere instead of $\omega^{\pm}_{sp_d}$.

The way we have presented these results allows for new or different approximations for the locations of the saddle points. This is a slight generalization over Oughstun and Sherman who, quite naturally, use their own expressions for the locations of the saddle points in the above equations.

We should comment that Oughstun and Sherman acknowledge that this expansion is not good for certain values for θ. One of the restrictions of the Olver method (and the method of steepest descent) is that our variable be bounded *away* from certain critical points. Two such in the problem at hand are for $\theta = 1^+$ and the point when the saddle points on the imaginary axis coalesce. In the first case, the distant saddle points are at infinity causing the integral in the expansion to diverge. For the case that the saddle points coalesce, the contribution to the integral is an

increasing exponential before they coalesce and then oscillatory afterwards. Because the variable must be bound away from this critical point, for very small values of θ around it, the expansion is no longer uniform. A third case arises for the modified sine wave for certain values of the carrier frequency, ω_c. The form of the transform of this signal has a simple pole singularity on the real axis at ω_c (We saw this in the original formulation of the problem by Sommerfeld in Section 3). If this carrier frequency is small, thus making the singularity near the imaginary axis, there will be a resonance peak in the Brillouin precursor as one of the near saddle points will pass near it. For these reasons, Oughstun and Sherman call their analysis the non-uniform expansion of the signal. In a subsequent paper they attempt to solve for these θ regions, but as of yet we have not spent much time with that paper.

In the appendices, we have included graphs of both precursor fields for the two signal forms which Oughstun and Sherman consider, the delta pulse and the modified sine wave. The second serves as a comparison with the same signal considered by Brillouin (figures 1-3). Again, we have plotted the amplitude of the signal versus the scaled time parameter, θ for a fixed distance z into the medium.

5 Numerical Calculation of the Location of the Saddle Points of the Phase Function

The original method of determining the behavior of precursors developed by Sommerfeld and Brillouin as well as the more recent improvements of Oughstun and Sherman have as a vital characteristic the need for calculating (at a given position in a medium), as a function of time, the location and behavior of the saddle points of the complex phase function. These saddle points are then used in the method of steepest descent which is used to give an asymptotic solution for the behavior of the precursors. For this reason, both pairs of researchers spent a significant amount of effort in calculating the number and position of these saddle points as a function of time. In fact, it is basically the improvement in their approximation of the position of the saddle points (and their ability to check these results with computer based numerics) that enables Oughstun and Sherman to claim a better analytic expression for the form which the precursors take.

Similarly, we found it necessary to calculate numerically the location of these saddle points. Among the FORTRAN programs found in the appendix is one which was developed to calculate the position of the saddle points of the complex phase function $\phi(\omega, \theta)$, given by

$$\phi(\omega, \theta) = i\omega[n(\omega) - \theta] \tag{48}$$

where ω is a complex variable and θ is a dimensionless parameter given by $\theta = ct/z$. z is the distance into the medium, c is the speed of light in vacuum, and t is the elapsed time.

The complex index of refraction, $n(\omega)$ in eq. (48) is given as

$$n(\omega) = \left(1 - \frac{b^2}{\omega^2 - \omega_0^2 + 2\delta i\omega}\right)^{1/2} \tag{49}$$

This is the equation which we derived in Section 2 using the Lorentz Model. It should be emphasized that b, ω_0, and δ are real parameters which describe physical characteristics of the medium. The complex frequency ω is the same as that in eq. (48). Note again that the local field correction factor ν discussed in Section 2 has been set equal to zero.

The numerical method used is Newton's method for two equations in two unknowns (the two unknowns being the real and imaginary parts of the complex frequency). The procedure for arriving at the two equations to be solved is as follows: To find the saddle points, the first partial derivative of the phase function ϕ with respect to ω is taken and set equal to zero

$$n(\omega) - \theta + \omega n'(\omega) = 0.$$

Substituting the expression for $n(\omega)$ given in eq. (49), we get

$$\left[\omega^2 - \omega_1^2 + 2\delta i\omega + \frac{b^2\omega(\omega + \delta i)}{\omega^2 - \omega_0^2 + 2\delta i\omega}\right]^2 - \theta^2(\omega^2 + \omega_1^2 + 2\delta i\omega)(\omega^2 - \omega_0^2 + 2\delta i\omega) = 0 \tag{50}$$

where $\omega_1^2 = \omega_0^2 + b^2$. Rearranging this yields an eighth order polynomial in the complex variable ω. From the theory of complex variables, we know that for this equation to be satisfied its respective real and imaginary parts must be equal to zero. If we let

$$\omega = \omega' + i\omega'',$$

two eighth order polynomials arise from setting the real and imaginary parts of eq. (50) equal to zero. Both of these polynomials will involve the variables ω' and ω'' as well as the parameter θ. These equations are

$$F(\omega',\omega'',\theta) =$$

$$\left((\omega'^2-\omega''^2-\omega_0^2-2\delta\omega'')+b^2\cdot\frac{(\omega'^2-\omega''^2-\delta\omega'')(\omega'^2-\omega''^2-\omega_1^2-2\delta\omega'')+2(\omega'(\delta+2\omega''))(\omega'(\delta+\omega''))}{(\omega'^2-\omega''^2-\omega_1^2-2\delta\omega'')^2+4(\omega'(\delta+\omega''))^2}\right)^2$$

$$-\left(2(\omega'(\delta+\omega''))+b^2\cdot\frac{(\omega'(\delta+2\omega''))(\omega'^2-\omega''^2-\omega_1^2-2\delta\omega'')-2(\omega'(\delta+\omega''))(\omega'^2-\omega''^2-\delta\omega'')}{(\omega'^2-\omega''^2-\omega_1^2-2\delta\omega'')^2+4(\omega'(\delta+\omega''))^2}\right)^2$$

$$-\theta^2\left((\omega'^2-\omega''^2-\omega_0^2-2\delta\omega'')(\omega'^2-\omega''^2-\omega_1^2-2\delta\omega'')-4(\omega'(\delta+\omega''))^2\right)$$

and

$$G(\omega',\omega'',\theta) =$$

$$\left(2(\omega'(\delta+\omega''))+b^2\cdot\frac{(\omega'(\delta+2\omega''))(\omega'^2-\omega''^2-\omega_1^2-2\delta\omega'')-2(\omega'(\delta+\omega''))(\omega'^2-\omega''^2-\delta\omega'')}{(\omega'^2-\omega''^2-\omega_1^2-2\delta\omega'')^2+4(\omega'(\delta+\omega''))^2}\right)$$

$$\times\left((\omega'^2-\omega''^2-\omega_0^2-2\delta\omega'')+b^2\cdot\frac{(\omega'^2-\omega''^2-\delta\omega'')(\omega'^2-\omega''^2-\omega_1^2-2\delta\omega'')+2(\omega'(\delta+2\omega''))(\omega'(\delta+\omega''))}{(\omega'^2-\omega''^2-\omega_1^2-2\delta\omega'')^2+4(\omega'(\delta+\omega''))^2}\right)$$

$$-\theta^2(\omega'(\delta+\omega''))\left((\omega'^2-\omega''^2-\omega_1^2-2\delta\omega'')+(\omega'^2-\omega''^2-\omega_0^2-2\delta\omega'')\right)$$

where F is the real part of eq. (50) and G is the imaginary part. As mentioned, both of these equations must be equal to zero

$$F(\omega',\omega'',\theta)=0, \qquad G(\omega',\omega'',\theta)=0. \tag{51}$$

The mutual solutions of these simlutaneous equations for ω' and ω'' will then give the locations of the saddle points as functions of θ. We will set $x=\omega'$ and $y=\omega''$ in all that follows.

Our aim is to find a solution point (x_0,y_0) which will make both $F(x,y)$ and $G(x,y)$ zero. This point will then solve the condition that the derivative of the complex phase function be zero which is the condition for a saddle point. Thus, if we can find (x_0,y_0), we have found a saddle point.

To derive Newton's method, we begin with a point which we assume is an approximate solution (x_k,y_k). We want to expand about this point in order to find a

better approximation to the solution. The Taylor's series expansion of $F(x,y)$ (and similarly $G(x,y)$) is given by

$$F(x,y) = F(x_k,y_k) + (x-x_k)F_x(x_k,y_k) + (y-y_k)F_y(x_k,y_k) + \cdots \qquad (52)$$

where the subscripted x and y on F represent partial differentiation with respect to those variables. For our approximation, we neglect all terms involving derivatives of second order and higher. Ideally, we would like a point which we call (x_{k+1}, y_{k+1}) to cause the $F(x,y)$ in eq. (52) to vanish. As an approximation to this, we say that this point (x_{k+1}, y_{k+1}) makes

$$F(x_{k+1},y_{k+1}) \approx F(x_k,y_k) + (x_{k+1}-x_k)F_x(x_k,y_k) + (y_{k+1}-y_k)F_y(x_k,y_k) = 0$$

or,

$$-F(x_k,y_k) = (x_{k+1}-x_k)F_x(x_k,y_k) + (y_{k+1}-y_k)F_y(x_k,y_k) \qquad (53)$$

Upon solving the above equation for x_{k+1} and y_{k+1}, we should get a better approximation for the value of (x_0, y_0), which would make $F(x,y)$ and $G(x,y)$ both equal to zero. To improve the accuracy of our approximation, we calculate a new solution point. The x_{k+1} we just calculated becomes the x_k in the new calculation and similarly, y_{k+1} becomes the new y_k. This iterative process is then continued until a certain predetermined accuracy is obtained.

Returning to our problem, we need a second equation in x_{k+1} and y_{k+1} to solve eq. (53). This second equation is provided by a similar equation for $G(x,y)$ which is obtained by the same manipulations as those which gave us eq. (53)

$$-G(x_k,y_k) = (x_{k+1}-x_k)G_x(x_k,y_k) + (y_{k+1}-y_k)G_y(x_k,y_k). \qquad (54)$$

With these two equations, we can then solve for the increments or steps in the two variables:

$$\Delta x = x_{k+1} - x_k = \frac{F_y G - F G_y}{J} \tag{55}$$

and

$$\Delta y = y_{k+1} - y_k = \frac{F G_x - F_x G}{J} \tag{56}$$

where, as before, the subscripts x and y represent partial differentiation with respect to x and y and where J is defined as

$$J = F_x G_y - F_y G_x. \tag{57}$$

Using the above relations, we were able to calculate numerically values for the position of the saddle points for different values of the parameter θ. The change in each variable tended to become smaller after each iteration, but to insure convergence we set the condition for accepting a value as that of a saddle point at a particular θ to be $\Delta x/x < 0.0001$ (and similarly for y, $\Delta y/y < 0.0001$). In this way, we knew that Δx wasn't just getting small because the value of x was very small to begin with.

In the initial stages of developing this program, it would sometimes alternate between two values for x or y. When this happened, convergence was not reached. To remedy this, after about 50 iterations, we added the last two calculated values (the offending values between which we found the program alternating) and divided by two. In other words, we took the median of the two recurring values. Using this "trick," we were then able to get convergence according to the conditions which we had set. It should be noted that calculating the location of the saddle points for θ

values between about 1 and 2 usually entailed upwards of 100 iterations. This was true even after the inclusion of our "trick." The values for the saddle points which we got using this method agree with the values obtained by Oughstun and Sherman to within the accuracy given in their paper.

This program calculates the position of the saddle points for specific values of θ. This series of θ values begins at values just barely greater than $\theta = 1$ and continues for increasing θ until the saddle points begin converging towards the ends of the branch cuts. To facilitate the process of finding saddle points for this series of θ values, once we had achieved convergence to a point for a single value of θ, we would use that point as our initial point for calculating the next higher θ value. For the most part, this worked very well and kept us from having to input new initial points every time we wanted to calculate the location of a saddle point for a different θ.

It is important to keep in mind that the program which we wrote does not itself distinguish between the different types of saddle points (the near and distant saddle points which are defined in the section on the original theory of Brillouin and Sommerfeld). After the main debugging of the programs was finished, we would always get convergence for the distant saddle points for all possible values of θ which we wanted to calculate *if* our choice of the initial point, (x_1, y_1), was relatively close to the value of the saddle point. In other words, if we wanted to find the distant saddle points for a θ value of 1.05, we recognized that the distant saddle points were going to be a little below the real axis and fairly far away from the origin. So if an initial point of $(25, -0.5)$ was chosen, we had no problem getting convergence. Even if we chose initial points at random, we would often obtain convergence to the distant saddle points. However, we had no guarantee that the points that we would find in

using random initial points would be values for the distant saddle points since the program calculated the location of a saddle point without being able to determine what kind of saddle point it was locating. They may have been initial points in the complex plane which ended up converging to values for one of the two near saddle points.

In general, calculating the near saddle points for all θ values proved to be a bit more problematic. Like the distant saddle points, on judicious choices of initial points (such as initial points very near the imaginary axis and relatively close to the origin), we got convergence to a point for *most* values of θ. The problem was twofold. First, as Brillouin has already shown, the path of steepest descent for the lower saddle point on the imaginary axis runs along the axis. This means that a local maximum exists along the imaginary axis for this saddle point. The increment in Newton's method for the imaginary variable y will thus tend to get larger as approximate points move down the "hill" which is this local maximum. Convergence for the real variable was no problem since it found itself in a local minimum and quickly found convergence to the imaginary axis. This problem was in part remedied by our calculating the median of the two last calculated points. This assumes that the increasing increment which is halved is centered about the saddle point.

Further, we found that as θ increased, the near saddle points approached each other, coalesced into a higher order saddle point at a single θ value, and then separated, moving apart from each other into the complex plane. Finding the location of the saddle points on the imaginary axis for θ values close to the value at which the saddle points coalesced ($\theta \approx 1.5$) proved to be more difficult. For θ values in this vicinity, the saddle points are very close together, either on the imaginary ais or just barely off it. A very small change in the variable in the program, say Δx, could cause

the next value of the variable, x_{k+1}, to be much farther away from the saddle points than the prior value of the variable x_k. As a result, obtaining convergence in this region was nearly impossible, and of this writing, we haven't completely solved the problem.

The only means we had of comparing our results with that of Oughstun and Sherman was to compare my computed values for the saddle points with the graphs of the locations of the saddle points for the six specific θ values which they attached with their paper (Oughstun and Sherman 1988, 822-823). The precision of our numerical values is about 1 in 10,000. Thus the final digit in the x and y values listed in the tables of the appendix may not always be in agreement with a similar run of the program which begins at a different θ value. Approximating a point on the graphs in Oughstun and Sherman's paper had a precision of about 1 in 20. Trying to compare the two in this way is an admittedly crude method (especially considering the limited number of graphs they gave when we had a much broader range of θ values), but to within the accuracy which such a method may allow, we consistently agreed with their results for the locations of the saddle points. We further tested our results by varying the initial points used in beginning the program. Regardless of what those initial points may have been, we consistently calculated the same points for the saddle points for all values of θ to within the precision given above (excepting of course the region about the imaginary axis where the near saddle points coalesced as mentioned above).

Tables 1-6 in the appendix give the locations of the saddle points in the complex frequency plane for specific θ values. The heading on each group gives the initial points which were used to begin that run of the program. For Table 1, we had θ increase by 0.05. For Tabel 2, θ increased by 0.02. As can be seen, by choosing an

appropriate initial point the approximation found convergence. These first two tables are the numerically calculated locations of the distant saddle points, and one can see that they are situated *exactly* symmetrically about the imaginary axis. This is true even though the initial points are not exactly the same.

The next four tables (Tables 3-6) are calculated points for the saddle points (both "upper" and "lower") located near the origin. To get Tables 3 and 5 we used an increment in θ of 0.05 and Tables 4 and 6, an increment of 0.02. As can be seen, very good agreement is obtained in comparing the tables which locate the position of these saddle points while they are on the imaginary axis. At about $\theta = 1.5$, the saddle points move off the axis into the plane. Beginning at this θ value, all four tables give excellent agreement with each other. It should be noted that although each table only gives positive values for x once the saddle points have moved off the axis, the near saddle points are located symmetrically about the y-axis so that the other saddle point is easily found. The reader will note that in the vicinity of $\theta \approx 1.5$, there is at least one asterix in each of these last four tables. It is at this point that the two near saddle points coalesce into a single second order saddle point and we have trouble gaining convergence even after 1000 iterations. In this θ range, the saddle points are so close together that the program has difficulty distinguishing them and hence converging to one or the other. After $\theta = 1.5$ the problem is resolved, but this illustrates the difficulty mentioned in getting appropriate convergence to the appropriate saddle point in this vicinity.

As can be seen in the tables, we have included the values of the real and imaginary parts of the phase function at each of these saddle points. One can then compare the relative importance of these saddle points as θ increases. Finally, the printout of the program which calculated these near and distant saddle points is

included in the appendices.

In comparing the two approximations with the numerical results graphically, we can see that the approximations due to Oughstun and Sherman are indeed better than those of Brillouin. The graph (figure 4) in the appendix gives the locations of the distant saddle points for increasing θ. The dotted line is the approximation due to Oughstun and Sherman, the straight solid line is the approximation due to Brillouin which he acknowledges breaks down as one approaches the region of the branch cuts. The curved solid line is our numerical result.

In conclusion, to find and verify the location of the saddle points of the phase function, we have developed FORTRAN programs based on Newton's method to numerically calculate these points. Our results reveal a general agreement with the numerical results presented by Oughstun and Sherman. To facilitate and speed convergence, we found it necessary to include a "trick" which took the median of the last two calculated values as the next trial value. However, this was still not sensitive enough for us to achieve convergence for values of θ close to that where the saddle points on the imaginary axis coalesce. This, as well as the dependence on initial conditions in determining which saddle points were found revealed the complexity of the structure of the analytic functions involved in the Lorentz model. Thus, except for the region mentioned, this is a valid method for numerically calculating the location of the saddle points for $1 < \theta < \infty$. Using this we also confirmed the improvements in the approximations to the locations of the saddle points by Oughstun and Sherman.

6 The Value of the Damping Constant

Understanding some this background, we can address the question of the parameter values. Brillouin gives certain parameter values for a dispersive dielectric and does not consider how a change in those values may affect his asymptotic analysis (Brillouin 1960, 56). Oughstun and Sherman similarly consider only these parameter values, and at one point mention that their analysis assumes $\delta^2 < \omega_0^2$ (Oughstun and Sherman 1988, 847). A natural question arises as to how the precursor fields would develop for different values of the parameters, and particularly for values for which this condition was no longer true.

We first consider the changes to the complex frequency plane as the damping constant, δ became larger. We find in general, five domains for the value of δ for a single resonance. These are

$$\delta < \omega_0$$

$$\delta = \omega_0$$

$$\omega_0 < \delta < \omega_1$$

$$\delta = \omega_1$$

$$\delta > \omega_1.$$

We recall that $\omega_1^2 = \omega_0^2 + b^2$ and thereby note that ω_1 will always be larger than ω_0 for a non-zero plasma frequency. The equations for the branch cuts remain the same since they arise from defining the critical points in the original form of the complex index of refraction (given by eq. (10)) independently of the parameter values.

$$\omega'_{\pm} = \pm(\omega_0^2 - \delta^2)^{1/2} - i\delta \tag{58}$$

$$\omega_{\pm} = \pm(\omega_0^2 - \delta^2)^{1/2} - i\delta$$

The graphs found in the appendix (figures 5-9) give an indication of where the branch cuts are in these five domains. For small δ, the branch cuts are situated symmetrically about the imaginary axis and slightly below the real axis along the line $y = -\delta$. As δ increases these branch points and the corresponding cuts which connect them, move away from the real axis and approach the imaginary axis until $\delta = \omega_0$. At this point they coalesce, in effect forming a single branch cut situated on the line $y = -i\delta$. At this point, it is interesting to note that the index of refraction can be written:

$$n(\omega) = \left(1 - \frac{b^2}{(\omega + i\delta)^2}\right)^{1/2}$$

As δ continues to increase, the branch points continue to move, two moving up and down the imaginary axis and the other two remaining off the imaginary axis until $\delta = \omega_1$ when the branch cuts again meet, this time on the imaginary axis and at the point $(0, -\delta)$. As with the special case of $\delta = \omega_0$, there is a simplification in the expression for the index of refraction when $\delta = \omega_1$.

$$n(\omega) = \left(1 - \frac{b^2}{(\omega + i\delta)^2 + b^2}\right)^{1/2}$$

Finally, as δ increases away from ω_1, the branch cuts move away from each other, the one approaching the real axis and the other $-\infty$ in the limit as $\delta \to \infty$.

Next, we want to find the location of the saddle points for these different domains. The program used for the special case of $\delta < \omega_0$ can again be used to calculate the saddle points for the new parameter values since it will calculate numerically the exact locations of the saddle points for all values of the parameters.

At this point, however, we find it worthwhile to retrace in some detail how we came to understand our original search for the saddle points. In the process, we discovered a few things which we had previously overlooked. In the course of attempting to find the saddle points for larger values of the damping constant, we discovered that the program would converge to six different points for the two regions $\delta = \omega_0$ and $\delta = \omega_1$ and eight points for the two other regions included in $\delta > \omega_0$. We naturally wondered how this could be seeing how we had found only four saddle points in the region we first considered, namely $\delta < \omega_0$ (and of course, Oughstun as well as Brillouin only mention four saddle points). Since with our program we were finding solution points to an eighth order equation (see Section 5 on Numerics for its form), in retrospect we thought we should find four additional solutions to it. After some additional analytical and numerical work, we located four more solutions to this equation. In the right half plane, for the case of $\delta < \omega_0$, one of these solutions was just above the cut line, and the other was just below it. Symmetrically placed solutions were found in the left half of the plane making a total of four additional solutions. After this rather astounding discovery we were disturbed that what we were calling four more saddle points were either ignored or completely unknown to previous researchers. On closer examination of this eighth order equation, we noticed that to put it in the form in which we were using it, we had squared both sides of the equation. By doing this we had introduced additional solutions in the following manner:

$$f(\omega) = g(\omega)$$

$$f^2(\omega) = g^2(\omega)$$

$$[f(\omega) - g(\omega)][f(\omega) + g(\omega)] = 0$$

The equation squared represents our eighth-order equation. In this final equation we have solutions which are true solutions of the original equation and hence are saddle points. However, by squaring we introduce additional solutions which, in the above example, are solutions of $f(x) + g(x) = 0$ and not the equation in which we were originally interested. Thus, these extra solutions we found numerically are not true saddle points of the complex phase function and are irrelevant to evaluating the behavior of the precursors.

After finding these extra solutions, it became necessary to know which of the solutions the program was converging to, in the various regions, were saddle points and which were not. It seemed reasonsable that if all the other parameters and variables were constant, the locations of the saddle points should vary continuously with increasing δ. Many runs of the program confirmed this which we double checked by substituting these solutions back into the original saddle point equation and finding which solutions satisfied it.

Having settled this subtle point, we were able to find numerically the location of the saddle points in all five regions of the parameter δ. In all cases there are four saddle points for all θ values larger than one except for the single θ value when $\delta < \omega_0$ at which two of the saddle points coalesce into a single saddle point. These saddle points (for a value of $\theta = 1.25$) have been added to the graphs (figures 5-9) showing the location of the branch cuts for the five domains. Also included (as circles as opposed to the "X"'s for the saddle points) are the additional solution points to which the program converged but which are not actual saddle points. Of these four saddle points, two always begin at infinity and as θ increases, approach the far branch points ($\omega'_{\pm}$) for the three regions where $\delta < \omega_1$. For $\delta \geq \omega_1$, both of these distant saddle points approach the branch point lowest on the imaginary axis, ω_+. As in the

case where $\delta < \omega_0$, all the other cases for δ also have two saddle points which begin on the imaginary axis. However, in these other cases these saddle points will never actually meet and move off into the complex plane, rather they will approach the nearest branch point to them on the axis. Thus, the upper saddle point will approach ω_- and the lower saddle point will approach ω_+ with increasing θ.

At this point we can make some qualitative predictions about the evolution and behavior of the precursors. To get asymptotic expressions for the precursors under the conditions mentioned in the additional four domains of the damping constant it would be necessary to rederive the analytic approximations for the location of the saddle points. Using the experience which we have gained in analyzing previous precursor forms will help us to get a general idea of what form these precursors will take. If we were to take a contour similar to the ones we have used before, one which goes from minus infinity to plus infinity through the available saddle points, only three saddle points would contribute for the cases where $\delta \geq \omega_0$. We will not be able to deform our contour in such a way that it will take in the lower saddle point on the imaginary axis.

In addition, we must note the relative values of the saddle points. In other words, we must know the value of the real part of the phase function at the saddle points. The computer program gives us these values. We have not included any tables of these as there would have been several for purposes of comparison. Therefore, we simply present the results of many runs of the computer program for increasing δ. As we saw for $\delta < \omega_0$, the distant saddle points are the largest contributions to the integral for θ values slightly larger than one and the near saddle points become predominant after a period of time. This difference in the relative values of the saddle points gives the distinction between the first and second precursor fields. For large

values of the damping constant, several things are changed. First, for δ just slightly larger than ω_0, the distant and near saddle points have nearly the same value. However, the value of the distant saddle points immediately begins to decrease whereas the upper near saddle point increases in value for a short time period. What this means is that the distant saddle points will contribute very little to the asymptotic expression for the precursor fields. If we can relate this to the precursor fields with which we are already familiar, we might say that the Sommerfeld precursor is extremely damped out with its amplitude and duration both being less than in the examples considered by both Brillouin and Oughstun.

Further, since the contour will never pass through the lower near saddle point, that contribution will not enter the equation. We note that it was the sum of the contributions of the two near saddle points after they had left the imaginary axis that gave the Brillouin precursor its oscillatory shape. It should also be pointed out that in the case $\delta < \omega_0$, the initial exponential behavior of the Brillouin precursor is a result of the single upper near saddle point contribution before the two saddle points coalesce and leave the axis. Though this is only a prediction and would need to be checked more carefully with further numerical and analytical work, it certainly seems a possibility that in the cases we are considering, since the lower saddle point will not be included, the Brillouin precursor will have an exponential increase for a short time and then an exponential decrease giving the whole precursor a somewhat Gaussian type of shape.

In conclusion, we see that a study of the analytic structure of the complex plane can be generalized without much difficulty for different values of the parameters. The more global perspective has enabled us to better understand the original case for $\delta < \omega_0$. However, whether these "supercritical" values of the damping constant can

be associated with physical media remains an open question. Nonetheless, we believe that our analysis has its place in the overall assesment of the applicability of the Lorentz model to realistic media.

7 A Double Resonance Medium

Until now we have only considered a material with a single resonance frequency. In general, most media will have several resonance frequencies and corresponding absorption bands. Brillouin speculated that in generalizing to the case of several resonances, additional precursors would arise with each additional resonance (Brillouin 1960, 81). In a paper by Shen and Oughstun, they confirm the presence of another precursor for a material with two resonances and give its shape graphically. They arrive at this through mostly numerical work as the index of refraction for two resonances and the resulting phase function in the integral for the signal become intractable to solve analytically. It is not our purpose to analyze too closely their numerical work, but we would like to extend what they have done.

Shen and Oughstun give the following for the index of refraction of a medium with two resonances (Shen and Oughstun 1989, 949):

$$n^2(\omega) = 1 - \frac{b_0^2}{\omega^2 - \omega_0^2 + 2i\delta_0\omega} - \frac{b_2^2}{\omega^2 - \omega_2^2 + 2i\delta_2\omega}. \tag{59}$$

This follows from eq. (7) in the section on the Lorentz model. However, as was pointed out there, this itself is a simplification in that the local field correction factor, ν, is assumed to be zero. This correction factor allows one to take into account the electric fields a particle in a material will feel which are exerted by neighboring particles. It is therefore a characteristic parameter of a material. Assuming that this correction factor is zero is not a serious problem in a material with a single resonance as the effect is to shift the resonant frequency (see Section 1). However, this simplification is not true for a multiple resonance medium.

We can take the general form we presented in the Lorentz section and show

that the above index of refraction does indeed follow when $\nu = 0$.

$$\frac{K-1}{1+\nu(K-1)} = \sum_i \frac{N_i q_i^2}{\epsilon_0 m_i} \cdot \frac{1}{\omega_{0_i}^2 - \omega^2 - 2i\delta_i\omega} \tag{60}$$

By multiplying both sides by the denominator on the left hand side and combining the $K-1$ terms, we get

$$K = n^2(\omega) = 1 + \frac{\sum_i \frac{b_i^2}{\omega_{0_i}^2 - \omega^2 - 2i\delta_i\omega}}{1 - \nu \sum_i \frac{b_i^2}{\omega_{0_i}^2 - \omega^2 - 2i\delta_i\omega}} \tag{61}$$

where we have set

$$b_i^2 = \frac{N_i q_i^2}{\epsilon_0 m_i}.$$

If $\nu = 0$ in the above equation, it reduces to the eq. (59). However, this approximation is only good for gases and other rarefied media. In general ν will not be zero for more dense materials.

We then ask, how will the inclusion of this local field correction factor affect the location of the branch points and of the saddle points in the complex frequency plane, and ultimately the resulting precursor behavior? To begin to answer this it may be well to put eq. (61) into a different form for two resonances.

$$n^2(\omega) = \frac{1 + (1-\nu)\left\{\frac{b_0^2}{\omega_0^2 - \omega^2 - 2i\delta_0\omega} + \frac{b_2^2}{\omega_2^2 - \omega^2 - 2i\delta_2\omega}\right\}}{1 - \nu\left\{\frac{b_0^2}{\omega_0^2 - \omega^2 - 2i\delta_0\omega} + \frac{b_2^2}{\omega_2^2 - \omega^2 - 2i\delta_2\omega}\right\}} \tag{62}$$

From this it can be seen that for $\nu = 0$ there will be four singularities at the ω values which satisfy the two equations

$$\omega^2 + 2i\delta_0\omega - \omega_0^2 = 0 \tag{63}$$

$$\omega^2 + 2i\delta_2\omega - \omega_2^2 = 0$$

However, for $\nu \neq 0$, these will no longer be singularities of the complex index of refraction since the zeros in both the numerator and denominator of eq. (62) cancel each other out. Simplification of eq. (62) leads to

$$n^2(\omega) = \frac{\omega^4 + ia\omega^3 - [c + (1-\nu)d]\omega^2 - i[e + (1-\nu)f]\omega + g + (1-\nu)h}{\omega^4 + ia\omega^3 - (c - \nu d)\omega^2 - i(e - \nu f)\omega + g - \nu h}. \qquad (64)$$

where a, c, d, e, f, g and h are combinations of the parameters of the material and are positive constants given by

$$\begin{aligned} a &= 2(\delta_0 + \delta_2) \\ c &= \omega_0^2 + \omega_2^2 + 4\delta_0\delta_2 \\ d &= b_0^2 + b_2^2 \\ e &= 2(\delta_0\omega_2^2 + \delta_2\omega_0^2) \\ f &= 2(b_0^2\delta_2 + b_2^2\delta_0) \\ g &= \omega_0^2\omega_2^2 \\ h &= b_0^2\omega_2^2 + b_2^2\omega_0^2. \end{aligned}$$

Shen and Oughstun give the following parameter values which we will use as well (Shen and Oughstun 1989, 949)

$$\begin{aligned} \delta_0 &= 0.1 \times 10^{16}\text{sec}^{-1} \\ \delta_2 &= 0.28 \times 10^{16}\text{sec}^{-1} \\ \omega_0 &= 1 \times 10^{16}\text{sec}^{-1} \\ \omega_2 &= 7 \times 10^{16}\text{sec}^{-1} \end{aligned}$$

$$b_0^2 = 5 \times 10^{32} \text{sec}^{-2}$$

$$b_2^2 = 20 \times 10^{32} \text{sec}^{-2}$$

To find the branch points and hence branch cuts of the above equation we must solve for the zero points of both the numerator and denominator of eq. (64). To do this exactly requires solving two complex quartic equations in a complex variable. With some work, this can be done exactly since methods for finding analytic solutions to these equations are known and available (see, for instance a CRC Math Handbook). But doing this will not give us much more information than solving them numerically since the resulting expressions are very complicated algebraically.

To garner some information, we again resort to numerics. To get an idea of the structure of the complex frequency plane, we graph the real part of the complex phase function which is given by

$$\Re\phi(\omega, \theta) = \Re\left(i\omega[n(\omega) - \theta]\right).$$

We let $\omega = \omega' + i\omega''$ and separated eq. (64) into real and imaginary parts. We wrote a program incorporating a 3 dimensional plotting subroutine to plot the real part of this phase function as a function of the real and imaginary parts of the complex frequency.

Several graphs (figures 12-24) are included in the appendix for increasing values of ν. We also include a graph of the real part of the phase function for a single resonance, showing that our derivation and the program does indeed reduce to that case when $b_2^2 = 0$, as it should (figure 11). This is, of course, no guarantee that our derivation and resulting program are correct, but it does provide a certain amount of validation for them.

For a double resonance medium with $\nu = 0$ there are two pairs of branch cuts which are situated symmetrically about the imaginary axis and which are below the real axis. One is relatively close to the imaginary axis for the parameters we are using, extending along the line $y = -\delta_0$ from $x \approx 1$ to $x \approx 1.9$. The other is further away from the axis and extends along the line $y = -\delta_2$ from $x \approx 7$ to $x \approx 8$. If we extend what we know from the case of a single resonance medium, we know that on each of the four branch cuts the branch point farthest away from the imaginary axis is the ω value which makes the index of refraction zero. The other end of the branch cut is thus the point that causes the denominator in the index of refraction to go to zero. These last four points are readily identifiable on the graphs as the peaks. They actually go to infinity since there are no maxima or minima in the complex plane, but since we are doing numerical work and dealing with finite intervals, the points that should go to infinity are effectively truncated and appear as peaks.

On inspection of the graphs one notices that as ν increases away from zero, two of the peaks (which are the ends of the branch cuts closest to the imaginary axis) begin to "move." In a manner not dissimilar to how the branch cuts moved for a single resonance as δ increased, these branch points approach the imaginary axis and at about the value $\nu = 0.2$ seem to become a single branch point on the imaginary axis. It may be that the branch points come together at the origin, but we are not sure of that at this point. There would seem to be some indication of this because as ν continues to increase, there appears to be a kind of separation as a peak in the lower half of the complex plane moves down the imaginary axis and a valley or "hole" in the upper half of the complex plane moves up the imaginary axis, each moving away from the point where they came together on the axis. By graphing the negative of the real part of the phase function, it appears that this valley is the mirror image

of the peak moving away from it for increasing ν.

To be able to say anything at all about the precursors we need to know the location of the saddle points and the value of the real part of the phase function at these saddle points. We have written a program to find the saddle points. Our methodology is the same as for a single resonance medium excepting that our index of refraction is more complicated. We set the first derivative of the phase function to zero, separated real and imaginary parts and were left with two equations in two unknowns, namely the real and imaginary components of the complex frequency. Using Newton's method for two variables, we are again able to calculate the solutions to these equations and thereby find the saddle points.

For $\nu = 0$, we are able to confirm the saddle point locations that Shen and Oughstun found. These include the original four saddle points for a single resonance medium plus four additional saddle points. A pair of saddle points are located between the branch cuts in both halves of the complex plane. For θ not much larger than one, in the right half of the complex plane, there is a saddle point approximately above and another below and to the right of the cut line closest to the imaginary axis. As θ increases away from one, these saddle points move onto the cut lines, the upper middle saddle point moving towards the far branch point on the cut closest to the imaginary axis and the lower middle saddle point moving towards the near branch point on the cut furthest away from the imaginary axis. As Shen and Oughstun point out, the importance of these middle saddle points depends on the parameters of the medium (Shen and Oughstun 1989, 960). For the previous choice of medium parameters, these saddle points will be of significance for a finite interval of time allowing for the evolution of an additional precursor which arrives after the end of the Sommerfeld precursor and the onset of the Brillouin precursor. Using our previous

interpretation, this is because the middle saddle points which contribute to a possible precursor are predominant over all other saddle points in a time period between the end of the Sommerfeld precursor and the arrival of the Brillouin precursor.

Having found the saddle points for a double resonance medium for $\nu = 0$, it is then necessary to find these saddle points for $\nu > 0$ and to determine roughly their behavior and their contribution to any expression for the precursor fields. As we did for a single resonance medium, we have listed in the appendices some of the locations for these saddle points as θ increases along with the values of the real and imaginary parts of the phase function. After some investigation it was found that the distant saddle points are barely affected by the increase in ν. They still approach the most distant branch cuts as θ increases and the relative positions of these saddle points for any given θ is nearly the same. Similarly, the value of the real part of the phase function $X(\omega, \theta)$ remains very nearly the same for a given θ value as ν increases. A look at the tables included in the appendices for the distant saddle points for a double resonance medium with ν included will bear this out (see Tables 7-9 in the appendices).

There is also not much change to the location of the middle saddle points. For small θ values, these saddle points begin and are found in approximately the same vicinity for $\nu \neq 0$. As θ increases these saddle points continue to move onto one of the nearby branch points. One difference is that the "upper" middle saddle point begins to converge to the branch cut farther away from the imaginary axis as ν becomes larger than about 0.4 rather than to the branch cut closer to the imaginary axis. The values of $X(\omega, \theta)$ at these middle saddle points remain about the same for increasing ν (again, see Tables 10-14 in the appendices).

On the other hand, there are some real changes to the near saddle points.

For all ν less than about 0.2 for the parameter values we are considering, the near saddle points still begin on the imaginary axis, move towards each other, coalesce, and move apart into the plane for increasing θ. However, for $0 < \nu < 0.2$ these saddle points begin closer to each other but take a longer time before coalescing. Further, the relative values of $X(\omega, \theta)$ are more pronounced. For example, for a given value of θ not much larger than one, $X(\omega, \theta)$ at the "upper" near saddle point becomes more negative as ν increases away from 0 to about 0.2. Thus, a longer time passes before these saddle points are of significance in comparison to the other saddle points. At $\nu \approx 0.2$ the branch points come together after which they move away from each other along the imaginary axis. This "motion" of the branch points along the axis for increasing ν effectively prevents the near saddle points from coalescing. For ν greater than about 0.2, the near saddle points still begin on the imaginary axis, however, they merely approach the branch points which are now located on the axis (see Tables 15-20).

As we did with the cases where δ increased, we can make a few predictions as to the resulting behavior and evolution of the precursors. Since the distant saddle points remain nearly unchanged in their position and contribution in terms of the value of the real part of the phase function as ν increases, we expect that the resulting Sommerfeld precursor fields should remain similar to those for $\nu = 0$. This would also appear to be true for the middle saddle points. Since their locations do not change much for increasing ν nor do the values of $X(\omega, \theta)$, we expect that the precursor fields arising from the extra resonance condition will also be close to those for $\nu = 0$. There is the question of whether there will be much change arising for larger values of ν (values greater than about 0.6) when one of the saddle points changes trajectories and converges to a different branch point. Additional numerical research would be

needed to answer this problem more carefully.

Though the other two precursors seem to remain largely the same with the inclusion of ν, this will not be true for the Brillouin precursor which arises from the contributions of the near saddle points. For values of ν such that $0 < \nu < 0.2$, the Brillouin precursor will arrive later than when $\nu = 0$. Further, this delay in its arrival will increase as ν increases towards 0.2. The main signal may then overshadow this precursor if the delay is long enough.

A troubling result, however, is the fact that for large enough ν, the upper near saddle point remains in the upper half of the plane. This is because one of the branch points (the "valley") is on the imaginary axis in the upper half of the plane and is actually the point to which the saddle point will converge. This is strange because it implies that the contribution from this saddle point will blow up as $\theta \to \infty$. We can show this by looking at the phase function

$$\begin{aligned} \phi(\omega, \theta) &= i\omega[n(\omega) - \theta] \\ &= y\theta - xn_i - yn_r + i(xn_r - yn_i - x\theta) \end{aligned}$$

where x and y are the real and imaginary parts of the complex frequency and n_r and n_i are the real and imaginary parts of the complex index of refraction. We are interested in the real part, so we have

$$\Re(\phi) = X = y\theta - yn_r$$

where the term involving x has been set to zero since we are dealing with a saddle point on the imaginary axis. Because the saddle point never moves below the real axis, as in all the cases with which we have dealt before, the first term remains positive and

goes to $+\infty$ with θ. In both the method of steepest descent as well as the method of Olver, the asymptotic expansion will now have a continuously increasing exponential term.

If we were to interpret this as before, we would have to say that the precursor field to which this saddle point makes its contribution (the Brillouin precursor) will have an exponentially increasing amplitude for increasing time. This would ultimately dwarf any possible signal which may follow. For example, in the case of the delta function which gives the impulse response of the medium, the Sommerfeld and second precusors would be followed by a Brillouin precursor which, instead of damping out, would increase in amplitude.

In conclusion, we have been able to incorporate a consideration of the local field correction factor present in the Lorentz model into an analysis of a double resonance medium. With numerical analysis we have been able to examine the structure of the complex plane. We have also given qualitative results for the forms of the precursors. A rather unphysical result does come out of the numerics for the Brillouin precursor, however. We strongly question this result, but at this time do not know the reason for it. Additional research will be necessary to determine the cause of this problem. But a significant start has been made to generalizing the analysis of precursors to a more complete Lorentz model of dielectrics.

A Complex Analysis

In this appendix, we present some basic results from complex analysis. We will also sketch a derivation of the method of steepest descent as well as briefly present the asymptotic technique of Olver which was used by Oughstun and Sherman in their calculation of the contribution of the saddle points. The results of complex analysis and the method of steepest descent can be found in chapters six and seven of *Mathematical Methods for Physicists*, by George Arfken as well as in other texts on complex analysis. The basic results which we present here are found discussed at greater length in those references.

A.1 Basic results

The complex variable z is defined in terms of two real variables, x and y

$$z = x + iy$$

where $i = \sqrt{-1}$ and x is called the real part of z and y is the imaginary part of z. The complex conjugate is $x - iy$ and can be expressed as z^*. It is found by simply replacing i with $-i$ everywhere. Complex variables also have a polar representation. If z is taken to be a vector, it can be graphed in the complex plane where the y-axis becomes the imaginary axis and the x-axis is the real axis. z can then be expressed in terms of its magnitude, r (often written as $|z|$), and the angle θ it makes with the real axis:

$$z = re^{i\theta}$$

where

$$r = |z| = \sqrt{x^2 + y^2}$$

$$\theta = \arctan \frac{y}{x}.$$

Complex functions defined in terms of the complex variable z can always be separated into the sum of two real functions, one comprising the real part and the other the imaginary part of the complex function.

$$f(z) = \Re[f(z)] + i\Im[f(z)] = u(x,y) + iv(x,y)$$

The complex conjugate of a complex function, $f^*(z)$, is found by simply replacing i with $-i$ everywhere i is found in the original function. The Schwarz reflection principle equates the complex conjugate of a function with the function of the conjugate of the complex variable:

$$f^*(z) = f(z^*)$$

provided that the function $f(z)$ is analytic in a region which includes the real axis and is real on the real axis.

In analogy with the complex variable z, $f(z)$ can be given a polar representation:

$$f(z) = |f(z)|e^{i\Theta}$$

where

$$|f(z)| = [f(z) \cdot f^*(z)]^{\frac{1}{2}} = \left(u^2 + v^2\right)^{\frac{1}{2}}$$

$$\Theta = \arctan \left[\frac{v(x,y)}{u(x,y)}\right]$$

When dealing with multivalued functions such as logarithms or functions involving powers of noninteger value, it becomes desirable to make the function single valued in the complex plane. Take, for example, the function

$$f(z) = z^{\frac{1}{2}} = r^{\frac{1}{2}} e^{i\theta/2}.$$

Assume for simplicity that r is 1. At $\theta = 0$, $f(z)$ will be 1 whereas $f(z)$ will be -1 at $\theta = 2\pi$. The significance of this is that the phase of the complex variable z has gone through an angle of 2π while the phase of the complex function

$$f(z) = z^{\frac{1}{2}}$$

has only gone through an angle of π. The following table illustrates this more clearly by showing values of z and $f(z) = z^{\frac{1}{2}}$ at various points in the complex plane. If a

θ	0	$\pi/2$	π	$3\pi/2$	2π	$5\pi/2$	3π	$7\pi/2$	4π
z	1	i	-1	$-i$	1	i	-1	$-i$	1
$f(z) = z^{1/2}$	1	$\frac{1}{\sqrt{2}}(1+i)$	i	$\frac{1}{\sqrt{2}}(-1+i)$	-1	$\frac{1}{\sqrt{2}}(-1-i)$	$-i$	$\frac{1}{\sqrt{2}}(1-i)$	1

function $f(z)$ is multivalued, we require that the phase of the function, θ, be restricted to an interval of 2π in order that the function be single-valued. Further, a branch point is created together with a line (called a cut line) in the complex plane (extending from the branch point) which no line integral may cross. For $f(z) = z^{\frac{1}{2}}$, or more generally, $f(z) = z^a$ where a is not an integer, the origin becomes the branch point and the positive (or negative) real axis may be taken as the cut line. (The choice of the cut line is arbitrary so long as we connect either two branch points or a branch point with infinity. We could have chosen the negative imaginary axis or any line beginning at the origin and extending to infinity to be the cut line.) In general, a function will not

be continuous across a cut line. Thus, the phase of the function on one side of the cut line will most likely be different from the phase on the other side. For functions which may have more than one compatible branch point, the cut lines can either be taken to infinity from the branch points or drawn between branch points. This is the case for the expression for the complex index of refraction where two branch cuts are found in the lower half of the complex plane.

Necessary and sufficient conditions for the differentiability of a complex function, $f(z)$, are the Cauchy-Riemann conditions,

$$\frac{\partial u}{\partial x} = \frac{\partial v}{\partial y}, \qquad \frac{\partial u}{\partial y} = -\frac{\partial v}{\partial x}$$

The importance of these conditions lies in the fact that they tell us whether or not a complex function, $f(z)$, is differentiable. That in turn tells us if a function is analytic, which is a condition for almost all significant operations in the complex plane and therefore a condition for almost all mathematical models of physical systems.

If a function is analytic, several properties of that function are then immediately known. Both the real and imaginary parts (u and v respectively) of an analytic function are harmonic. In other words, they satisfy Laplace's equation. Analyticity of a function also guarantees the existence of all derivatives of that function. A function which is both analytic and finite over the entire complex plane can be shown to be a constant. If a function is analytic in a given region of the complex plane, though they may have saddle points, the real and imaginary parts of the function will have no minimums or maximums in that region. The last two conditions imply that any function which is not a constant will have at least one singularity somewhere in the complex plane. Further, if a function is continuous and analytic on the boundary which defines a region within which the function is also analytic, the line integral of

the function along that contour (taken in a couterclockwise direction) will be zero:

$$\oint_C f(z)dz = 0$$

where C is a closed contour. This is known as Cauchy's integral theorem.

Another significant result is the Cauchy integral formula. It gives the value of the function at a specific point within a given closed contour once the value of the integral on the contour is known. The condition for this formula is that the function $f(z)$ be analytic everywhere within and on a closed contour C. Then, if z_0 is a point within C,

$$\oint_C \frac{f(z)}{z - z_0}dz = 2\pi i f(z_0)$$

where again the contour is traversed in a counterclockwise direction. (If the contour is followed clockwise, a negative sign would be introduced.) For the above, if z_0 is on the outside of the contour, the integrand remains analytic on and in C, and hence, by the Cauchy integral theorem, the integral is zero.

By using the Cauchy integral formula, higher order derivatives of $f(z)$ can be found. The equation for finding the nth order derivative at z_0 is given by

$$f^{(n)}(z_0) = \frac{n!}{2\pi i}\oint_C \frac{f(z)}{(z - z_0)^{n+1}}.$$

Using the Cauchy integral formula, a Taylor series expansion can be derived for functions of a complex variable:

$$f(z) = \sum_{n=0}^{\infty}(z - z_0)^n \frac{f^{(n)}(z_0)}{n!}.$$

For annular, analytic regions in the complex plane, a series expansion known as a Laurent series can be found from the Cauchy integral formula:

$$f(z) = \sum_{n=-\infty}^{\infty} a_n (z - z_0)^n$$

where

$$a_n = \frac{1}{2\pi i} \oint_C \frac{f(z')dz'}{(z' - z_0)^{n+1}}.$$

If the Laurent series given above is integrated term by term over a region enclosed by C in which $f(z)$ is analytic except for an isolated singularity z_0, all the terms integrate to zero except the $n = -1$ term. This term is given by

$$\oint_C f(z)dz = a_{-1} \oint_C \frac{dz}{z - z_0} = 2\pi i a_{-1}$$

and a_{-1} is called the residue of $f(z)$ at z_0 and is

$$a_{-1} = \frac{1}{2\pi i} \oint_C f(z')dz'.$$

For a region, C', which encloses n singularities the residues of $f(z)$ at each of those singularities add towards giving the integral of the function around C'

$$\begin{aligned} \oint_{C'} f(z)dz &= 2\pi i(a_{-1_{z_0}} + a_{-1_{z_1}} + \cdots + a_{-1_{z_n}}) \\ &= 2\pi i \cdot \sum(\text{enclosed residues}). \end{aligned}$$

This result is known as the residue theorem. It is extremely important in evaluating definite integrals through contour integration. Basically, the process of integration is reduced to choosing an appropriate closed contour C and finding the residues at the singular points enclosed by this contour. By appropriate we mean a contour which, when the integral is evaluated, will cause the integral to go to zero (or be otherwise easily evaluated), except along the portion of interest (often the x-axis).

A.2 The method of steepest descent

At this point we introduce the method of steepest descent. This is a method which determines the asymptotic behavior of a function when it can be expressed in an integral form of the following type:

$$I(s) = \int_C g(z)e^{sf(z)}dz$$

where s is assumed to be real, large, and positive and $f(z)$ and $g(z)$ are complex functions of the complex variable z and independent of s. (Born and Wolf point out that the method can still be derived for s complex, but since in our physical problem, for which we are using the method of steepest descent, this parameter is real, we will derive it only for the real case.) In this way the exponential involving s and $f(z)$ will dominate the function $g(z)$. It is further assumed that $f(z)$ is analytic along the contour. The contour is chosen in such a way that it is independent of s and that the real part of $f(z)$ (which we will call $u(x, y)$ from now on) goes to minus infinity at both limits of the contour. Hence the integrand goes to zero and does not contribute to the integral in those points. Since s is large and positive in the asymptotic domain, the main contribution to the integrand comes when u is large and positive. We require that the imaginary part of $f(z)$ (to be called $v(x, y)$ from now on) is constant in the region where u attains its maximum.

A maximum in u means that the first derivative of $f(z)$ will be zero:

$$\frac{\partial u}{\partial x} = \frac{\partial u}{\partial y} = 0 \Rightarrow \frac{df(z)}{dz} = \frac{\partial u}{\partial x} + i\frac{\partial u}{\partial y} = 0.$$

This implies that we have a saddle point since Laplace's equation $\nabla^2 u = 0$ gives

$$\frac{\partial^2 u}{\partial x^2} = -\frac{\partial^2 u}{\partial y^2}$$

which shows us that u (and similarly v since it also satisfies Laplace's equation) cannot have an absolute maximum or minimum. This condition, that we demand that u have a maximum at the saddle point restricts how we can pass through the saddle point with our contour. We further restrict this to a single path by requiring that along this contour $v(x, y)$ be constant, namely the value of v at the saddle point, $v(x_0, y_0)$. That only a single curve satisfies this is a result of the fact that the curves $u =$ constant are orthogonal to the curves $v =$ constant. We can show this by using the gradients of the two functions:

$$\begin{aligned} \nabla u \cdot \nabla v &= \frac{\partial u}{\partial x}\frac{\partial v}{\partial x} + \frac{\partial u}{\partial y}\frac{\partial v}{\partial y} \\ &= \frac{\partial u}{\partial x}\left(-\frac{\partial u}{\partial y}\right) + \frac{\partial u}{\partial y}\left(\frac{\partial u}{\partial x}\right) \\ &= 0 \end{aligned}$$

Thus, if the gradients are perpendicular for all x and y, the curves are orthogonal, which is the same as saying that the gradient of u is tangent to a curve of constant v. In our problem, remaining on a contour where v is constant is identical to moving along the gradient, i.e. in the direction of most rapidly decreasing (or increasing) u. By our previous condition that we go through the saddle point such that u will have a maximum there, we must go through the saddle point in the direction of most rapidly decreasing u. Hence, we have *the* path of steepest descent.

On expanding $f(z)$ in a Taylor series about our saddle point at z_0, we see that the first derivative vanishes and for a small region around the saddle point $f(z)$ can be approximated by

$$f(z) \approx f(z_0) + \frac{1}{2}f''(z_0) \cdot (z - z_0)^2$$

such that the integral over the contour can, in turn, be approximated as being entirely made up by the contribution at this saddle point at z_0:

$$I(s) \approx g(z_0)e^{sf(z_0)} \int_{-\infty}^{\infty} e^{\frac{1}{2}sf''(z_0)(z-z_0)^2} dz.$$

The term involving the second derivative can be shown to be purely real since we are taking the path of steepest descent. This is equivalent to keeping the imaginary part of $f(z)$ constant along the contour.

$$\begin{aligned} f(z) - f(z_0) &= u(x,y) + iv(x,y) - u(x_0,y_0) - iv(x_0,y_0) \\ &= u(x,y) - u(x_0,y_0) \\ &\approx \frac{1}{2}f''(z_0) \cdot (z - z_0)^2 \end{aligned}$$

We then set the term involving the second derivative equal to $-t^2/2s$ where s is real according to our original assumption and hence t is also real. By expressing $z - z_0$ and $f''(z_0)$ in polar form

$$(z - z_0) = \delta e^{i\alpha} \qquad f''(z_0) = |f''(z_0)|e^{i\beta},$$

where α and β are arbitrary phase constants, we can then rewrite our substitution as

$$\frac{1}{2}|f''(z_0)|e^{i\beta}\delta^2 e^{i2\alpha} = e^{i\pi}\frac{t^2}{2s}.$$

The phases on both side of this equation must be equal so we can write

$$e^{i(2\alpha+\beta)} = e^{i\pi} \quad \Rightarrow \quad 2\alpha + \beta = \pi,$$

where we have taken only the first branch of the function. We can now express the integral in terms of t rather than z by using

$$(z - z_0) = \pm \frac{te^{i(\pi-\beta)/2}}{\sqrt{s|f''(z_0)|}}$$

where the exponent of the exponential of this last equation is simply $i\alpha$. We set

$$dz = \frac{dz}{dt} \cdot dt = \frac{e^{i\alpha}}{\sqrt{s|f''(z_0)|}} \cdot dt$$

and rewrite our integral as

$$I(s) \approx \frac{g(z_0)e^{sf(z_0)}e^{i\alpha}}{|sf''(z_0)|^{1/2}} \int_{-\infty}^{\infty} e^{-t^2/2} dt.$$

This gives, on recognizing the remaining integral as the error integral, the final result for the method of steepest descent.

$$I(s) \approx \frac{\sqrt{2\pi}g(z_0)e^{sf(z_0)}e^{i\alpha}}{|sf''(z_0)|^{1/2}}$$

A few things should be pointed out. It is critical that the correct path is chosen, in this case the path of steepest descent. This is done by correctly choosing α, the phase factor which indicates the direction taken through the saddle point. The location of the saddle point z_0 is determined for a given $f(z)$ by setting its first derivative equal to zero and solving for z. This must be the maximum for $u(x_0, y_0)$, the real part of $f(z)$. Therefore,

$$\Re[f(z)] < \Re[f(z)]|_{z=z_0}$$

for all the rest of the points on the contour C where $z \neq z_0$. Substituting $z = z_0 + \delta e^{i\alpha}$ into the left hand side of the above equation makes it possible to solve for the appropriate value of the phase factor, α.

Should it be the case that the contour passes through more than one saddle point, the final result for the integral will be the sum of the contributions to the integral of the individual saddle points.

The method of steepest descent, originally due to P. Debye is related to the method of stationary phases due to Stokes and Kelvin, which was later set on firmer foundation by Watson. For more details see Born and Wolf (Born and Wolf 1970, 747). All these methods give asymptotic approximations to integrals by choosing a path of integration such that the integrand only contributes to the integral in certain critical points where the integral can be evaluated exactly. In the method of steepest descent these points are the saddle points.

A.3 The Olver method

Oughstun and Sherman use in their analysis the asymptotic expansion derived by Olver (Olver 1970, 228). The most significant improvement of this method over that of steepest descent is that it does not require a knowledge of the path of steepest descent through the saddle points to evaluate the appropriate integral. In addition, Olver's paper presents the entire asymptotic series for an integral given in the above form. His derivation is also more general in that it is applicable to saddle points of higher order. (A higher order saddle point is one where, in addition to the first derivative, higher order derivatives in the Taylor expansion of $f(z)$ go to zero.) Although, I have not shown them, these last two results of Olver can be found using the method of steepest descent. I will not attempt to reproduce Olver's derivation, but I do want to show that for the conditions of a first order saddle point, the first term of his asymptotic expansion does reduce to the expression derived here using the method of steepest descent.

Consider a contour integral of the form

$$I(z) = \int_a^b e^{-zp(t)} q(t) dt,$$

where $p(t)$ and $q(t)$ are analytic functions of the complex variable t and the following conditions are met:

1) $p(t)$ and $q(t)$ are independent of z, single-valued, and analytic in an open domain which we will call **T**.

2) The contour is independent of z, a is finite, b is finite or infinite, and the interval between a and b is in the open domain **T**.

3) Around a, $p(t)$ and $q(t)$ can be expanded in convergent series of the form

$$p(t) = p(a) + \sum_{s=0}^{\infty} p_s (t-a)^{s+\mu}, \qquad q(t) = \sum_{s=0}^{\infty} q_s (t-a)^{s+\lambda-1},$$

where p_s and q_s are coefficients in the expansion and $p_0 \neq 0$ (we will take μ and λ as positive integers although Olver has conditions which include a more general range for the two).

4) z ranges along a ray or over a subsector given by $\theta_1 \leq \theta \leq \theta_2$ and $|z| \geq Z$ where θ is defined as the phase of z, $\theta_2 - \theta_1 < \pi$, and $Z > 0$. $I(z)$ converges at its upper limit absolutely and uniformly with respect to z.

5) $\Re\left[e^{i\theta}p(t) - e^{i\theta}p(a)\right]$ is positive when t is on the contour and is bounded away from zero uniformly with respect to θ as $t \to b$ along the contour.

If these conditions hold for an integral of the form given above, Olver shows:

$$I(z) = \int_b^a e^{-zp(t)} q(t) dt \sim e^{-zp(a)} \sum_{s=0}^{\infty} \Gamma\left(\frac{s+\lambda}{\mu}\right) \frac{a_s}{z^{(s+\lambda)/\mu}}$$

uniformly with respect to θ (the phase of z) where $|z| \to \infty$. In addition, the coefficients a_s are given by reverting the series for $p(t)$ and $q(t)$.

The first term of this asymptotic expansion is given by

$$e^{-zp(a)}\Gamma\left(\frac{\lambda}{\mu}\right)\frac{q_0}{\mu p_0^{\lambda/\mu}}\cdot\frac{1}{z^{\lambda/\mu}}$$

where Olver has given $a_0 = q_0/\mu p_0^{\lambda/\mu}$. By expanding $p(t)$ and $q(t)$ in terms of power series we can determine p_0 and q_0. Olver's definition of $p(t)$ is

$$p(t) = p(a) + p_0(t-a)^{\mu} + p_1(t-a)^{1+\mu} + p_2(t-a)^{2+\mu} + \cdots$$

For a first order saddle point, which is what we considered in deriving the method of steepest descent, the Taylor's expansion of $p(t)$ will be

$$p(t) = p(a) + \frac{1}{2!}p''(a)\cdot(t-a)^2 + \frac{1}{3!}p'''(a)\cdot(t-a)^3 + \cdots$$

since for a first order saddle point the first derivative is zero. For higher order saddle points, correspondingly higher order derivatives will also vanish. By the uniqueness of power series, we can then say that $p_0 = \frac{1}{2}p''(a)$ and $\mu = 2$. Expanding $q(t)$ in like manner, we get

$$\begin{aligned} q(t) &= q_0(t-a)^{\lambda-1} + q_1(t-a)^{\lambda} + q_2(t-a)^{\lambda+1} + \cdots \\ &= q(a) + q'(a)\cdot(t-a) + \frac{1}{2}q''(a)\cdot(t-a)^2 + \cdots \end{aligned}$$

where again, by the uniqueness of power series, we can say that $q_0 = q(a)$ and $\lambda = 1$. Using these values, the first term in Olver's expansion becomes

$$e^{-zp(a)}\Gamma\left(\frac{1}{2}\right)\frac{q(a)}{2\left(\frac{1}{2}p''(a)\right)^{1/2}}\cdot\frac{1}{z^{1/2}} = \sqrt{\frac{\pi}{2}}\cdot\frac{q(a)e^{-zp(a)}}{[zp''(a)]^{1/2}}.$$

Referring back to our discussion of the method of steepest descent and using our prior notation, we see that a and z_0 are the same point, in this case a first order

saddle point. $q(a)$ is the same as $g(z_0)$, $p(a)$ becomes $f(z_0)$, and $-z$ corresponds to s. However, if we write $-z$ as $e^{i\pi}z$, we can set

$$z = e^{-i\pi}s.$$

Substituting this into Olver's first term yields

$$\sqrt{\frac{\pi}{2}}\frac{g(z_0)e^{sf(z_0)}}{(e^{-i\pi}sf''(z_0))^{1/2}} = \sqrt{\frac{\pi}{2}}\frac{g(z_0)e^{sf(z_0)}}{e^{-i\pi/2}e^{i\beta/2}\left|sf''(z_0)\right|^{1/2}}$$

where we have used our earlier notation in putting $f''(z_0)$ into polar representation. Olver's theorem calculates the integral over a contour which begins at the critical point (in this case a saddle point) and extends to a point where the integrand goes uniformly to zero. Since we took our original contour between two points (between $-\infty$ and $+\infty$) at which the integrand vanished uniformly with the saddle point on the contour, we must multiply Olver's result by two to account for the difference in contours. We can consider Olver's method as having calculated half the contribution of the saddle point since we "went down" only one side of it. We also recognize that the sum of the phases in the denominator above, $(-\pi + \beta)/2$, is identical to the α which we had defined earlier in our derivation of the method of steepest descent. With these substitutions, the first term of Olver's asymptotic expansion is seen to be identical to the approximation which we calculated using the method of steepest descent:

$$I(s) \approx \frac{\sqrt{2\pi}g(z_0)e^{sf(z_0)}e^{i\alpha}}{\left|sf''(z_0)\right|^{1/2}}.$$

B Graphs

The following are various sets of graphs which we felt would be appropriate to include. The first set of three graphs (figures 1-3) are amplitudes of the Sommerfeld and Brillouin precursors versus θ for two types of signals: a delta pulse and a sine wave modulated by the Heaviside function. The graph for the delta pulse is to give an idea of the general shape of the precursors. We graphed it using the formulation of Oughstun and Sherman. The first graph of the sine wave is using the equations of Brillouin while the second is using those of Oughstun and Sherman. They are distinguished by the "O" or "B" which follow them to indicate either Oughstun or Brillouin. The two graphs of the two sine waves disregard the arrival of the signal itself in order that we may compare the two formulations by Brillouin and Oughstun and Sherman. One should note on the graphs that they do not exactly begin at $\theta = 1$ since we are working with the non-uniform expansion. The Sommerfeld precursor goes to infinity at that θ value. So we begin at $\theta = 1.02$ for the delta pulse and at $\theta = 1.05$ for the two sine waves. The Brillouin precursor also seems to have a discontinuity at $\theta \approx 1.5$. This is again because we are using the non-uniform expansion at the point where the near saddle points coalesce and separate. We used the parameter values set forth in the text for these graphs. We considered the distance into the medium as $z = 1 \times 10^{-4}$ cm making c/z 0.03×10^{16} sec^{-1} and the carrier frequency for the modified sine wave as 5×10^{16} sec^{-1}.

Figure 4 is a graph comparing the approximations for the distant saddle points with the numerically calculated values. The curved solid line leading to the far ends of the branch cuts are the numerical values while the dotted line is the approximation of Oughstun and Sherman and the straight solid line is the approximation due to

Brillouin. These are graphed in the complex plane with the real part of the frequency (which we also call x) along the horizontal axis and the imaginary part of the frequency (also called y) along the vertical axis. The graph shows the trajectories of the saddle points and how they approach the branch cuts for increasing θ.

The next graphs (figures 5-9) are graphs of the complex frequency plane for a medium with a single resonance showing the locations of the branch cuts, the saddle points (given as "X"'s) and the extra solutions (given as "O"'s) to which our programs would converge but which are not saddle points. We have also included a graph of the complex plane for a double resonance medium with $\nu = 0$ (figure 10).

The remaining graphs are three dimensional plots for both a single and a double resonance medium which show the real part of the phase function (which we have called $X(\omega, \theta)$) for a given value of θ plotted against the real and imaginary parts of the complex frequency (which we have called x and y respectively). There are 13 of these three dimensional plots. All of them were calculated for a θ value of 1.25. The parameter values are those listed in Section 7 for a double resonance medium. The first three are for ν values from 0 to 0.2 showing a broad view of the plane. In these, both x and y extend from -10 to $+10$. The next five are plots for ν values from 0.2 to 0.6 where x and y extend from -5 to $+5$. The final five plots are identical to the previous five except that instead of looking along the $+y$ axis, the viewer is looking along the $-x$ axis. In effect, we have turned the graph around to get a "reverse" view of the surface of the complex plane. The programs to graph these three dimensional plots used a subroutine found in the p6 library on the VAX used in the Physics Department at BYU.

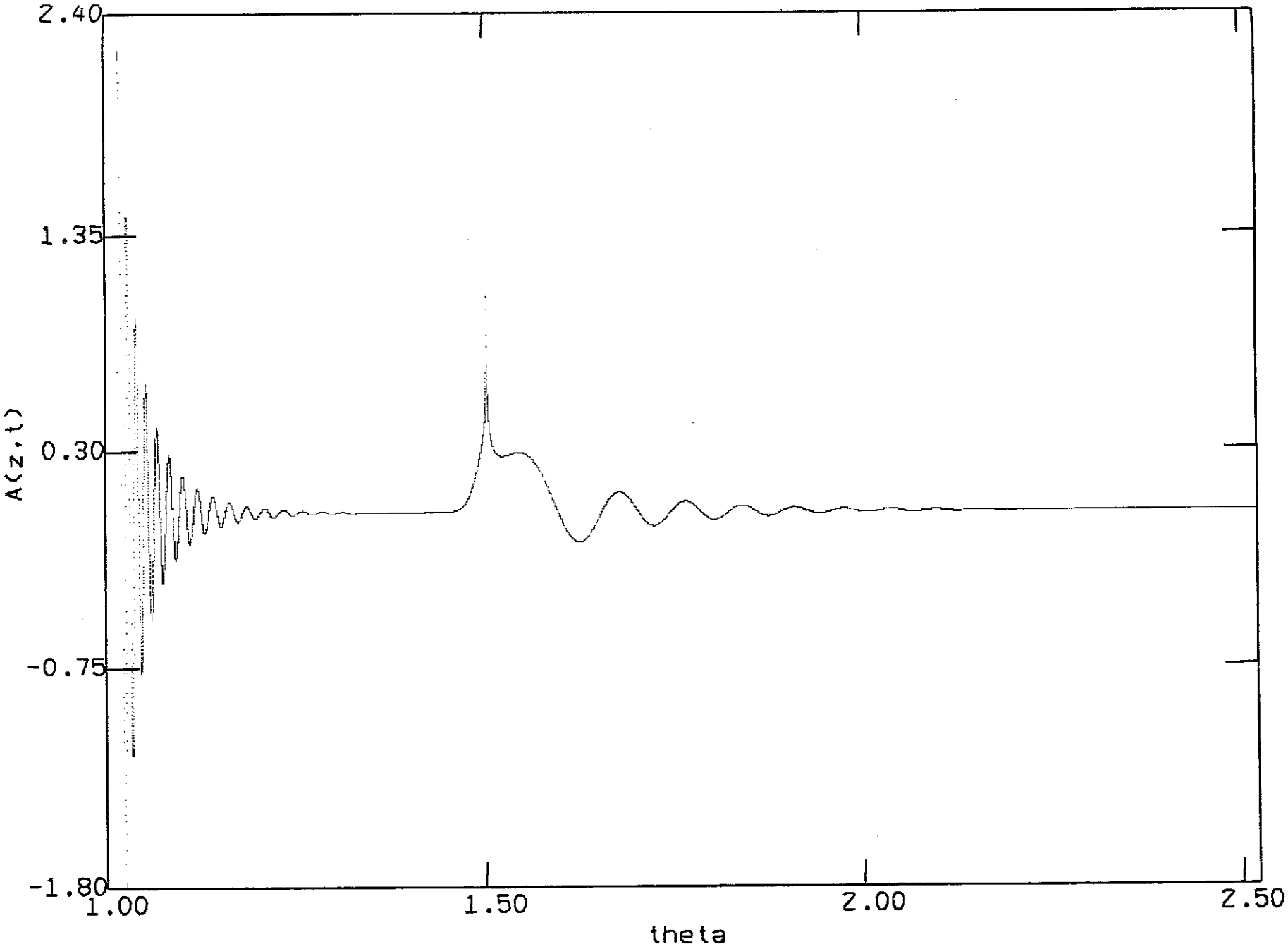

22:18:23
10-JUN-91

PRECURSORS FOR AN INPUT DELTA PULSE

FIG 1

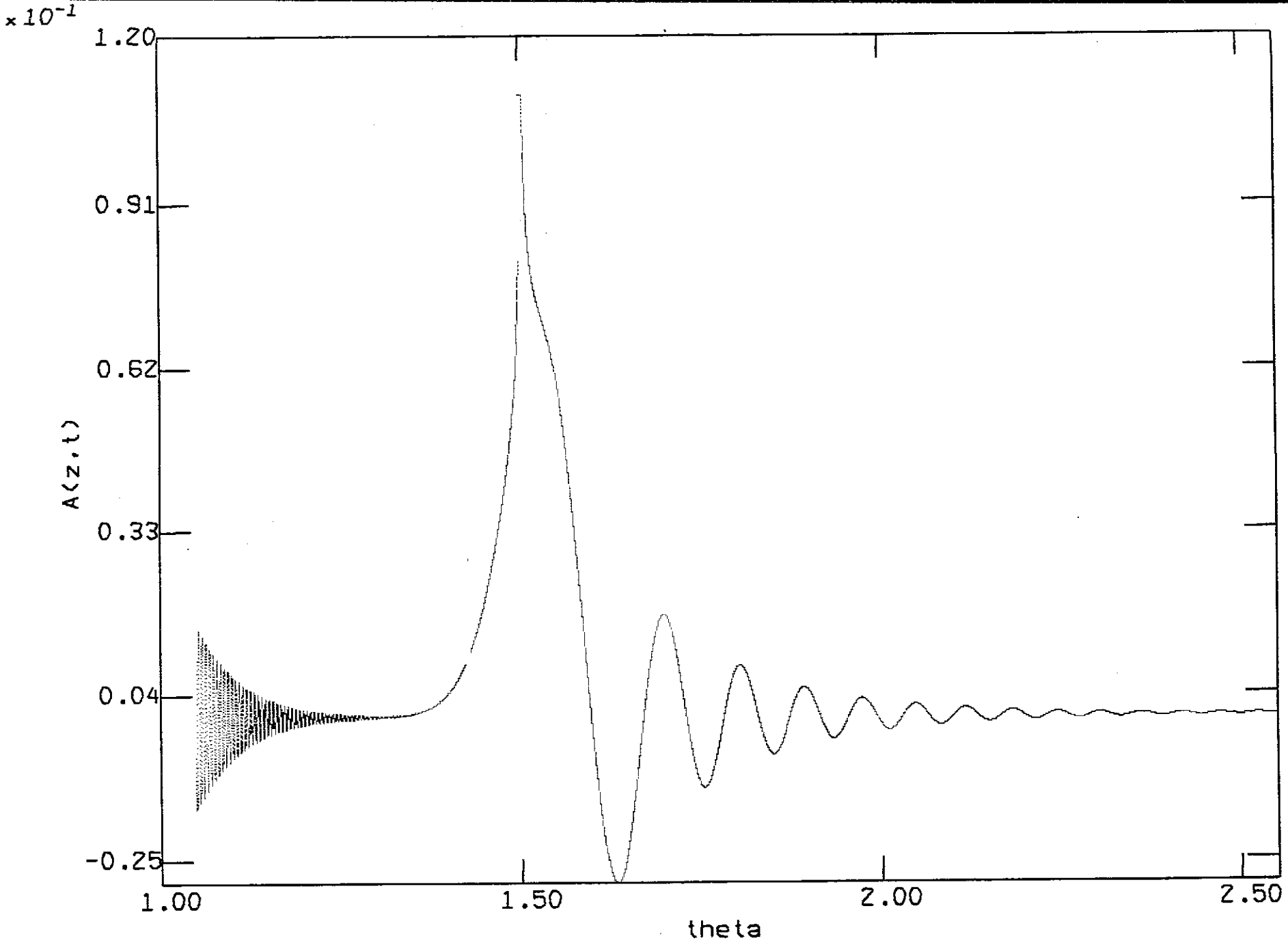

22:20:40
10-JUN-91

PRECURSORS FOR A MODIFIED SINE WAVE - B

FIG 2

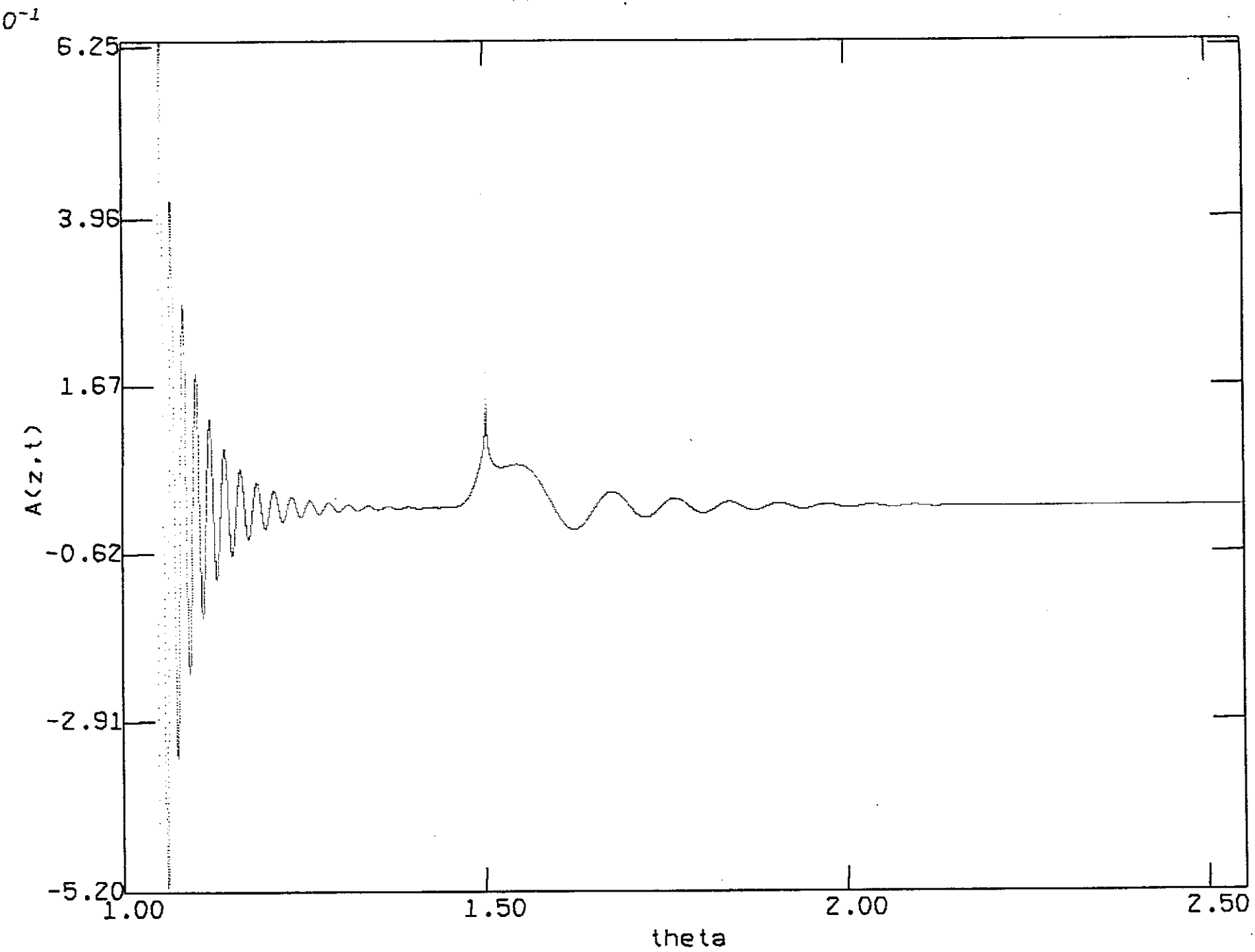

22:49:14
10 JUN-91

PRECURSORS FOR A MODIFIED SINE WAVE - 0

FIG 3

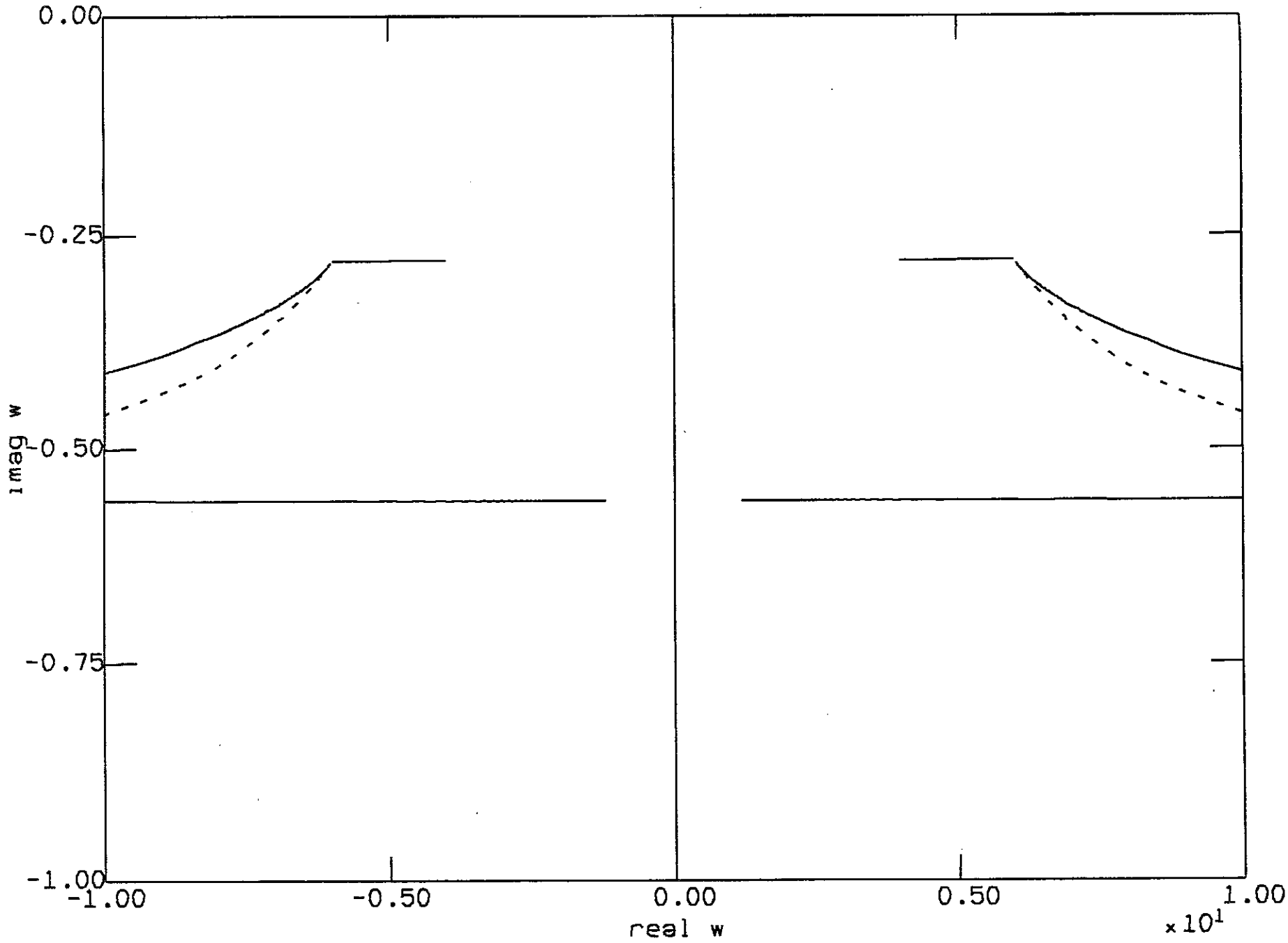

23:46:34
10-JUN-91

A COMPARISON OF THE SAD. PT. LOCATIONS

FIG 4

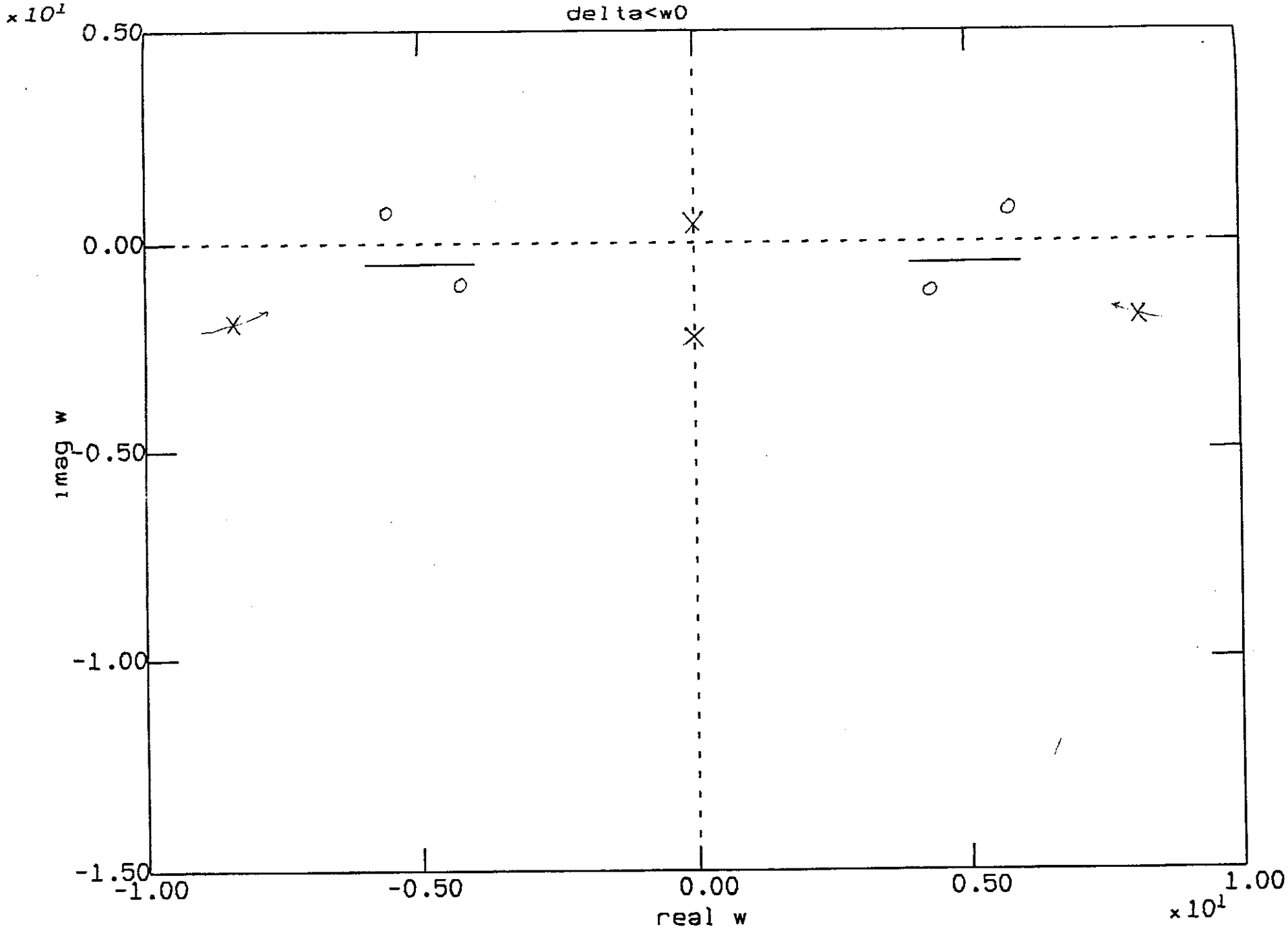

00:11:38
9-JUN-91

THE COMPLEX PLANE AS DELTA INCREASES

FIG 5

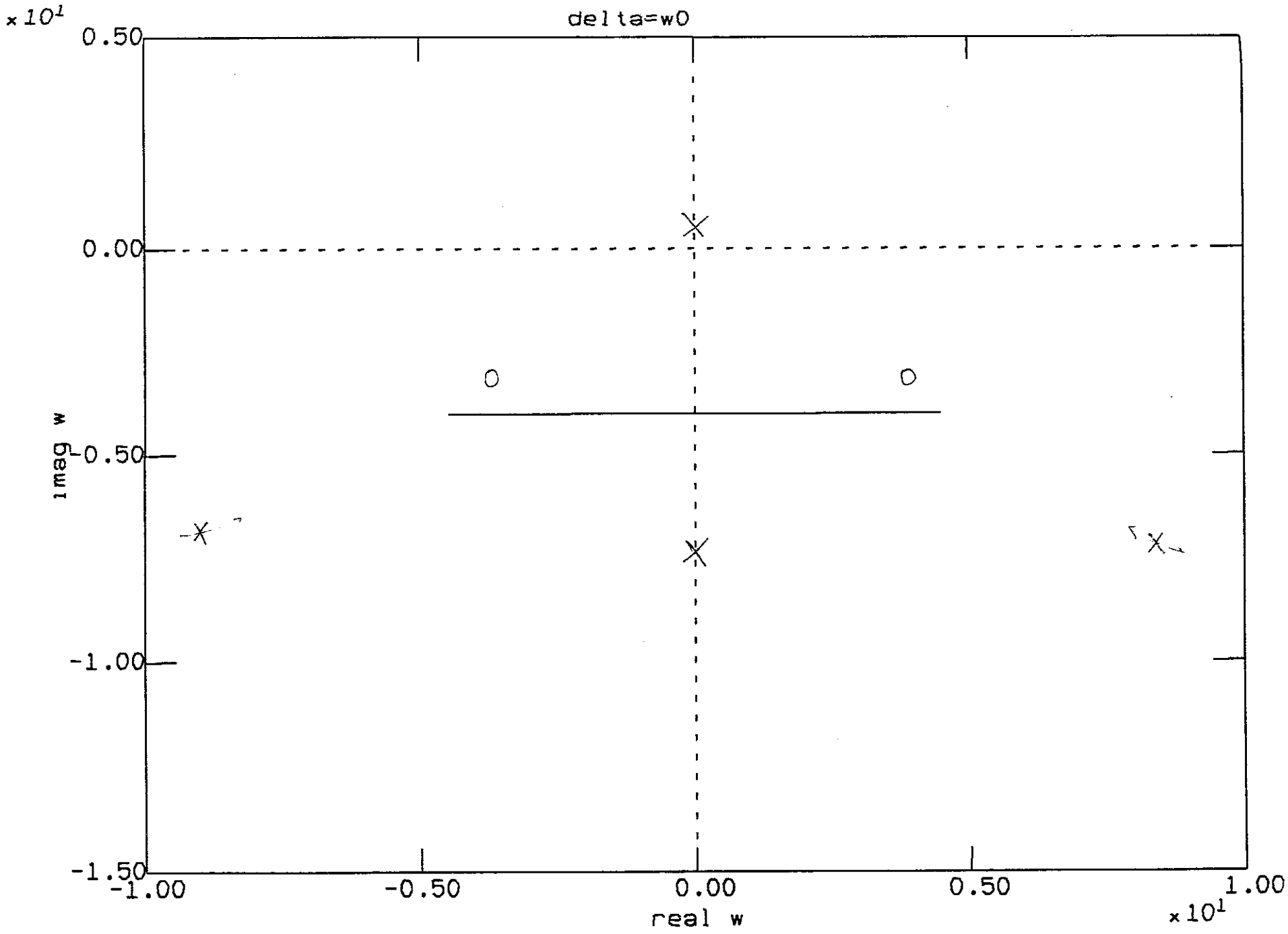

00:11:38
9-JUN-91

THE COMPLEX PLANE AS DELTA INCREASES

FIG 6

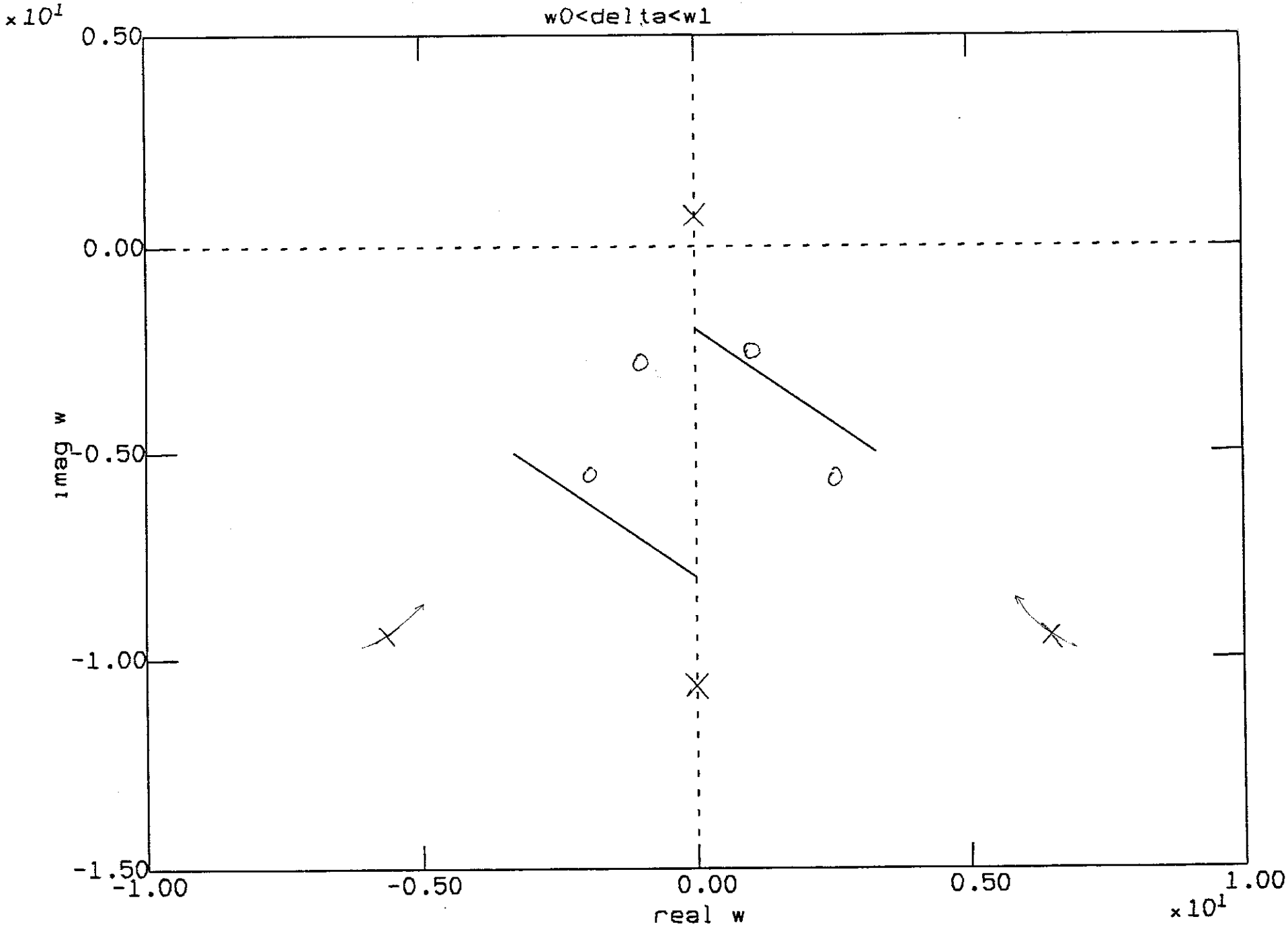

00:11:38
9-JUN-91

THE COMPLEX PLANE AS DELTA INCREASES

FIG 7

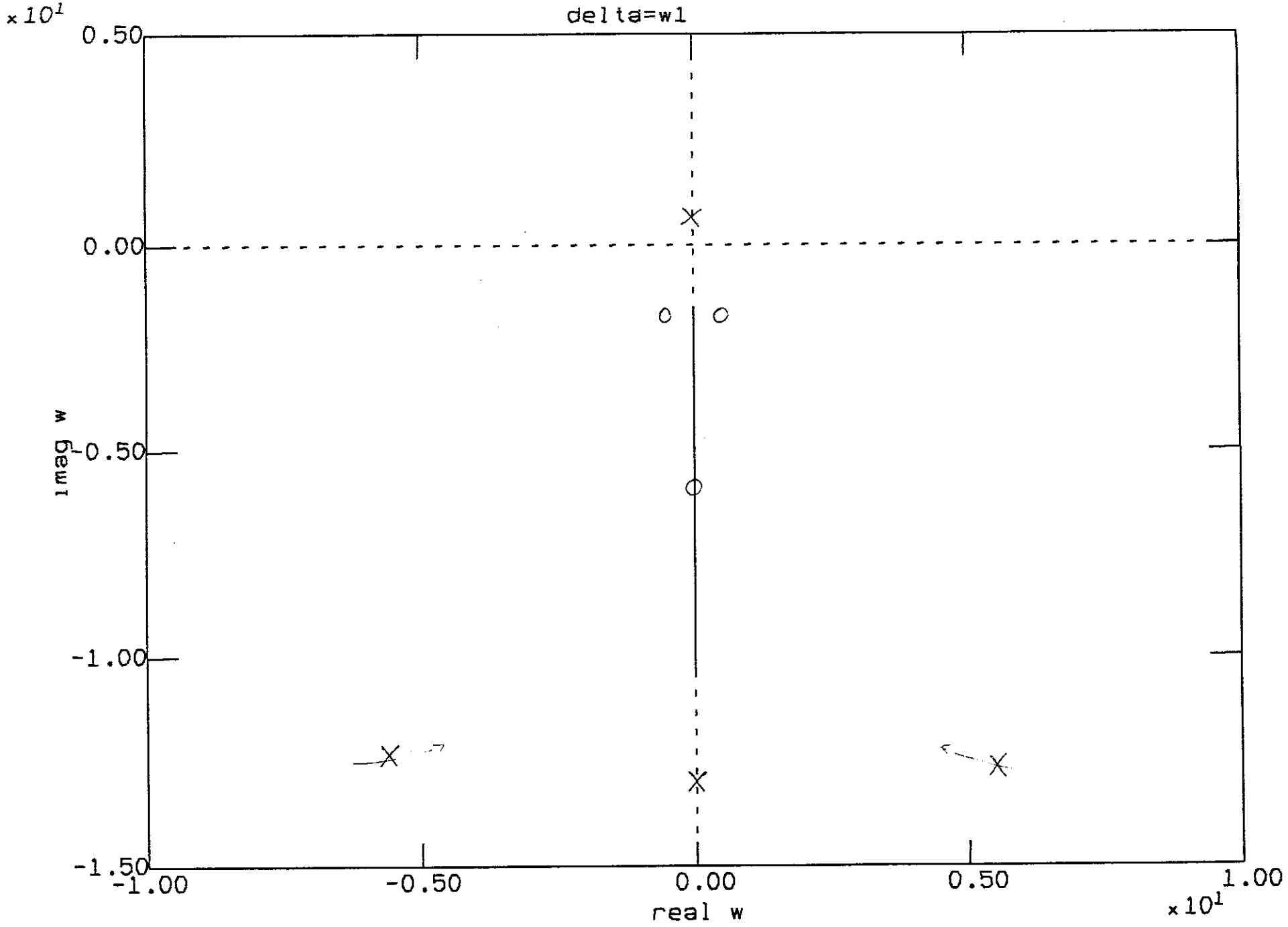

00:11:38
9-JUN-91

THE COMPLEX PLANE AS DELTA INCREASES

FIG 8

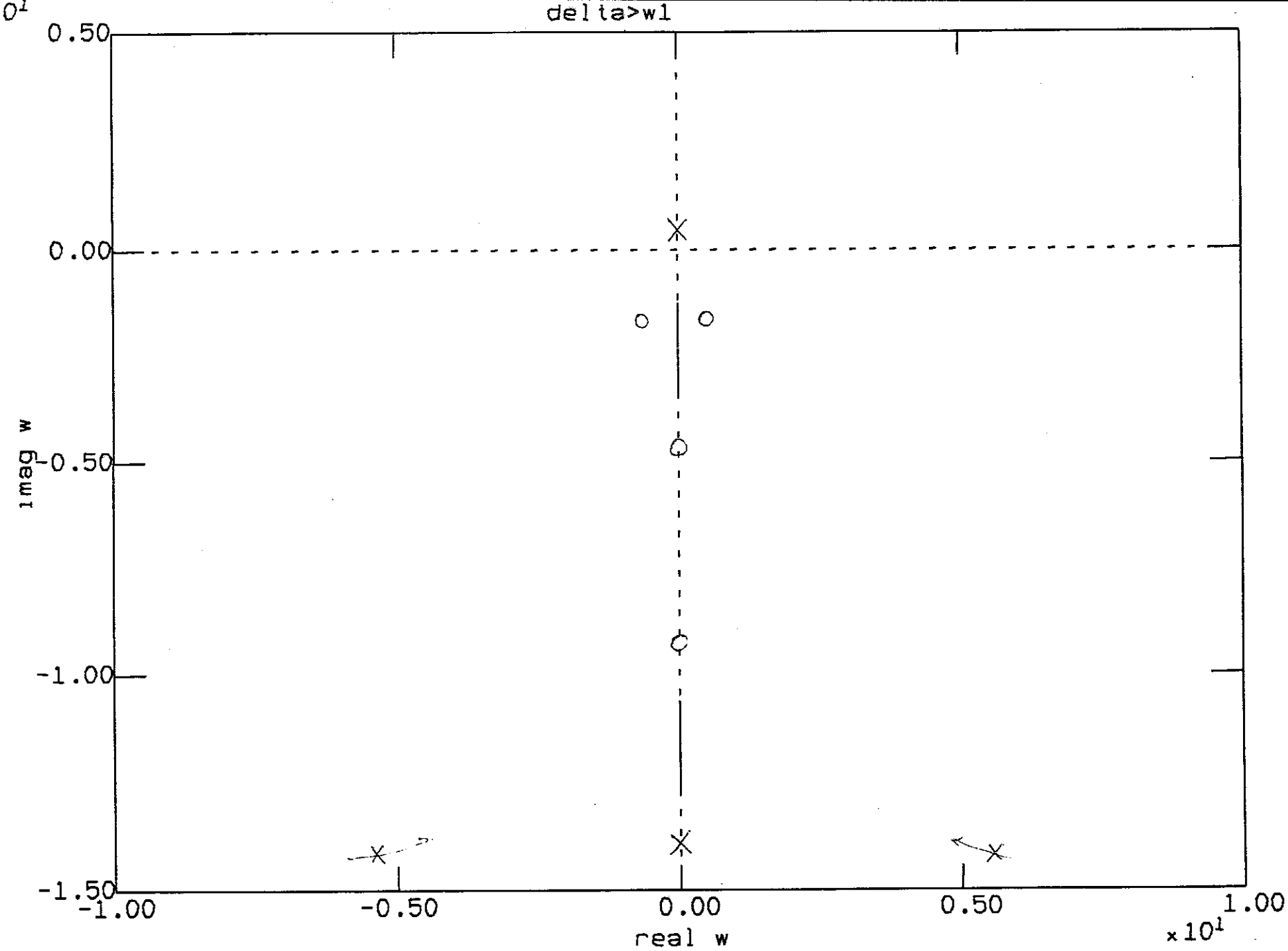

00:11:38
9-JUN-91

THE COMPLEX PLANE AS DELTA INCREASES

FIG 9

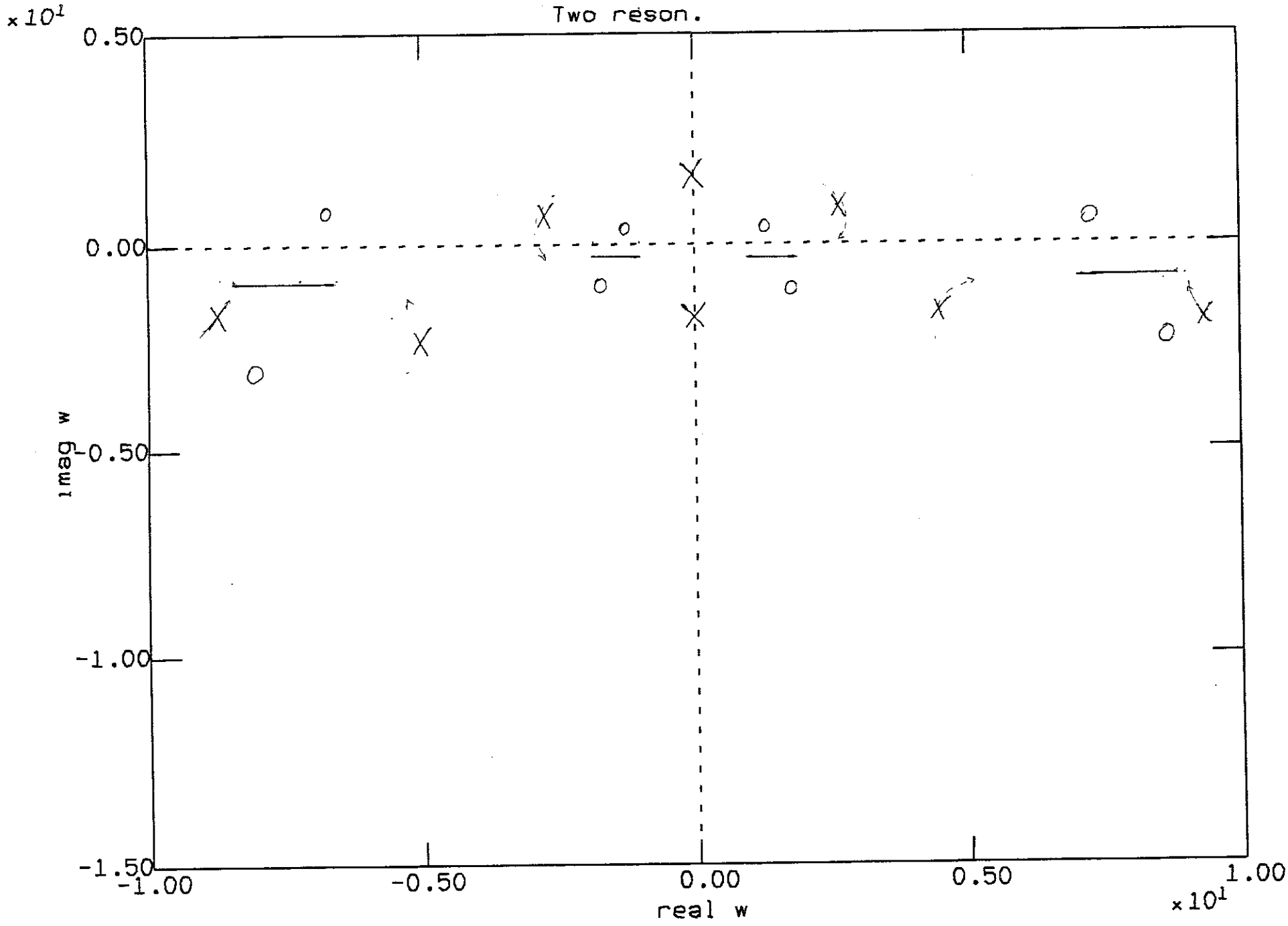

00:11:38
9-JUN-91

THE COMPLEX PLANE AS DELTA INCREASES

FIG 10

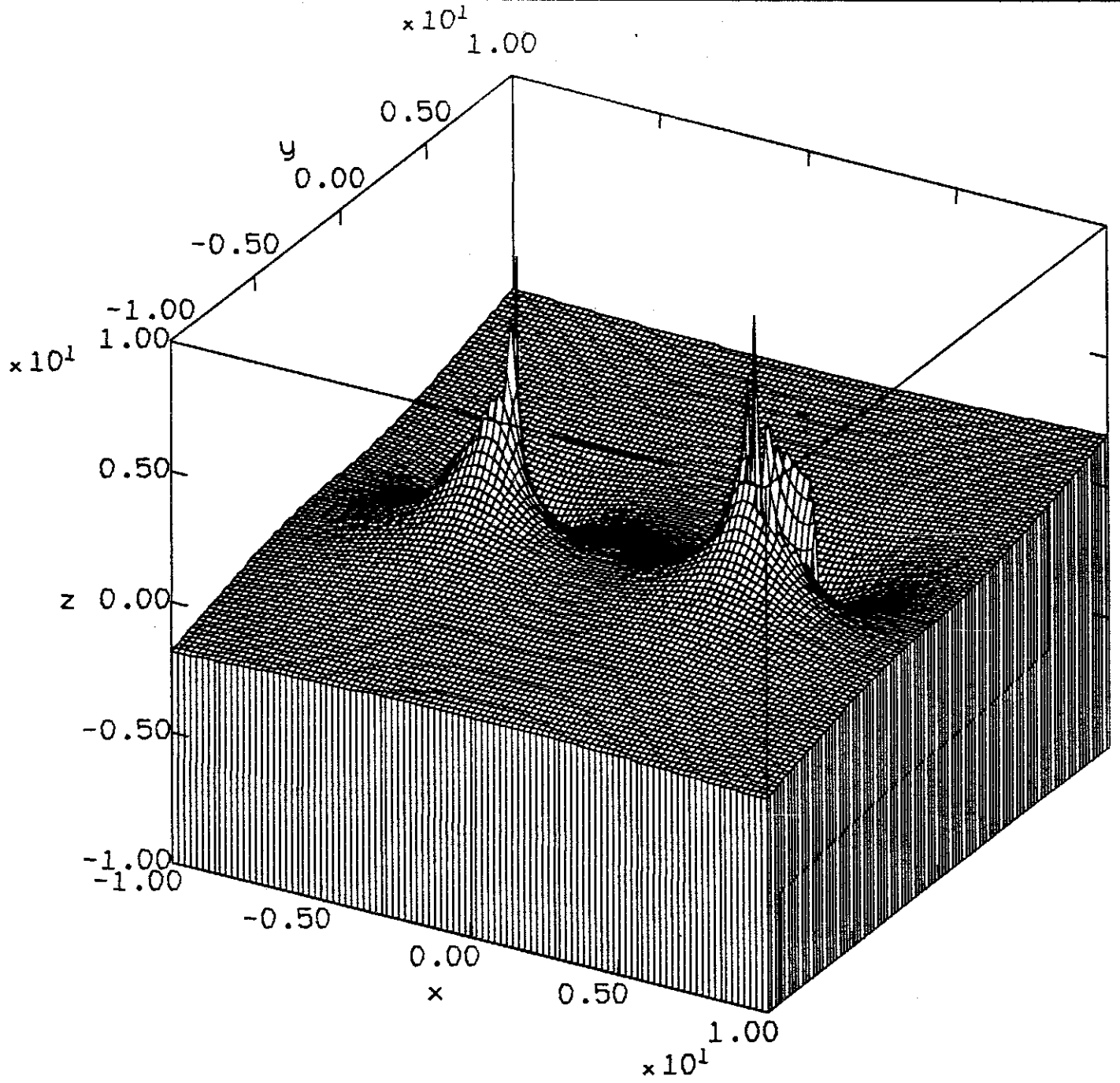

21:50:22
20-JUN-91

Real part of phi for a single resonance

FIG 11

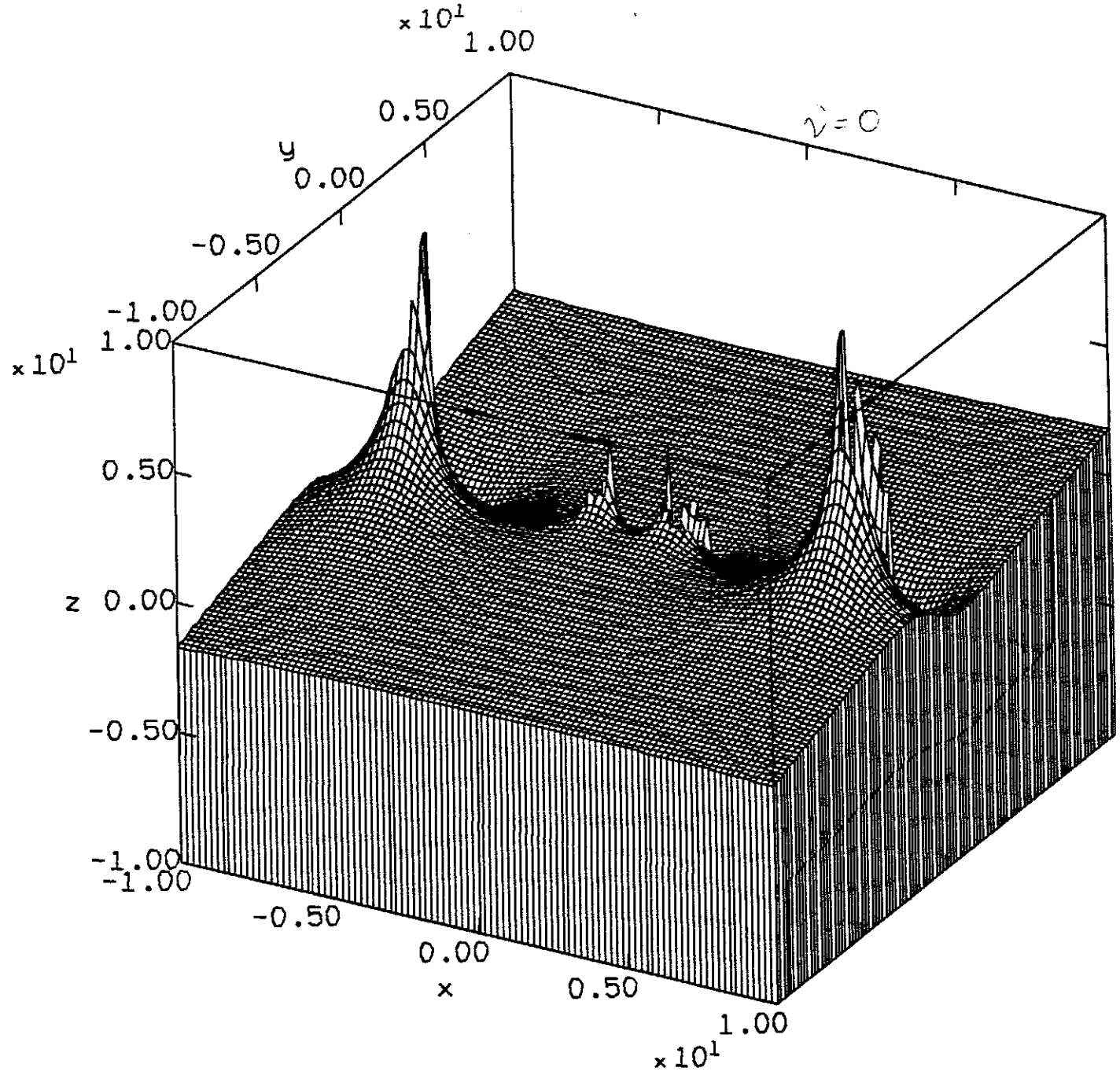

22:03:53
10-JUN-91

Real part of phi for a double resonance

FIG 12

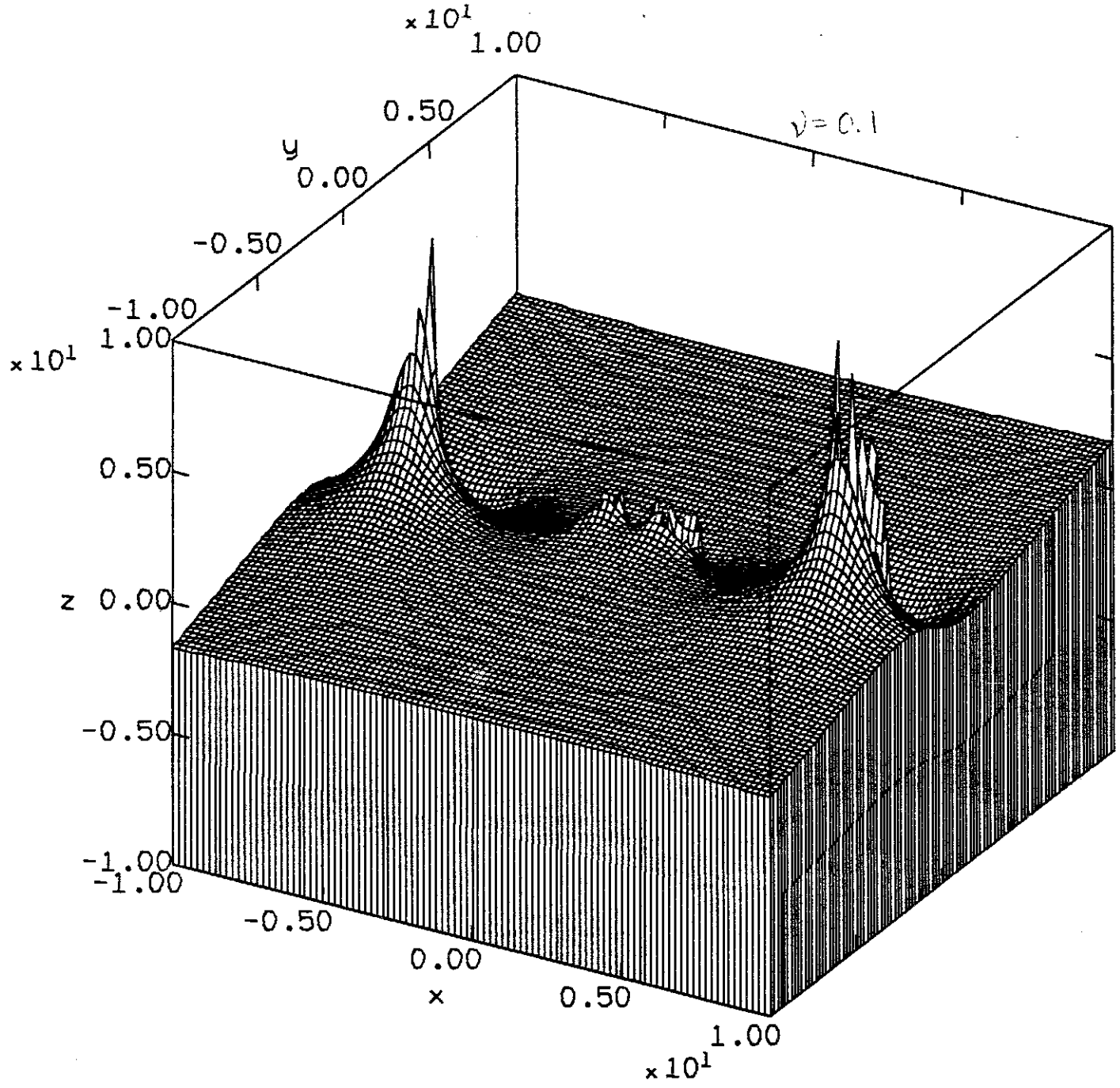

22:03:53
10-JUN-91

Real part of phi for a double resonance

FIG 13

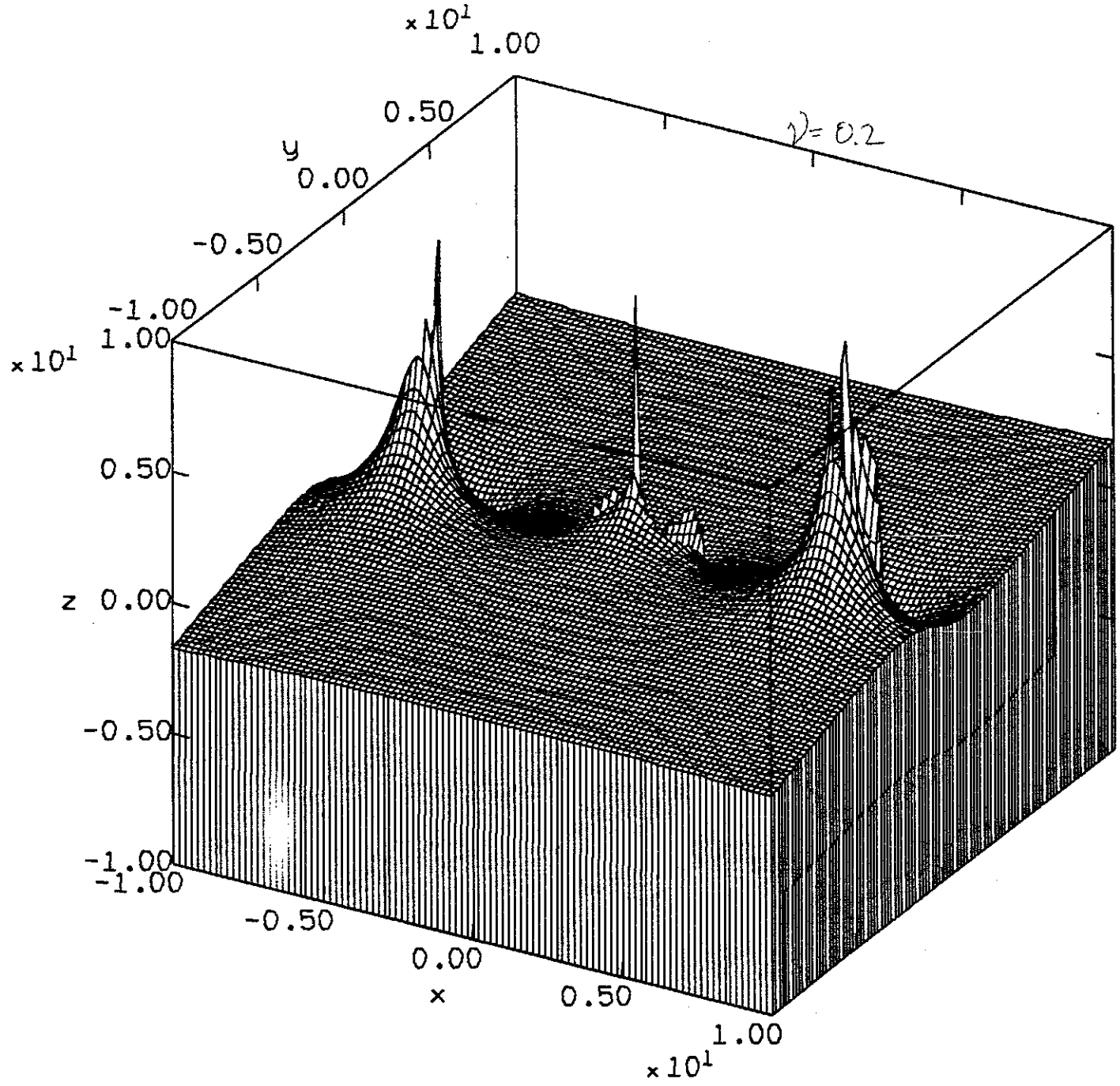

22:03:53
10-JUN-91

Real part of phi for a double resonance

FIG 14

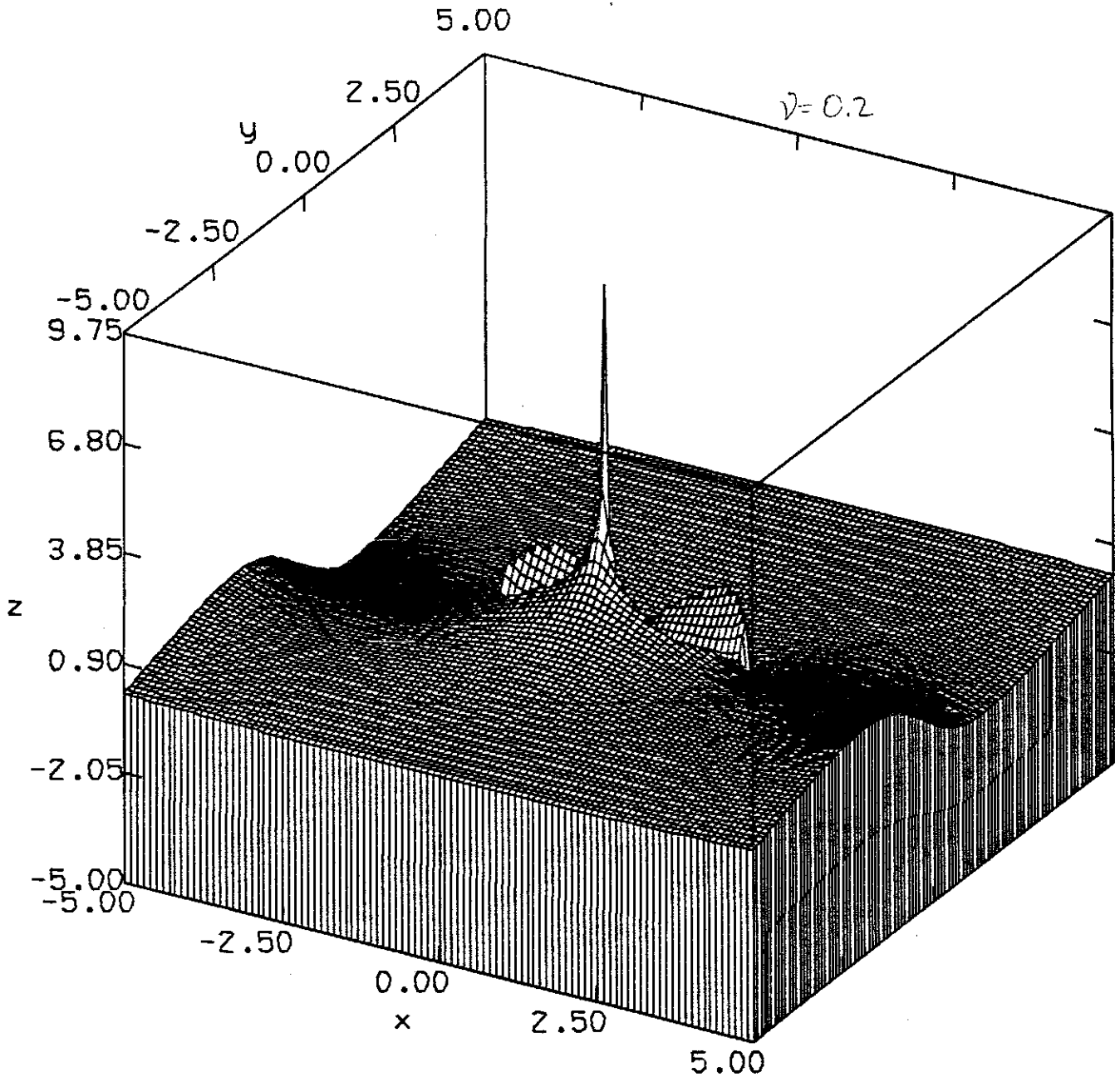

22:03:53
10-JUN-91

Real part of phi for a double resonance

FIG 15

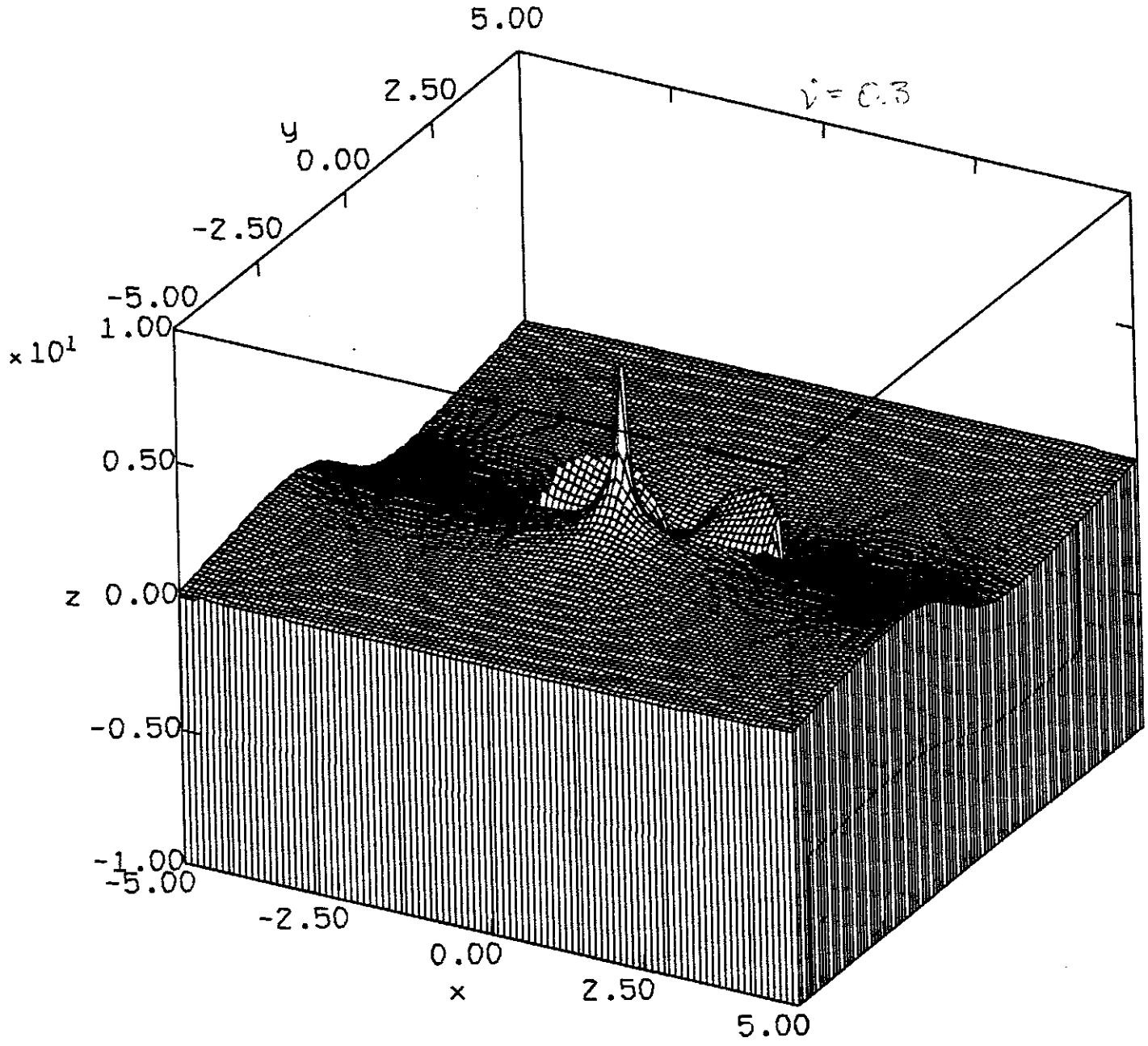

22:03:53
10-JUN-91

Real part of phi for a double resonance

FIG 16

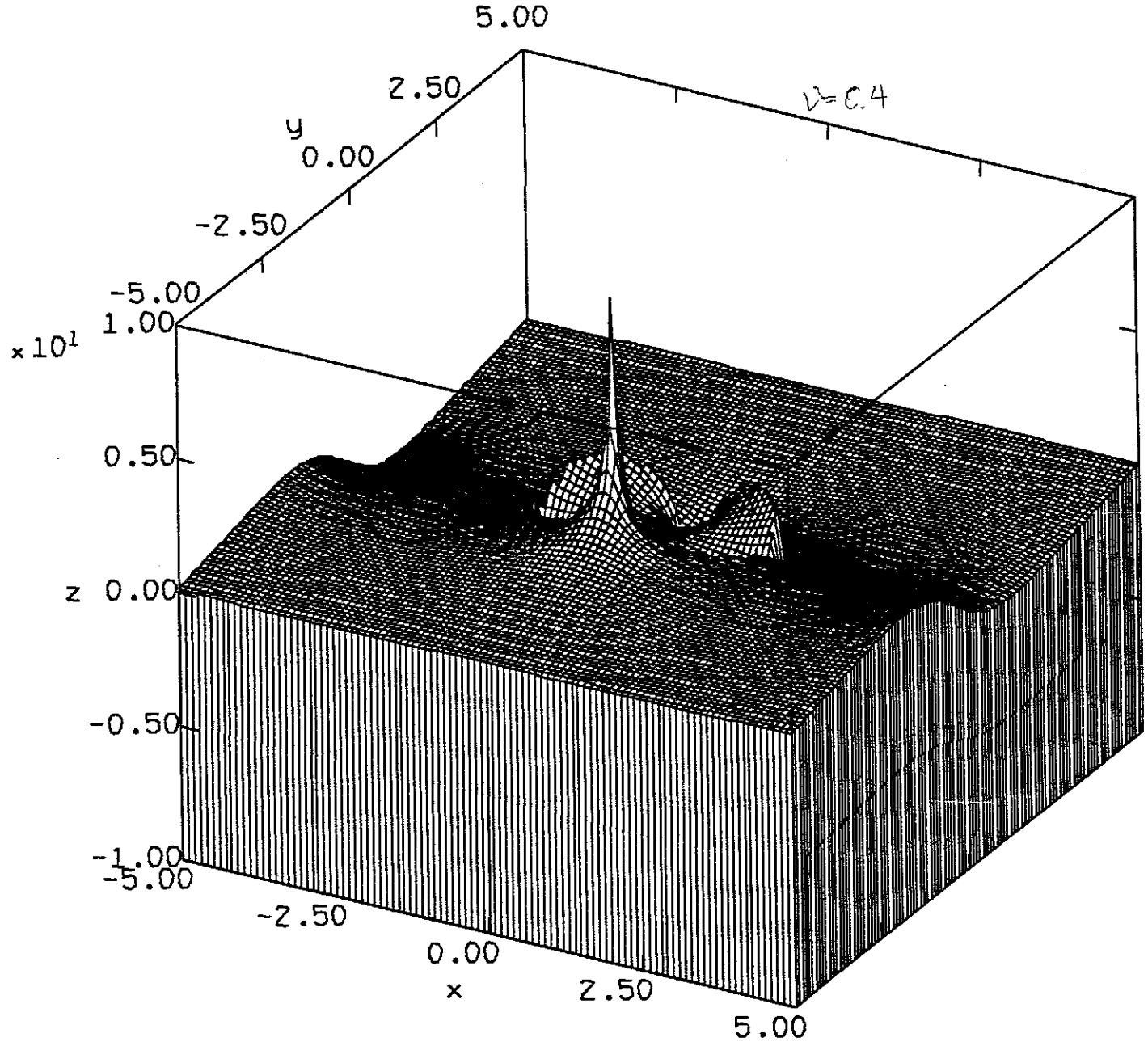

22:03:53
10-JUN-91

Real part of phi for a double resonance

FIG 17

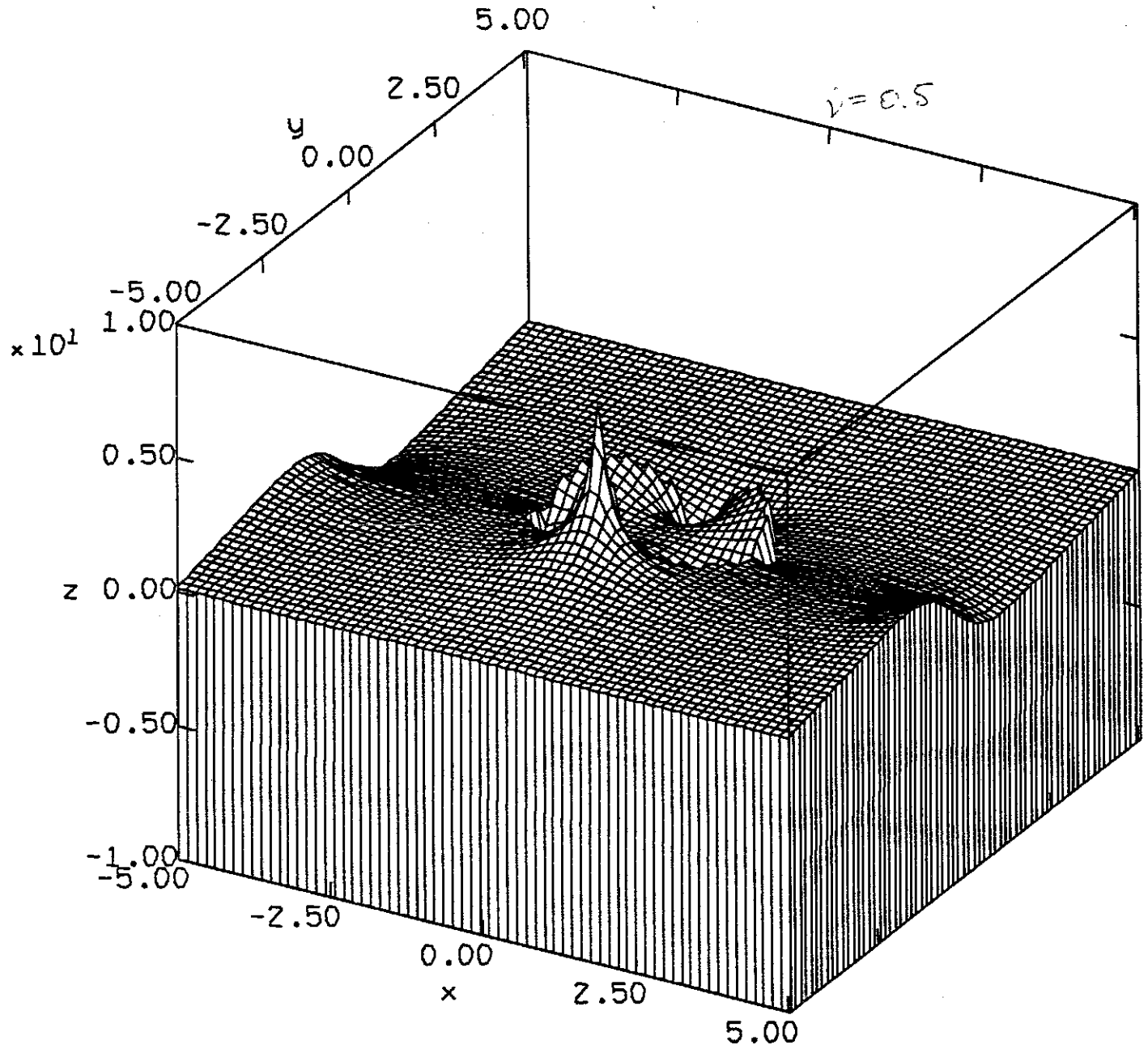

00:36:11
11-JUN-91

Real part of phi for a double resonance

FIG 18

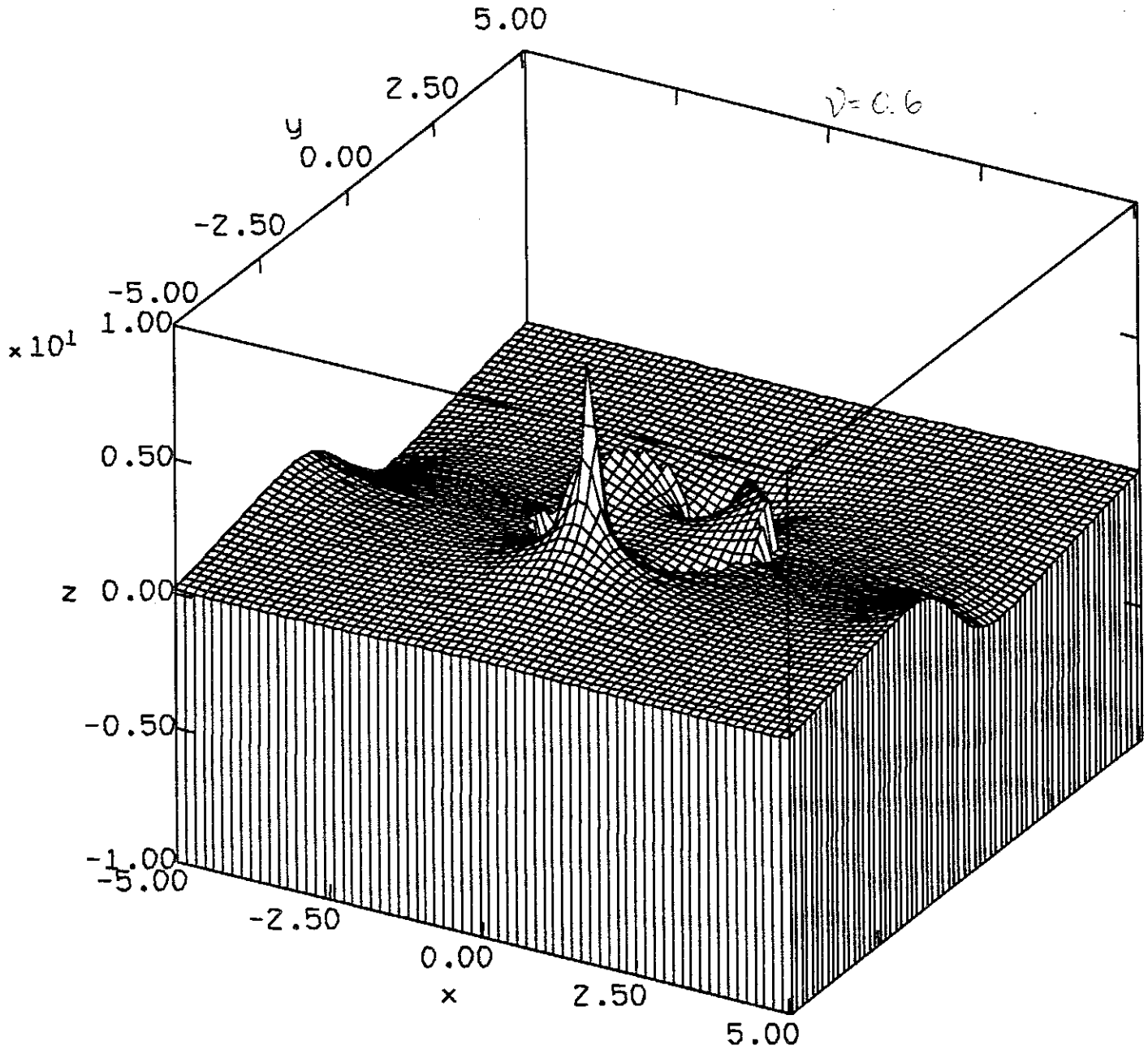

00:36:11
11-JUN-91

Real part of phi for a double resonance

FIG 19

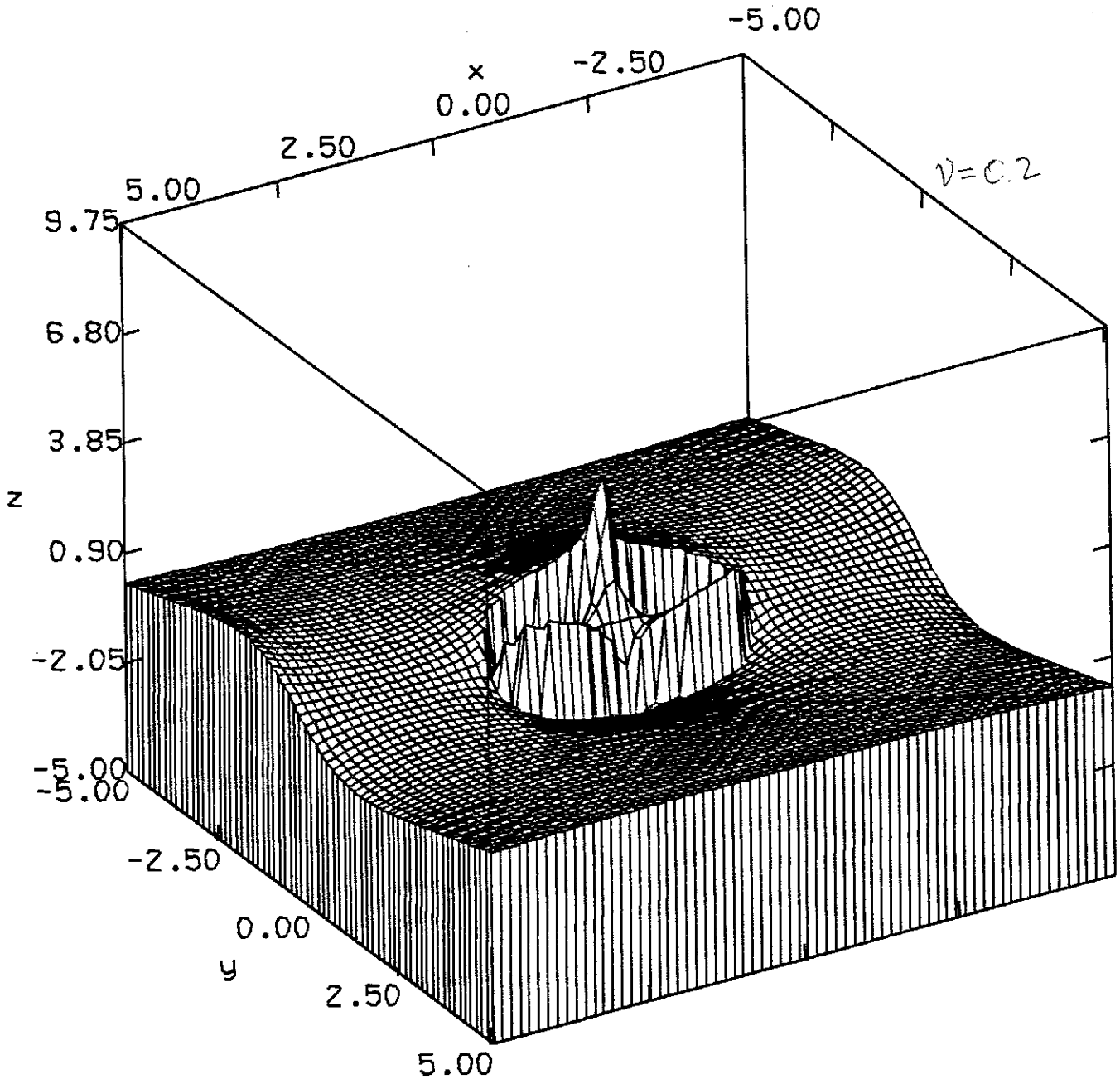

00:36:11
11-JUN-91

Real part of phi for a double resonance

FIG 20

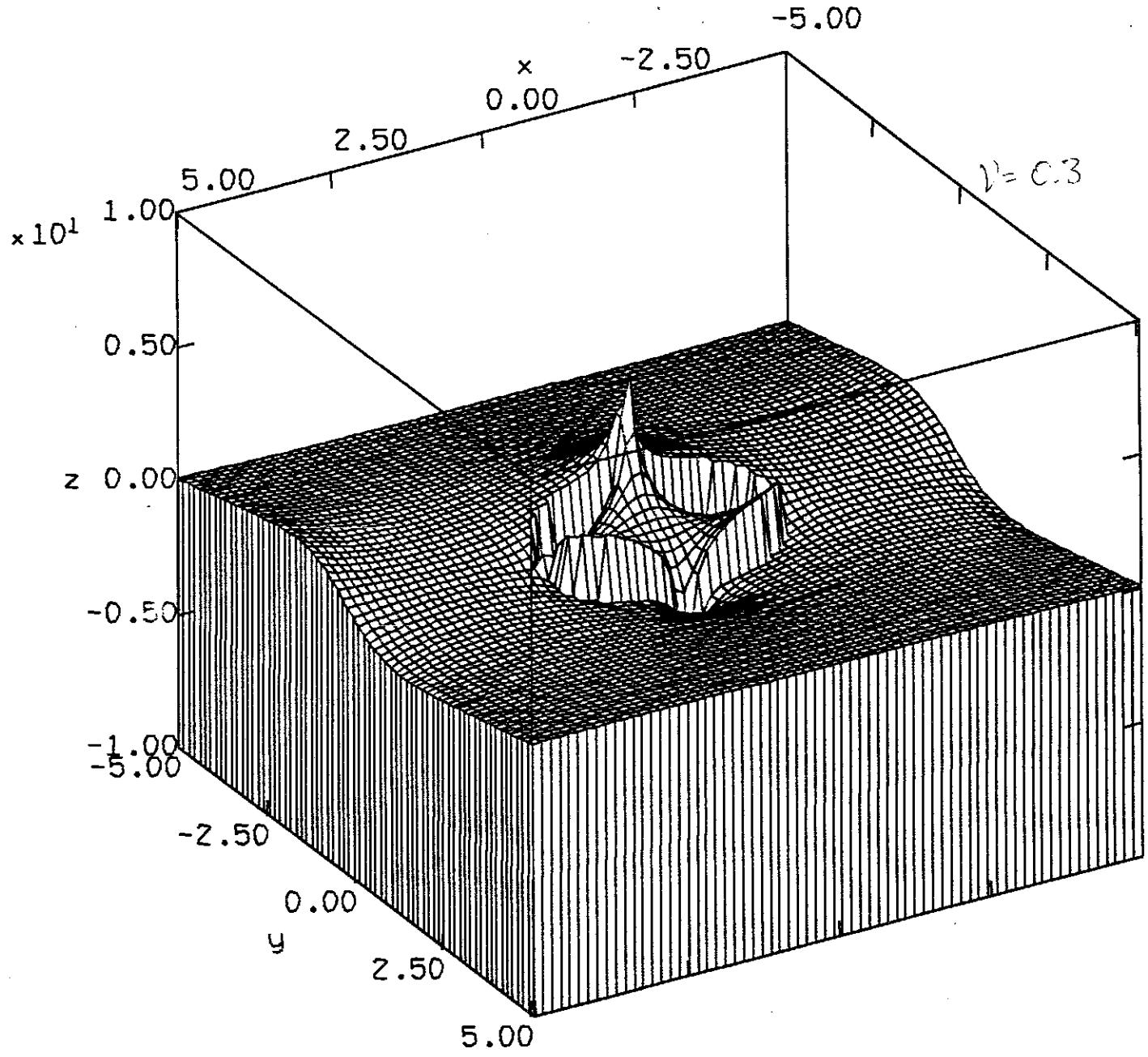

00:36:11
11-JUN-91

Real part of phi for a double resonance

FIG 21

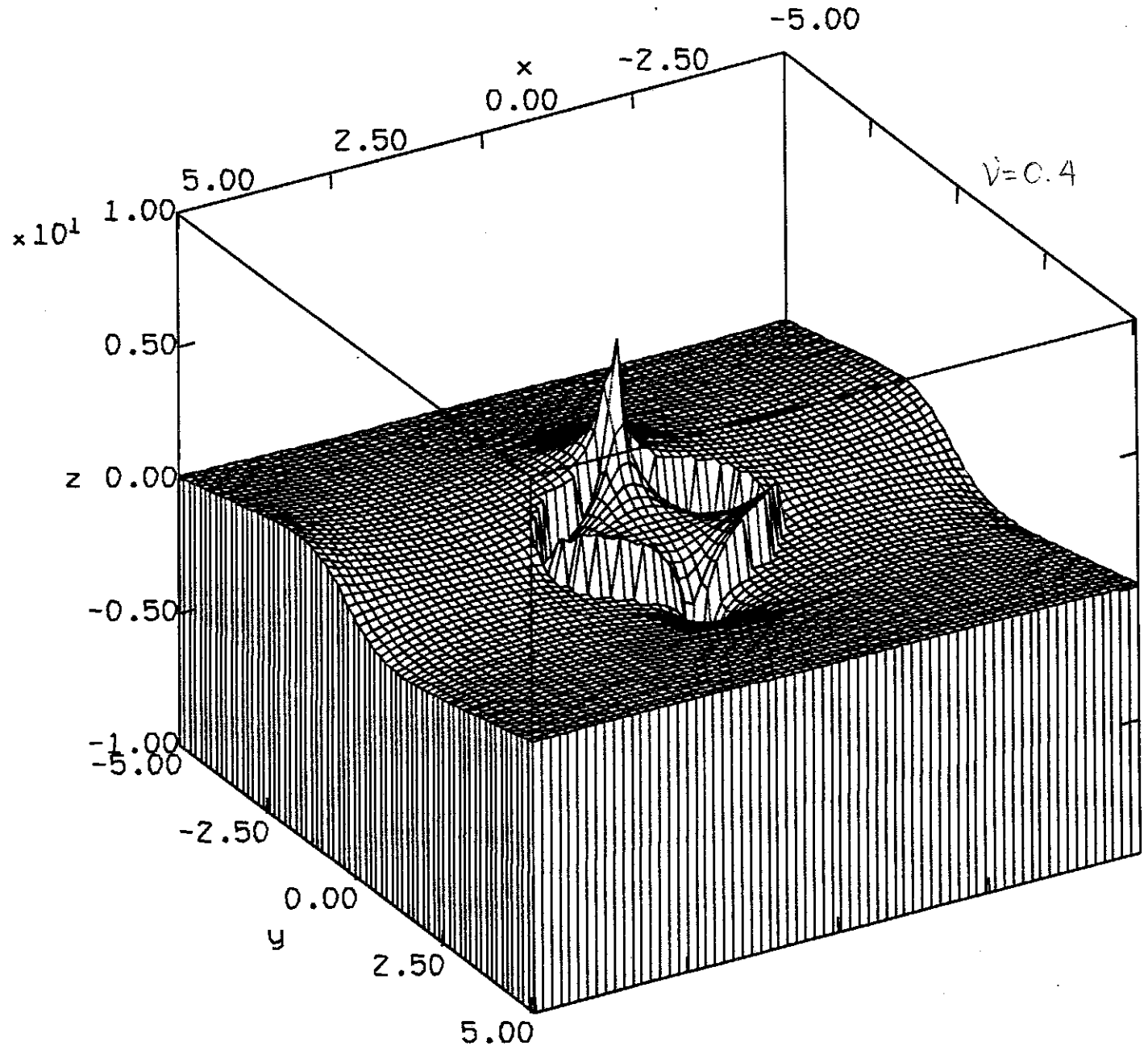

00:36:11
11-JUN-91

Real part of phi for a double resonance

FIG 22

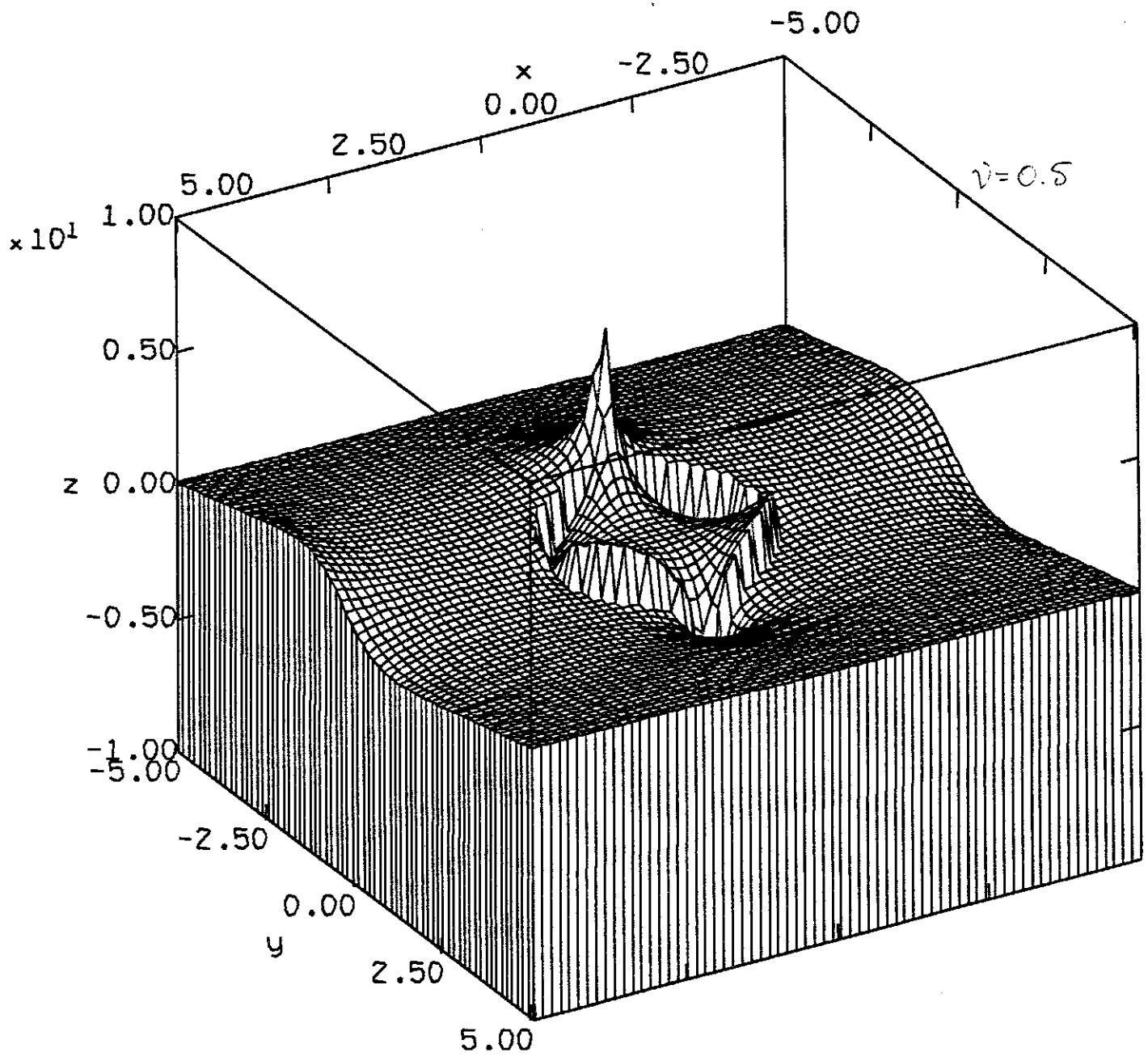

00:36:11
11-JUN-91

Real part of phi for a double resonance

FIG 23

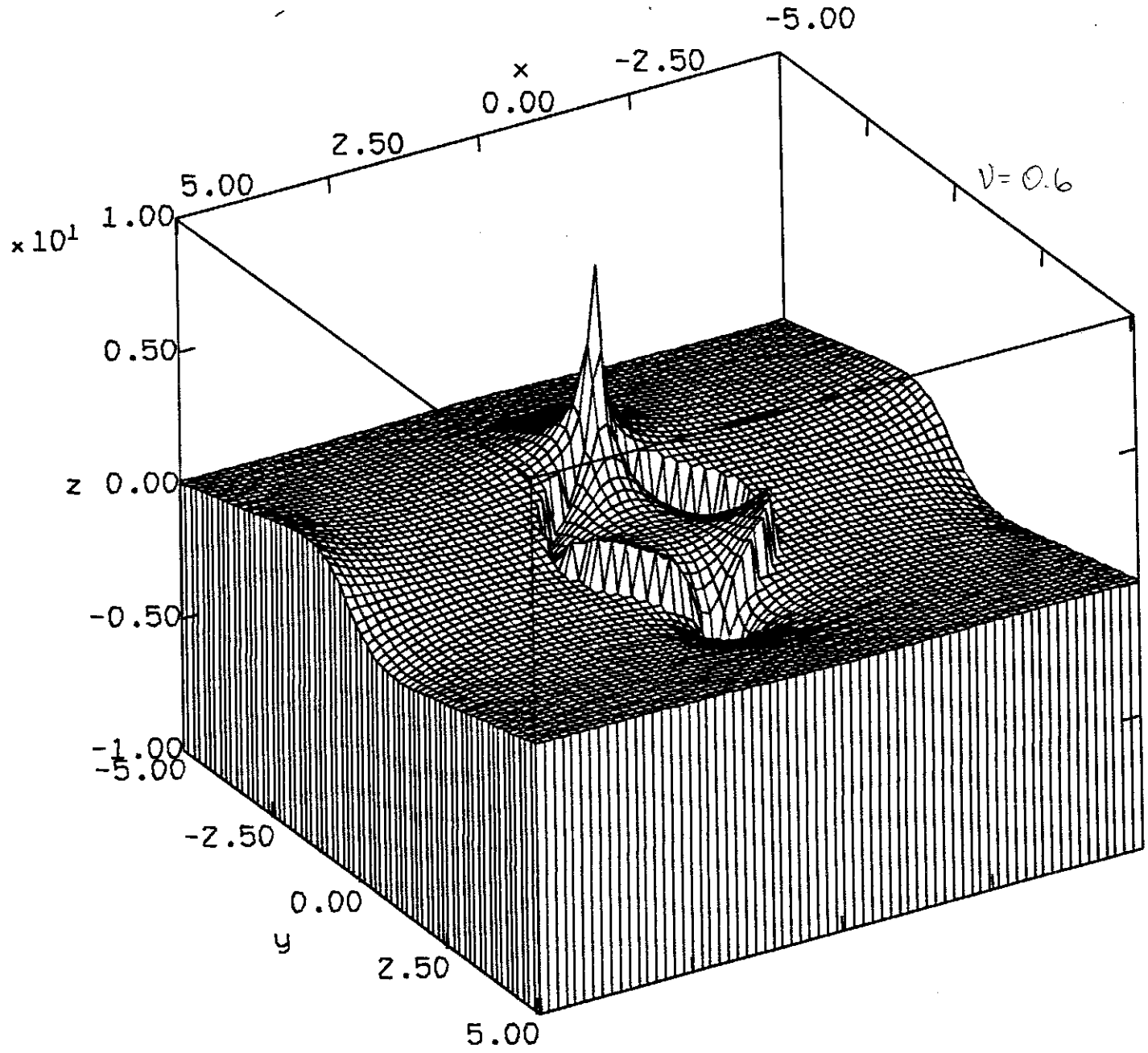

00:36:11
11-JUN-91

Real part of phi for a double resonance

FIG 24

C Tables

The following pages are tables which contain locations of the saddle points for increasing θ under various conditions. They also show the relative importance of these saddle points by giving the real and imaginary parts of the phase function at these saddle points. The calculations for single resonance media show differences in both the initial values and the increment of θ.

For double resonance media, we changed the value of ν and the initial values while keeping the increment in θ the same. It should be noted that we had difficulty in getting convergence for the middle saddle points for a double resonance medium for $\theta < 1.6$ so we started the tables at this value. This is actually not so terrible since the importance of these saddle points comes shortly after this θ value for the parameters we used.

Also, any asterisks indicate that we had a problem with convergence. This happened in particular for certain θ values for the near saddle points as they coalesced. This is discussed in the text.

TABLE 1:

The distant saddle point in the right half of the plane for a single resonance medium.

initial x = 40.00
initial y = -0.10

theta	x-value	y-value	Re phi	Im phi
1.05	16.03171	-0.48565	-0.02587	-1.48110
1.10	12.38877	-0.44927	-0.04916	-2.17518
1.15	10.84923	-0.42659	-0.07102	-2.75201
1.20	9.96039	-0.41066	-0.09193	-3.27055
1.25	9.36848	-0.39865	-0.11215	-3.75290
1.30	8.94024	-0.38917	-0.13183	-4.21010
1.35	8.61309	-0.38141	-0.15109	-4.64859
1.40	8.35340	-0.37491	-0.17000	-5.07252
1.45	8.14128	-0.36934	-0.18860	-5.48472
1.50	7.96413	-0.36449	-0.20694	-5.88723
1.55	7.81358	-0.36022	-0.22506	-6.28158
1.60	7.68379	-0.35642	-0.24297	-6.66893
1.65	7.57055	-0.35300	-0.26071	-7.05023
1.70	7.47077	-0.34990	-0.27828	-7.42621
1.75	7.38208	-0.34707	-0.29570	-7.79749
1.80	7.30268	-0.34447	-0.31299	-8.16458
1.85	7.23112	-0.34208	-0.33015	-8.52789
1.90	7.16627	-0.33986	-0.34720	-8.88780
1.95	7.10721	-0.33779	-0.36414	-9.24462
2.00	7.05317	-0.33586	-0.38098	-9.59861
2.05	7.00353	-0.33405	-0.39773	-9.95001
2.10	6.95776	-0.33235	-0.41439	-10.29902
2.15	6.91543	-0.33075	-0.43097	-10.64584
2.20	6.87616	-0.32924	-0.44747	-10.99062
2.25	6.83962	-0.32780	-0.46389	-11.33350
2.30	6.80554	-0.32644	-0.48025	-11.67462
2.35	6.77369	-0.32515	-0.49654	-12.01409
2.40	6.74385	-0.32392	-0.51276	-12.35202
2.45	6.71583	-0.32274	-0.52893	-12.68851
2.50	6.68949	-0.32162	-0.54504	-13.02363
2.55	6.66467	-0.32055	-0.56109	-13.35748
2.60	6.64125	-0.31952	-0.57709	-13.69012
2.65	6.61912	-0.31854	-0.59304	-14.02163
2.70	6.59818	-0.31760	-0.60895	-14.35205
2.75	6.57833	-0.31669	-0.62481	-14.68146
2.80	6.55950	-0.31582	-0.64062	-15.00990
2.85	6.54161	-0.31498	-0.65639	-15.33743
2.90	6.52460	-0.31417	-0.67212	-15.66408
2.95	6.50840	-0.31338	-0.68780	-15.98990
3.00	6.49297	-0.31263	-0.70346	-16.31493
3.05	6.47824	-0.31190	-0.71907	-16.63921
3.10	6.46419	-0.31120	-0.73465	-16.96276
3.15	6.45075	-0.31053	-0.75019	-17.28563
3.20	6.43790	-0.30987	-0.76570	-17.60785
3.25	6.42561	-0.30924	-0.78118	-17.92943
3.30	6.41383	-0.30863	-0.79663	-18.25042
3.35	6.40253	-0.30803	-0.81204	-18.57082
3.40	6.39170	-0.30746	-0.82743	-18.89068
3.45	6.38130	-0.30690	-0.84279	-19.21000
3.50	6.37131	-0.30636	-0.85812	-19.52881

TABLE 1:
The distant saddle point in the right half of the plane for a single resonance medium.

initial x = 40.00
initial y = -0.10

theta	x-value	y-value	Re phi	Im phi
1.05	16.03171	-0.48565	-0.02587	-1.48110
1.10	12.38877	-0.44927	-0.04916	-2.17518
1.15	10.84923	-0.42659	-0.07102	-2.75201
1.20	9.96039	-0.41066	-0.09193	-3.27055
1.25	9.36848	-0.39865	-0.11215	-3.75290
1.30	8.94024	-0.38917	-0.13183	-4.21010
1.35	8.61309	-0.38141	-0.15109	-4.64859
1.40	8.35340	-0.37491	-0.17000	-5.07252
1.45	8.14128	-0.36934	-0.18860	-5.48472
1.50	7.96413	-0.36449	-0.20694	-5.88723
1.55	7.81358	-0.36022	-0.22506	-6.28158
1.60	7.68379	-0.35642	-0.24297	-6.66893
1.65	7.57055	-0.35300	-0.26071	-7.05023
1.70	7.47077	-0.34990	-0.27828	-7.42621
1.75	7.38208	-0.34707	-0.29570	-7.79749
1.80	7.30268	-0.34447	-0.31299	-8.16458
1.85	7.23112	-0.34208	-0.33015	-8.52789
1.90	7.16627	-0.33986	-0.34720	-8.88780
1.95	7.10721	-0.33779	-0.36414	-9.24462
2.00	7.05317	-0.33586	-0.38098	-9.59861
2.05	7.00353	-0.33405	-0.39773	-9.95001
2.10	6.95776	-0.33235	-0.41439	-10.29902
2.15	6.91543	-0.33075	-0.43097	-10.64584
2.20	6.87616	-0.32924	-0.44747	-10.99062
2.25	6.83962	-0.32780	-0.46389	-11.33350
2.30	6.80554	-0.32644	-0.48025	-11.67462
2.35	6.77369	-0.32515	-0.49654	-12.01409
2.40	6.74385	-0.32392	-0.51276	-12.35202
2.45	6.71583	-0.32274	-0.52893	-12.68851
2.50	6.68949	-0.32162	-0.54504	-13.02363
2.55	6.66467	-0.32055	-0.56109	-13.35748
2.60	6.64125	-0.31952	-0.57709	-13.69012
2.65	6.61912	-0.31854	-0.59304	-14.02163
2.70	6.59818	-0.31760	-0.60895	-14.35205
2.75	6.57833	-0.31669	-0.62481	-14.68146
2.80	6.55950	-0.31582	-0.64062	-15.00990
2.85	6.54161	-0.31498	-0.65639	-15.33743
2.90	6.52460	-0.31417	-0.67212	-15.66408
2.95	6.50840	-0.31338	-0.68780	-15.98990
3.00	6.49297	-0.31263	-0.70346	-16.31493
3.05	6.47824	-0.31190	-0.71907	-16.63921
3.10	6.46419	-0.31120	-0.73465	-16.96276
3.15	6.45075	-0.31053	-0.75019	-17.28563
3.20	6.43790	-0.30987	-0.76570	-17.60785
3.25	6.42561	-0.30924	-0.78118	-17.92943
3.30	6.41383	-0.30863	-0.79663	-18.25042
3.35	6.40253	-0.30803	-0.81204	-18.57082
3.40	6.39170	-0.30746	-0.82743	-18.89068
3.45	6.38130	-0.30690	-0.84279	-19.21000
3.50	6.37131	-0.30636	-0.85812	-19.52881

TABLE 2:

The distant saddle point in the left half of the plane for a single resonance medium.

initial x =-30.00
initial y = -4.00

theta	x-value	y-value	Re phi	Im phi
1.02	-23.66715	-0.52205	-0.01079	0.91236
1.04	-17.54819	-0.49598	-0.02096	1.31364
1.06	-14.92805	-0.47662	-0.03068	1.63564
1.08	-13.40601	-0.46151	-0.04005	1.91783
1.10	-12.38877	-0.44927	-0.04916	2.17518
1.12	-11.65087	-0.43909	-0.05804	2.41522
1.14	-11.08590	-0.43044	-0.06673	2.64235
1.16	-10.63643	-0.42297	-0.07526	2.85942
1.18	-10.26844	-0.41644	-0.08366	3.06835
1.20	-9.96039	-0.41066	-0.09193	3.27055
1.22	-9.69790	-0.40549	-0.10009	3.46707
1.24	-9.47095	-0.40083	-0.10815	3.65871
1.26	-9.27236	-0.39659	-0.11612	3.84610
1.28	-9.09680	-0.39273	-0.12402	4.02975
1.30	-8.94024	-0.38918	-0.13183	4.21010
1.32	-8.79955	-0.38590	-0.13958	4.38747
1.34	-8.67231	-0.38286	-0.14727	4.56217
1.36	-8.55654	-0.38003	-0.15490	4.73444
1.38	-8.45067	-0.37739	-0.16247	4.90450
1.40	-8.35340	-0.37491	-0.17000	5.07252
1.42	-8.26367	-0.37258	-0.17747	5.23868
1.44	-8.18057	-0.37039	-0.18490	5.40311
1.46	-8.10336	-0.36832	-0.19229	5.56594
1.48	-8.03140	-0.36636	-0.19963	5.72728
1.50	-7.96413	-0.36450	-0.20694	5.88723
1.52	-7.90109	-0.36273	-0.21421	6.04588
1.54	-7.84188	-0.36104	-0.22145	6.20330
1.56	-7.78612	-0.35943	-0.22866	6.35957
1.58	-7.73352	-0.35789	-0.23583	6.51477
1.60	-7.68379	-0.35642	-0.24297	6.66893
1.62	-7.63670	-0.35501	-0.25009	6.82213
1.64	-7.59204	-0.35366	-0.25717	6.97442
1.66	-7.54961	-0.35236	-0.26423	7.12583
1.68	-7.50923	-0.35111	-0.27127	7.27642
1.70	-7.47077	-0.34990	-0.27828	7.42621
1.72	-7.43408	-0.34874	-0.28526	7.57526
1.74	-7.39903	-0.34762	-0.29223	7.72359
1.76	-7.36551	-0.34653	-0.29917	7.87123
1.78	-7.33343	-0.34549	-0.30609	8.01822
1.80	-7.30268	-0.34447	-0.31299	8.16457
1.82	-7.27318	-0.34349	-0.31987	8.31033
1.84	-7.24486	-0.34254	-0.32673	8.45551
1.86	-7.21765	-0.34162	-0.33357	8.60013
1.88	-7.19147	-0.34073	-0.34039	8.74422
1.90	-7.16628	-0.33986	-0.34720	8.88780
1.92	-7.14200	-0.33901	-0.35399	9.03088
1.94	-7.11860	-0.33819	-0.36076	9.17348
1.96	-7.09602	-0.33740	-0.36752	9.31563
1.98	-7.07423	-0.33662	-0.37426	9.45733
2.00	-7.05317	-0.33586	-0.38098	9.59860

TABLE 3:

The "upper" near saddle point for a single resonance medium.

initial x = -0.05
initial y = 4.00

theta	x-value	y-value	Re phi	Im phi
1.05	0.00000	3.67312	-0.83841	0.00000
1.10	0.00000	3.12691	-0.66906	0.00000
1.15	0.00000	2.69509	-0.52385	0.00000
1.20	0.00000	2.32577	-0.39852	0.00000
1.25	0.00000	1.99233	-0.29068	0.00000
1.30	0.00000	1.67736	-0.19899	0.00000
1.35	0.00000	1.36594	-0.12289	0.00000
1.40	0.00000	1.03972	-0.06263	0.00000
*				
*				
1.55	0.75420	-0.19057	-0.00909	-0.02401
1.60	1.05429	-0.19414	-0.01871	-0.06977
1.65	1.26614	-0.19732	-0.02850	-0.12802
1.70	1.43221	-0.20019	-0.03844	-0.19563
1.75	1.56909	-0.20279	-0.04851	-0.27076
1.80	1.68538	-0.20517	-0.05871	-0.35220
1.85	1.78625	-0.20735	-0.06903	-0.43904
1.90	1.87509	-0.20935	-0.07944	-0.53062
1.95	1.95429	-0.21121	-0.08996	-0.62639
2.00	2.02555	-0.21294	-0.10056	-0.72592
2.05	2.09019	-0.21455	-0.11125	-0.82884
2.10	2.14921	-0.21605	-0.12202	-0.93484
2.15	2.20340	-0.21747	-0.13285	-1.04368
2.20	2.25341	-0.21879	-0.14376	-1.15511
2.25	2.29976	-0.22005	-0.15473	-1.26896
2.30	2.34289	-0.22123	-0.16576	-1.38503
2.35	2.38315	-0.22235	-0.17685	-1.50320
2.40	2.42086	-0.22341	-0.18800	-1.62331
2.45	2.45628	-0.22442	-0.19919	-1.74524
2.50	2.48963	-0.22538	-0.21044	-1.86890
2.55	2.52110	-0.22630	-0.22173	-1.99418
2.60	2.55087	-0.22718	-0.23307	-2.12098
2.65	2.57909	-0.22801	-0.24445	-2.24924
2.70	2.60588	-0.22881	-0.25587	-2.37887
2.75	2.63137	-0.22958	-0.26733	-2.50980
2.80	2.65565	-0.23032	-0.27883	-2.64198
2.85	2.67881	-0.23103	-0.29036	-2.77535
2.90	2.70095	-0.23171	-0.30193	-2.90985
2.95	2.72212	-0.23237	-0.31353	-3.04543
3.00	2.74241	-0.23300	-0.32517	-3.18204
3.05	2.76186	-0.23361	-0.33683	-3.31965
3.10	2.78054	-0.23420	-0.34853	-3.45822
3.15	2.79849	-0.23476	-0.36025	-3.59769
3.20	2.81576	-0.23531	-0.37200	-3.73805
3.25	2.83239	-0.23585	-0.38378	-3.87926
3.30	2.84842	-0.23636	-0.39559	-4.02128
3.35	2.86388	-0.23686	-0.40742	-4.16409
3.40	2.87881	-0.23734	-0.41927	-4.30766
3.45	2.89323	-0.23781	-0.43115	-4.45196
3.50	2.90718	-0.23826	-0.44305	-4.59698

TABLE 4:

The "upper" near saddle point for a single resonance medium

initial x = 1.00
initial y = 6.00

theta	x-value	y-value	Re phi	Im phi
1.02	0.00000	4.10450	-0.95480	0.00000
1.04	0.00000	3.80502	-0.87580	0.00000
1.06	0.00000	3.55041	-0.80230	0.00000
1.08	0.00000	3.32714	-0.73357	0.00000
1.10	0.00000	3.12691	-0.66906	0.00000
1.12	0.00000	2.94426	-0.60838	0.00000
1.14	0.00000	2.77532	-0.55120	0.00000
1.16	0.00000	2.61729	-0.49729	0.00000
1.18	0.00000	2.46801	-0.44645	0.00000
1.20	0.00000	2.32577	-0.39852	0.00000
1.22	0.00000	2.18918	-0.35338	0.00000
1.24	0.00000	2.05705	-0.31093	0.00000
1.26	0.00000	1.92834	-0.27108	0.00000
1.28	0.00000	1.80208	-0.23378	0.00000
1.30	0.00000	1.67735	-0.19899	0.00000
1.32	0.00000	1.55323	-0.16668	0.00000
1.34	0.00000	1.42871	-0.13686	0.00000
1.36	0.00000	1.30263	-0.10954	0.00000
1.38	0.00000	1.17359	-0.08477	0.00000
1.40	0.00000	1.03972	-0.06263	0.00000
1.42	0.00000	0.89835	-0.04323	0.00000
1.44	0.00000	0.74513	-0.02677	0.00000
1.46	0.00000	0.57201	-0.01356	0.00000
1.48	0.00000	0.35929	-0.00415	0.00000
*				
1.52	0.46335	-0.18822	-0.00341	-0.00535
1.54	0.67329	-0.18981	-0.00719	-0.01686
1.56	0.82576	-0.19132	-0.01100	-0.03192
1.58	0.94925	-0.19276	-0.01484	-0.04970
1.60	1.05429	-0.19414	-0.01871	-0.06977
1.62	1.14623	-0.19545	-0.02261	-0.09179
1.64	1.22821	-0.19671	-0.02653	-0.11555
1.66	1.30231	-0.19792	-0.03047	-0.14087
1.68	1.36996	-0.19908	-0.03444	-0.16760
1.70	1.43221	-0.20019	-0.03844	-0.19563
1.72	1.48988	-0.20126	-0.04245	-0.22486
1.74	1.54357	-0.20229	-0.04649	-0.25520
1.76	1.59379	-0.20329	-0.05054	-0.28658
1.78	1.64095	-0.20424	-0.05462	-0.31893
1.80	1.68537	-0.20517	-0.05871	-0.35219
1.82	1.72735	-0.20606	-0.06282	-0.38633
1.84	1.76712	-0.20692	-0.06695	-0.42127
1.86	1.80489	-0.20776	-0.07110	-0.45700
1.88	1.84083	-0.20857	-0.07526	-0.49346
1.90	1.87509	-0.20935	-0.07944	-0.53062
1.92	1.90782	-0.21011	-0.08364	-0.56845
1.94	1.93913	-0.21085	-0.08785	-0.60692
1.96	1.96913	-0.21157	-0.09207	-0.64601
1.98	1.99791	-0.21226	-0.09631	-0.68568
2.00	2.02555	-0.21294	-0.10056	-0.72592

TABLE 5:
The "lower" near saddle point for a single resonance medium.

initial x = 0.05
initial y = -7.00

theta	x-value	y-value	Re phi	Im phi
1.05	0.00000	-3.80870	0.97394	0.00000
1.10	0.00000	-3.33469	0.79584	0.00000
1.15	0.00000	-2.94768	0.63904	0.00000
1.20	0.00000	-2.60966	0.50026	0.00000
1.25	0.00000	-2.29968	0.37761	0.00000
1.30	0.00000	-2.00314	0.27007	0.00000
1.35	0.00000	-1.70672	0.17729	0.00000
1.40	0.00000	-1.39300	0.09968	0.00000
1.45	0.00000	-1.02575	0.03885	0.00000
*				
1.55	0.75420	-0.19057	-0.00909	-0.02401
1.60	1.05429	-0.19414	-0.01871	-0.06977
1.65	1.26614	-0.19732	-0.02850	-0.12802
1.70	1.43221	-0.20019	-0.03844	-0.19563
1.75	1.56909	-0.20279	-0.04851	-0.27076
1.80	1.68538	-0.20517	-0.05871	-0.35220
1.85	1.78625	-0.20735	-0.06903	-0.43904
1.90	1.87509	-0.20935	-0.07944	-0.53062
1.95	1.95429	-0.21121	-0.08996	-0.62639
2.00	2.02555	-0.21294	-0.10056	-0.72592
2.05	2.09019	-0.21455	-0.11125	-0.82884
2.10	2.14921	-0.21605	-0.12202	-0.93484
2.15	2.20340	-0.21747	-0.13285	-1.04368
2.20	2.25341	-0.21879	-0.14376	-1.15511
2.25	2.29976	-0.22005	-0.15473	-1.26896
2.30	2.34289	-0.22123	-0.16576	-1.38503
2.35	2.38315	-0.22235	-0.17685	-1.50320
2.40	2.42086	-0.22341	-0.18800	-1.62331
2.45	2.45628	-0.22442	-0.19919	-1.74524
2.50	2.48963	-0.22538	-0.21044	-1.86890
2.55	2.52110	-0.22630	-0.22173	-1.99418
2.60	2.55087	-0.22718	-0.23307	-2.12098
2.65	2.57909	-0.22801	-0.24445	-2.24924
2.70	2.60588	-0.22881	-0.25587	-2.37887
2.75	2.63137	-0.22958	-0.26733	-2.50980
2.80	2.65565	-0.23032	-0.27883	-2.64198
2.85	2.67881	-0.23103	-0.29036	-2.77535
2.90	2.70095	-0.23171	-0.30193	-2.90985
2.95	2.72212	-0.23237	-0.31353	-3.04543
3.00	2.74241	-0.23300	-0.32517	-3.18204
3.05	2.76186	-0.23361	-0.33683	-3.31965
3.10	2.78054	-0.23420	-0.34853	-3.45822
3.15	2.79849	-0.23476	-0.36025	-3.59769
3.20	2.81576	-0.23531	-0.37200	-3.73805
3.25	2.83239	-0.23585	-0.38378	-3.87926
3.30	2.84842	-0.23636	-0.39559	-4.02128
3.35	2.86388	-0.23686	-0.40742	-4.16409
3.40	2.87881	-0.23734	-0.41927	-4.30766
3.45	2.89323	-0.23781	-0.43115	-4.45196
3.50	2.90718	-0.23826	-0.44305	-4.59698

TABLE 6:
The "lower" near saddle point for a single resonance medium.

initial x = -0.20
initial y = -5.00

theta	x-value	y-value	Re phi	Im phi
1.02	0.00000	-4.16763	1.09339	0.00000
1.04	0.00000	-3.92007	1.01257	0.00000
1.06	0.00000	-3.70394	0.93638	0.00000
1.08	0.00000	-3.51067	0.86426	0.00000
1.10	0.00000	-3.33469	0.79584	0.00000
1.12	0.00000	-3.17217	0.73079	0.00000
1.14	0.00000	-3.02030	0.66888	0.00000
1.16	0.00000	-2.87698	0.60992	0.00000
1.18	0.00000	-2.74055	0.55375	0.00000
1.20	0.00000	-2.60966	0.50026	0.00000
1.22	0.00000	-2.48320	0.44934	0.00000
1.24	0.00000	-2.36017	0.40091	0.00000
1.26	0.00000	-2.23971	0.35491	0.00000
1.28	0.00000	-2.12097	0.31131	0.00000
1.30	0.00000	-2.00314	0.27007	0.00000
1.32	0.00000	-1.88536	0.23118	0.00000
1.34	0.00000	-1.76671	0.19466	0.00000
1.36	0.00000	-1.64608	0.16053	0.00000
1.38	0.00000	-1.52212	0.12884	0.00000
1.40	0.00000	-1.39300	0.09968	0.00000
1.42	0.00000	-1.25607	0.07317	0.00000
1.44	0.00000	-1.10704	0.04951	0.00000
1.46	0.00000	-0.93786	0.02902	0.00000
1.48	0.00000	-0.72886	0.01226	0.00000
*				
1.52	0.46335	-0.18822	-0.00341	-0.00535
1.54	0.67329	-0.18981	-0.00719	-0.01686
1.56	0.82576	-0.19132	-0.01100	-0.03192
1.58	0.94925	-0.19276	-0.01484	-0.04970
1.60	1.05429	-0.19414	-0.01871	-0.06977
1.62	1.14623	-0.19545	-0.02261	-0.09179
1.64	1.22821	-0.19671	-0.02653	-0.11555
1.66	1.30231	-0.19792	-0.03047	-0.14087
1.68	1.36996	-0.19908	-0.03444	-0.16760
1.70	1.43221	-0.20019	-0.03844	-0.19563
1.72	1.48988	-0.20126	-0.04245	-0.22486
1.74	1.54357	-0.20229	-0.04649	-0.25520
1.76	1.59379	-0.20329	-0.05054	-0.28658
1.78	1.64095	-0.20424	-0.05462	-0.31893
1.80	1.68537	-0.20517	-0.05871	-0.35219
1.82	1.72735	-0.20606	-0.06282	-0.38633
1.84	1.76712	-0.20692	-0.06695	-0.42127
1.86	1.80489	-0.20776	-0.07110	-0.45700
1.88	1.84083	-0.20857	-0.07526	-0.49346
1.90	1.87509	-0.20935	-0.07944	-0.53062
1.92	1.90782	-0.21011	-0.08364	-0.56845
1.94	1.93913	-0.21085	-0.08785	-0.60692
1.96	1.96913	-0.21157	-0.09207	-0.64601
1.98	1.99791	-0.21226	-0.09631	-0.68568
2.00	2.02555	-0.21294	-0.10056	-0.72592

TABLE 7:

The distant saddle points for a double resonance medium. (The points in the left half of the plane are the same as these with a negative sign in front of the x-value.)

initial x = 37.20
initial y = -0.47 nu = 0.00

theta	x-value	y-value	Re phi	Im phi
1.02	27.45406	-0.44876	-0.00933	-1.03410
1.04	20.86954	-0.42546	-0.01805	-1.50548
1.06	18.08478	-0.40962	-0.02639	-1.89204
1.08	16.47833	-0.39788	-0.03446	-2.23644
1.10	15.40925	-0.38881	-0.04233	-2.55468
1.12	14.63581	-0.38146	-0.05003	-2.85476
1.14	14.04461	-0.37538	-0.05759	-3.14132
1.16	13.57472	-0.37036	-0.06505	-3.41734
1.18	13.19021	-0.36587	-0.07241	-3.68487
1.20	12.86837	-0.36198	-0.07969	-3.94537
1.22	12.59408	-0.35855	-0.08689	-4.19993
1.24	12.35686	-0.35550	-0.09403	-4.44938
1.26	12.14917	-0.35276	-0.10111	-4.69440
1.28	11.96544	-0.35028	-0.10814	-4.93551
1.30	11.80146	-0.34802	-0.11512	-5.17315
1.32	11.65399	-0.34594	-0.12206	-5.40767
1.34	11.52047	-0.34403	-0.12896	-5.63940
1.36	11.39887	-0.34227	-0.13582	-5.86857
1.38	11.28757	-0.34080	-0.14265	-6.09542
1.40	11.18517	-0.33924	-0.14945	-6.32013
1.42	11.09058	-0.33778	-0.15622	-6.54288
1.44	11.00288	-0.33642	-0.16296	-6.76380
1.46	10.92129	-0.33515	-0.16967	-6.98304
1.48	10.84515	-0.33394	-0.17636	-7.20069
1.50	10.77387	-0.33281	-0.18303	-7.41687
1.52	10.70698	-0.33173	-0.18967	-7.63167
1.54	10.64405	-0.33071	-0.19629	-7.84518
1.56	10.58472	-0.32974	-0.20290	-8.05746
1.58	10.52865	-0.32882	-0.20948	-8.26859
1.60	10.47558	-0.32793	-0.21605	-8.47863
1.62	10.42524	-0.32709	-0.22260	-8.68763
1.64	10.37742	-0.32629	-0.22913	-8.89565
1.66	10.33191	-0.32552	-0.23565	-9.10274
1.68	10.28855	-0.32478	-0.24215	-9.30894
1.70	10.24716	-0.32406	-0.24864	-9.51430
1.72	10.20762	-0.32338	-0.25511	-9.71884
1.74	10.16978	-0.32272	-0.26157	-9.92261
1.76	10.13354	-0.32209	-0.26802	-10.12564
1.78	10.09879	-0.32147	-0.27446	-10.32796
1.80	10.06543	-0.32088	-0.28088	-10.52960
1.82	10.03338	-0.32031	-0.28729	-10.73059
1.84	10.00254	-0.31976	-0.29369	-10.93095
1.86	9.97286	-0.31922	-0.30008	-11.13070
1.88	9.94426	-0.31870	-0.30646	-11.32987
1.90	9.91668	-0.31820	-0.31283	-11.52847
1.92	9.89006	-0.31771	-0.31919	-11.72654
1.94	9.86436	-0.31724	-0.32554	-11.92408
1.96	9.83951	-0.31678	-0.33188	-12.12112
1.98	9.81548	-0.31633	-0.33821	-12.31767

TABLE 8:

The distant saddle points for a double resonance medium with a non-zero nu. (An identical saddle point is found reflected across the imaginary axis.)

initial x = 30.00
initial y = -1.00 nu = 0.40

theta	x-value	y-value	Re phi	Im phi
1.02	26.97527	-0.45763	-0.00943	-1.02715
1.04	20.29582	-0.43726	-0.01837	-1.48786
1.06	17.46815	-0.42241	-0.02696	-1.86246
1.08	15.83907	-0.41085	-0.03529	-2.19429
1.10	14.75709	-0.40168	-0.04341	-2.49961
1.12	13.97604	-0.39405	-0.05137	-2.78655
1.14	13.38035	-0.38765	-0.05918	-3.05987
1.16	12.90790	-0.38235	-0.06688	-3.32258
1.18	12.52207	-0.37750	-0.07447	-3.57676
1.20	12.19972	-0.37326	-0.08198	-3.82389
1.22	11.92550	-0.36951	-0.08940	-4.06507
1.24	11.68871	-0.36615	-0.09676	-4.30116
1.26	11.48172	-0.36312	-0.10405	-4.53282
1.28	11.29887	-0.36037	-0.11129	-4.76059
1.30	11.13591	-0.35785	-0.11847	-4.98491
1.32	10.98952	-0.35554	-0.12560	-5.20613
1.34	10.85715	-0.35340	-0.13269	-5.42458
1.36	10.73673	-0.35142	-0.13974	-5.64050
1.38	10.62660	-0.34958	-0.14675	-5.85412
1.40	10.52541	-0.34786	-0.15372	-6.06562
1.42	10.43205	-0.34639	-0.16066	-6.27519
1.44	10.34555	-0.34485	-0.16757	-6.48295
1.46	10.26514	-0.34340	-0.17445	-6.68905
1.48	10.19015	-0.34204	-0.18130	-6.89359
1.50	10.12002	-0.34075	-0.18813	-7.09669
1.52	10.05426	-0.33953	-0.19493	-7.29842
1.54	9.99244	-0.33837	-0.20171	-7.49888
1.56	9.93419	-0.33727	-0.20846	-7.69814
1.58	9.87919	-0.33622	-0.21520	-7.89627
1.60	9.82715	-0.33522	-0.22191	-8.09333
1.62	9.77783	-0.33426	-0.22861	-8.28937
1.64	9.73101	-0.33334	-0.23528	-8.48446
1.66	9.68648	-0.33246	-0.24194	-8.67863
1.68	9.64407	-0.33162	-0.24858	-8.87193
1.70	9.60362	-0.33081	-0.25520	-9.06440
1.72	9.56499	-0.33003	-0.26181	-9.25609
1.74	9.52805	-0.32928	-0.26840	-9.44701
1.76	9.49269	-0.32855	-0.27498	-9.63722
1.78	9.45879	-0.32785	-0.28154	-9.82673
1.80	9.42627	-0.32718	-0.28809	-10.01558
1.82	9.39503	-0.32653	-0.29463	-10.20379
1.84	9.36501	-0.32590	-0.30116	-10.39139
1.86	9.33611	-0.32529	-0.30767	-10.57840
1.88	9.30828	-0.32469	-0.31417	-10.76484
1.90	9.28146	-0.32412	-0.32065	-10.95074
1.92	9.25559	-0.32356	-0.32713	-11.13610
1.94	9.23061	-0.32302	-0.33360	-11.32097
1.96	9.20647	-0.32249	-0.34005	-11.50534
1.98	9.18314	-0.32198	-0.34650	-11.68923

TABLE 9:

The distant saddle points for a double resonance medium with a non-zero nu. (An identical saddle point is found reflected across the imaginary axis.)

initial x = 30.00
initial y = -1.00 nu = 0.80

theta	x-value	y-value	Re phi	Im phi
1.02	26.47458	-0.46768	-0.00955	-1.01999
1.04	19.68323	-0.45155	-0.01874	-1.46941
1.06	16.80292	-0.43839	-0.02763	-1.83118
1.08	15.14579	-0.42726	-0.03629	-2.14940
1.10	14.04804	-0.41806	-0.04474	-2.44067
1.12	13.25807	-0.41008	-0.05301	-2.71334
1.14	12.65749	-0.40323	-0.06115	-2.97225
1.16	12.18266	-0.39724	-0.06915	-3.22047
1.18	11.79605	-0.39208	-0.07704	-3.46014
1.20	11.47398	-0.38731	-0.08483	-3.69275
1.22	11.20070	-0.38304	-0.09253	-3.91942
1.24	10.96534	-0.37920	-0.10015	-4.14102
1.26	10.76006	-0.37571	-0.10770	-4.35823
1.28	10.57912	-0.37253	-0.11518	-4.57159
1.30	10.41818	-0.36961	-0.12260	-4.78153
1.32	10.27390	-0.36691	-0.12997	-4.98843
1.34	10.14367	-0.36441	-0.13728	-5.19258
1.36	10.02539	-0.36209	-0.14455	-5.39425
1.38	9.91739	-0.35992	-0.15177	-5.59367
1.40	9.81831	-0.35789	-0.15894	-5.79101
1.42	9.72700	-0.35599	-0.16608	-5.98645
1.44	9.64256	-0.35436	-0.17318	-6.18013
1.46	9.56414	-0.35265	-0.18025	-6.37219
1.48	9.49110	-0.35104	-0.18729	-6.56274
1.50	9.42287	-0.34952	-0.19429	-6.75187
1.52	9.35896	-0.34807	-0.20126	-6.93968
1.54	9.29894	-0.34670	-0.20821	-7.12625
1.56	9.24245	-0.34540	-0.21513	-7.31166
1.58	9.18916	-0.34415	-0.22202	-7.49597
1.60	9.13880	-0.34297	-0.22889	-7.67924
1.62	9.09110	-0.34183	-0.23574	-7.86154
1.64	9.04586	-0.34075	-0.24256	-8.04291
1.66	9.00286	-0.33971	-0.24937	-8.22339
1.68	8.96195	-0.33871	-0.25615	-8.40303
1.70	8.92296	-0.33775	-0.26292	-8.58188
1.72	8.88576	-0.33683	-0.26966	-8.75996
1.74	8.85020	-0.33594	-0.27639	-8.93732
1.76	8.81619	-0.33508	-0.28310	-9.11398
1.78	8.78361	-0.33426	-0.28979	-9.28998
1.80	8.75238	-0.33346	-0.29647	-9.46533
1.82	8.72240	-0.33269	-0.30313	-9.64008
1.84	8.69359	-0.33195	-0.30977	-9.81424
1.86	8.66589	-0.33123	-0.31641	-9.98783
1.88	8.63923	-0.33053	-0.32302	-10.16088
1.90	8.61355	-0.32985	-0.32963	-10.33341
1.92	8.58879	-0.32919	-0.33622	-10.50543
1.94	8.56490	-0.32856	-0.34279	-10.67696
1.96	8.54183	-0.32794	-0.34936	-10.84803
1.98	8.51954	-0.32734	-0.35591	-11.01864

TABLE 10:
The "upper" middle saddle point for a double resonance medium.

initial x = 3.58
initial y = 0.42 nu = 0.00

theta	x-value	y-value	Re phi	Im phi
1.60	3.57979	0.42358	-0.11201	-1.92273
1.62	3.58184	0.33611	-0.10439	-1.99436
1.64	3.57895	0.23599	-0.09864	-2.06598
1.66	3.56124	0.11365	-0.09510	-2.13742
1.68	3.48177	-0.03292	-0.09430	-2.20804
1.70	3.34643	-0.09689	-0.09576	-2.27627
1.72	3.24771	-0.11449	-0.09790	-2.34216
1.74	3.17207	-0.12202	-0.10027	-2.40633
1.76	3.11104	-0.12603	-0.10276	-2.46915
1.78	3.05902	-0.12842	-0.10531	-2.53083
1.80	3.01364	-0.12991	-0.10789	-2.59154
1.82	2.97339	-0.13084	-0.11050	-2.65140
1.84	2.93723	-0.13141	-0.11312	-2.71050
1.86	2.90443	-0.13174	-0.11575	-2.76890
1.88	2.87443	-0.13191	-0.11839	-2.82669
1.90	2.84683	-0.13195	-0.12103	-2.88389
1.92	2.82129	-0.13191	-0.12367	-2.94056
1.94	2.79755	-0.13180	-0.12631	-2.99675
1.96	2.77540	-0.13164	-0.12894	-3.05247
1.98	2.75465	-0.13145	-0.13157	-3.10777
2.00	2.73516	-0.13122	-0.13420	-3.16266
2.02	2.71680	-0.13098	-0.13682	-3.21718
2.04	2.69947	-0.13072	-0.13944	-3.27134
2.06	2.68307	-0.13045	-0.14205	-3.32516
2.08	2.66752	-0.13017	-0.14466	-3.37866
2.10	2.65274	-0.12988	-0.14726	-3.43186
2.12	2.63869	-0.12959	-0.14985	-3.48477
2.14	2.62529	-0.12930	-0.15244	-3.53741
2.16	2.61251	-0.12901	-0.15502	-3.58979
2.18	2.60029	-0.12871	-0.15760	-3.64191
2.20	2.58860	-0.12842	-0.16017	-3.69380
2.22	2.57741	-0.12813	-0.16274	-3.74546
2.24	2.56667	-0.12784	-0.16530	-3.79690
2.26	2.55637	-0.12755	-0.16785	-3.84813
2.28	2.54647	-0.12727	-0.17040	-3.89915
2.30	2.53694	-0.12699	-0.17294	-3.94999
2.32	2.52778	-0.12671	-0.17548	-4.00063
2.34	2.51895	-0.12643	-0.17801	-4.05110
2.36	2.51045	-0.12616	-0.18054	-4.10139
2.38	2.50224	-0.12590	-0.18306	-4.15152
2.40	2.49431	-0.12563	-0.18557	-4.20148
2.42	2.48666	-0.12537	-0.18808	-4.25129
2.44	2.47926	-0.12512	-0.19059	-4.30095
2.46	2.47211	-0.12487	-0.19309	-4.35046
2.48	2.46518	-0.12462	-0.19558	-4.39983
2.50	2.45848	-0.12437	-0.19807	-4.44907

TABLE 11:

The "upper" middle saddle point for a double resonance medium.

initial x = 3.15
initial y = 0.60 nu = 0.40

theta	x-value	y-value	Re phi	Im phi
1.60	3.14431	0.59266	-0.13511	-1.96311
1.62	3.15160	0.51441	-0.12403	-2.02607
1.64	3.15770	0.43123	-0.11456	-2.08917
1.66	3.16298	0.34006	-0.10683	-2.15238
1.68	3.16656	0.23556	-0.10105	-2.21568
1.70	3.16409	0.10401	-0.09759	-2.27900
1.72	3.09460	-0.11429	-0.09745	-2.34196
1.74	2.89531	-0.16141	-0.10046	-2.40157
1.76	2.78718	-0.16398	-0.10372	-2.45833
1.78	2.70835	-0.16354	-0.10700	-2.51325
1.80	2.64527	-0.16223	-0.11026	-2.56677
1.82	2.59245	-0.16063	-0.11349	-2.61913
1.84	2.54698	-0.15892	-0.11668	-2.67051
1.86	2.50713	-0.15719	-0.11985	-2.72105
1.88	2.47171	-0.15548	-0.12297	-2.77083
1.90	2.43993	-0.15382	-0.12606	-2.81994
1.92	2.41117	-0.15221	-0.12912	-2.86845
1.94	2.38515	-0.15071	-0.13215	-2.91640
1.96	2.36113	-0.14921	-0.13515	-2.96386
1.98	2.33902	-0.14776	-0.13812	-3.01085
2.00	2.31859	-0.14637	-0.14106	-3.05742
2.02	2.29965	-0.14504	-0.14397	-3.10360
2.04	2.28202	-0.14377	-0.14686	-3.14942
2.06	2.26558	-0.14255	-0.14972	-3.19489
2.08	2.25019	-0.14138	-0.15256	-3.24004
2.10	2.23577	-0.14027	-0.15538	-3.28490
2.12	2.22221	-0.13919	-0.15817	-3.32948
2.14	2.20945	-0.13817	-0.16095	-3.37379
2.16	2.19741	-0.13718	-0.16370	-3.41786
2.18	2.18603	-0.13624	-0.16643	-3.46169
2.20	2.17526	-0.13533	-0.16915	-3.50530
2.22	2.16506	-0.13446	-0.17185	-3.54870
2.24	2.15537	-0.13363	-0.17453	-3.59190
2.26	2.14616	-0.13283	-0.17719	-3.63492
2.28	2.13740	-0.13206	-0.17984	-3.67775
2.30	2.12905	-0.13131	-0.18247	-3.72042
2.32	2.12109	-0.13060	-0.18509	-3.76292
2.34	2.11349	-0.12991	-0.18770	-3.80526
2.36	2.10623	-0.12925	-0.19029	-3.84746
2.38	2.09928	-0.12861	-0.19287	-3.88951
2.40	2.09263	-0.12800	-0.19543	-3.93143
2.42	2.08625	-0.12741	-0.19799	-3.97322
2.44	2.08014	-0.12684	-0.20053	-4.01488
2.46	2.07427	-0.12628	-0.20306	-4.05642
2.48	2.06863	-0.12575	-0.20558	-4.09785
2.50	2.06321	-0.12524	-0.20809	-4.13917

TABLE 12:
The "upper" middle saddle point for a double resonance medium.

initial x = 2.54
initial y = 0.05 nu = 0.80

theta	x-value	y-value	Re phi	Im phi
1.60	2.68335	-0.03006	-0.08488	-1.98248
1.62	2.80390	-0.06837	-0.08588	-2.03737
1.64	2.91268	-0.09601	-0.08754	-2.09455
1.66	3.01066	-0.11653	-0.08967	-2.15380
1.68	3.09922	-0.13218	-0.09217	-2.21492
1.70	3.17974	-0.14442	-0.09494	-2.27772
1.72	3.25318	-0.15414	-0.09793	-2.34206
1.74	3.32061	-0.16205	-0.10109	-2.40780
1.76	3.38283	-0.16861	-0.10440	-2.47485
1.78	3.44051	-0.17413	-0.10783	-2.54309
1.80	3.49421	-0.17883	-0.11136	-2.61244
1.82	3.54438	-0.18289	-0.11498	-2.68283
1.84	3.59141	-0.18643	-0.11868	-2.75419
1.86	3.63565	-0.18955	-0.12244	-2.82647
1.88	3.67738	-0.19232	-0.12626	-2.89960
1.90	3.71683	-0.19480	-0.13013	-2.97355
1.92	3.75423	-0.19704	-0.13405	-3.04826
1.94	3.78975	-0.19907	-0.13801	-3.12370
1.96	3.82355	-0.20093	-0.14201	-3.19984
1.98	3.85578	-0.20263	-0.14605	-3.27664
2.00	3.88656	-0.20420	-0.15012	-3.35406
2.02	3.91601	-0.20565	-0.15421	-3.43209
2.04	3.94421	-0.20700	-0.15834	-3.51069
2.06	3.97127	-0.20826	-0.16249	-3.58985
2.08	3.99725	-0.20944	-0.16667	-3.66954
2.10	4.02224	-0.21054	-0.17087	-3.74973
2.12	4.04629	-0.21159	-0.17509	-3.83042
2.14	4.06947	-0.21257	-0.17934	-3.91158
2.16	4.09183	-0.21350	-0.18360	-3.99319
2.18	4.11342	-0.21438	-0.18788	-4.07525
2.20	4.13428	-0.21522	-0.19217	-4.15773
2.22	4.15446	-0.21602	-0.19648	-4.24061
2.24	4.17399	-0.21678	-0.20081	-4.32390
2.26	4.19291	-0.21751	-0.20516	-4.40757
2.28	4.21125	-0.21821	-0.20951	-4.49161
2.30	4.22903	-0.21887	-0.21388	-4.57602
2.32	4.24630	-0.21952	-0.21827	-4.66077
2.34	4.26307	-0.22013	-0.22267	-4.74586
2.36	4.27937	-0.22072	-0.22707	-4.83129
2.38	4.29521	-0.22129	-0.23149	-4.91704
2.40	4.31063	-0.22184	-0.23593	-5.00309
2.42	4.32564	-0.22238	-0.24037	-5.08946
2.44	4.34025	-0.22289	-0.24482	-5.17612
2.46	4.35449	-0.22339	-0.24928	-5.26307
2.48	4.36838	-0.22387	-0.25376	-5.35030
2.50	4.38191	-0.22433	-0.25824	-5.43780

TABLE 13:
The "lower" middle saddle point for a double resonance medium.

initial x = 3.62
initial y = -0.80 nu = 0.00

theta	x-value	y-value	Re phi	Im phi
1.60	3.62934	-0.79927	-0.04956	-1.91090
1.62	3.65094	-0.71149	-0.06468	-1.98370
1.64	3.67655	-0.61131	-0.07794	-2.05697
1.66	3.71649	-0.48879	-0.08899	-2.13086
1.68	3.81684	-0.34214	-0.09728	-2.20600
1.70	3.97243	-0.27808	-0.10333	-2.28394
1.72	4.09061	-0.26023	-0.10868	-2.36463
1.74	4.18474	-0.25250	-0.11380	-2.44741
1.76	4.26439	-0.24834	-0.11881	-2.53192
1.78	4.33415	-0.24584	-0.12375	-2.61792
1.80	4.39660	-0.24425	-0.12865	-2.70524
1.82	4.45335	-0.24321	-0.13352	-2.79375
1.84	4.50548	-0.24241	-0.13838	-2.88334
1.86	4.55377	-0.24200	-0.14322	-2.97394
1.88	4.59880	-0.24175	-0.14806	-3.06547
1.90	4.64100	-0.24161	-0.15290	-3.15787
1.92	4.68074	-0.24157	-0.15773	-3.25109
1.94	4.71828	-0.24159	-0.16256	-3.34509
1.96	4.75386	-0.24166	-0.16740	-3.43981
1.98	4.78769	-0.24177	-0.17223	-3.53523
2.00	4.81992	-0.24191	-0.17707	-3.63131
2.02	4.85070	-0.24207	-0.18191	-3.72802
2.04	4.88014	-0.24225	-0.18675	-3.82533
2.06	4.90836	-0.24245	-0.19160	-3.92322
2.08	4.93545	-0.24265	-0.19645	-4.02166
2.10	4.96149	-0.24286	-0.20131	-4.12063
2.12	4.98655	-0.24308	-0.20617	-4.22011
2.14	5.01070	-0.24330	-0.21103	-4.32008
2.16	5.03401	-0.24352	-0.21590	-4.42053
2.18	5.05651	-0.24375	-0.22077	-4.52144
2.20	5.07827	-0.24398	-0.22565	-4.62279
2.22	5.09932	-0.24421	-0.23053	-4.72456
2.24	5.11971	-0.24443	-0.23542	-4.82676
2.26	5.13947	-0.24466	-0.24031	-4.92935
2.28	5.15864	-0.24488	-0.24520	-5.03233
2.30	5.17725	-0.24511	-0.25010	-5.13569
2.32	5.19532	-0.24533	-0.25501	-5.23942
2.34	5.21288	-0.24555	-0.25992	-5.34350
2.36	5.22996	-0.24576	-0.26483	-5.44793
2.38	5.24658	-0.24598	-0.26975	-5.55269
2.40	5.26276	-0.24619	-0.27467	-5.65779
2.42	5.27852	-0.24640	-0.27960	-5.76320
2.44	5.29388	-0.24661	-0.28453	-5.86893
2.46	5.30886	-0.24681	-0.28946	-5.97495
2.48	5.32348	-0.24701	-0.29440	-6.08128
2.50	5.33774	-0.24721	-0.29934	-6.18789

TABLE 14:
The "lower" middle saddle point for a double resonance medium.

initial x = 3.12
initial y = -1.00 nu = 0.40

theta	x-value	y-value	Re phi	Im phi
1.60	3.12358	-0.99760	-0.01236	-1.96148
*				
*				
1.66	3.16241	-0.73957	-0.06477	-2.15003
1.68	3.17803	-0.63350	-0.07853	-2.21343
1.70	3.19906	-0.50019	-0.08994	-2.27718
1.72	3.28696	-0.28030	-0.09798	-2.34167
1.74	3.50428	-0.23151	-0.10285	-2.40987
1.76	3.63023	-0.22732	-0.10742	-2.48129
1.78	3.72658	-0.22627	-0.11196	-2.55489
1.80	3.80689	-0.22615	-0.11648	-2.63024
1.82	3.87664	-0.22638	-0.12101	-2.70709
1.84	3.93873	-0.22677	-0.12554	-2.78526
1.86	3.99491	-0.22724	-0.13008	-2.86460
1.88	4.04634	-0.22764	-0.13463	-2.94502
1.90	4.09383	-0.22819	-0.13919	-3.02643
1.92	4.13800	-0.22873	-0.14376	-3.10875
1.94	4.17932	-0.22927	-0.14834	-3.19193
1.96	4.21813	-0.22980	-0.15293	-3.27591
1.98	4.25475	-0.23032	-0.15753	-3.36064
2.00	4.28940	-0.23082	-0.16215	-3.44609
2.02	4.32230	-0.23132	-0.16677	-3.53221
2.04	4.35360	-0.23180	-0.17140	-3.61897
2.06	4.38346	-0.23226	-0.17604	-3.70634
2.08	4.41199	-0.23272	-0.18069	-3.79430
2.10	4.43931	-0.23316	-0.18535	-3.88281
2.12	4.46551	-0.23359	-0.19002	-3.97186
2.14	4.49068	-0.23402	-0.19469	-4.06143
2.16	4.51488	-0.23442	-0.19938	-4.15148
2.18	4.53819	-0.23482	-0.20407	-4.24201
2.20	4.56066	-0.23521	-0.20877	-4.33301
2.22	4.58235	-0.23559	-0.21348	-4.42444
2.24	4.60331	-0.23596	-0.21820	-4.51629
2.26	4.62357	-0.23632	-0.22292	-4.60856
2.28	4.64319	-0.23667	-0.22765	-4.70123
2.30	4.66220	-0.23702	-0.23239	-4.79429
2.32	4.68062	-0.23735	-0.23713	-4.88772
2.34	4.69850	-0.23768	-0.24188	-4.98151
2.36	4.71585	-0.23800	-0.24664	-5.07565
2.38	4.73271	-0.23831	-0.25140	-5.17014
2.40	4.74911	-0.23862	-0.25617	-5.26496
2.42	4.76505	-0.23892	-0.26095	-5.36010
2.44	4.78057	-0.23921	-0.26573	-5.45556
2.46	4.79568	-0.23950	-0.27051	-5.55132
2.48	4.81041	-0.23978	-0.27531	-5.64738
2.50	4.82476	-0.24005	-0.28011	-5.74373

TABLE 15:

This is the "upper" near saddle point for a double resonance medium.

initial x = 0.01
initial y = 2.12 nu = 0.00

theta	x-value	y-value	Re phi	Im phi
1.02	0.00000	1.99701	-0.99017	0.00000
1.04	0.00000	1.78245	-0.95268	0.00000
1.06	0.00000	1.64568	-0.91855	0.00000
1.08	0.00000	1.54227	-0.88676	0.00000
1.10	0.00000	1.46011	-0.85679	0.00000
1.12	0.00000	1.39163	-0.82832	0.00000
1.14	0.00000	1.33289	-0.80111	0.00000
1.16	0.00000	1.28031	-0.77501	0.00000
1.18	0.00000	1.23343	-0.74990	0.00000
1.20	0.00000	1.19178	-0.72567	0.00000
1.22	0.00000	1.15285	-0.70225	0.00000
1.24	0.00000	1.11699	-0.67957	0.00000
1.26	0.00000	1.08369	-0.65758	0.00000
1.28	0.00000	1.05259	-0.63622	0.00000
1.30	0.00000	1.02337	-0.61547	0.00000
1.32	0.00000	0.99580	-0.59529	0.00000
1.34	0.00000	0.97022	-0.57564	0.00000
1.36	0.00000	0.94528	-0.55650	0.00000
1.38	0.00000	0.92149	-0.53784	0.00000
1.40	0.00000	0.89872	-0.51965	0.00000
1.42	0.00000	0.87689	-0.50190	0.00000
1.44	0.00000	0.85589	-0.48458	0.00000
1.46	0.00000	0.83564	-0.46768	0.00000
1.48	0.00000	0.81609	-0.45116	0.00000
1.50	0.00000	0.79717	-0.43504	0.00000
1.52	0.00000	0.77883	-0.41928	0.00000
1.54	0.00000	0.76102	-0.40389	0.00000
1.56	0.00000	0.74369	-0.38884	0.00000
1.58	0.00000	0.72681	-0.37414	0.00000
1.60	0.00000	0.71035	-0.35977	0.00000
1.62	0.00000	0.69427	-0.34573	0.00000
1.64	0.00000	0.67854	-0.33200	0.00000
1.66	0.00000	0.66314	-0.31859	0.00000
1.68	0.00000	0.64804	-0.30548	0.00000
1.70	0.00000	0.63322	-0.29267	0.00000
1.72	0.00000	0.61867	-0.28015	0.00000
1.74	0.00000	0.60435	-0.26792	0.00000
1.76	0.00000	0.59025	-0.25597	0.00000
1.78	0.00000	0.57635	-0.24431	0.00000
1.80	0.00000	0.56264	-0.23292	0.00000
1.82	0.00000	0.54911	-0.22180	0.00000
1.84	0.00000	0.53573	-0.21096	0.00000
1.86	0.00000	0.52249	-0.20037	0.00000
1.88	0.00000	0.50938	-0.19006	0.00000
1.90	0.00000	0.49638	-0.18000	0.00000
1.92	0.00000	0.48348	-0.17020	0.00000
1.94	0.00000	0.47068	-0.16066	0.00000
1.96	0.00000	0.45794	-0.15137	0.00000
1.98	0.00000	0.44527	-0.14234	0.00000
2.00	0.00000	0.43265	-0.13356	0.00000

TABLE 16:

This is the "upper" near saddle point for a double resonance medium with non-zer nu.

initial x = 0.01
initial y = 2.12 nu = 0.40

theta	x-value	y-value	Re phi	Im phi
1.02	0.00000	1.59084	-2.31523	0.00000
1.04	0.00000	1.58740	-2.29190	0.00000
1.06	0.00000	1.58433	-2.26676	0.00000
1.08	0.00000	1.58134	-2.24151	0.00000
1.10	0.00000	1.57840	-2.21631	0.00000
1.12	0.00000	1.57550	-2.19119	0.00000
1.14	0.00000	1.57264	-2.16615	0.00000
1.16	0.00000	1.56983	-2.14118	0.00000
1.18	0.00000	1.56706	-2.11628	0.00000
1.20	0.00000	1.56433	-2.09146	0.00000
1.22	0.00000	1.56163	-2.06670	0.00000
1.24	0.00000	1.55898	-2.04202	0.00000
1.26	0.00000	1.55636	-2.01739	0.00000
1.28	0.00000	1.55378	-1.99284	0.00000
1.30	0.00000	1.55124	-1.96834	0.00000
1.32	0.00000	1.54873	-1.94391	0.00000
1.34	0.00000	1.54625	-1.91954	0.00000
1.36	0.00000	1.54381	-1.89522	0.00000
1.38	0.00000	1.54139	-1.87096	0.00000
1.40	0.00000	1.53902	-1.84676	0.00000
1.42	0.00000	1.53667	-1.82261	0.00000
1.44	0.00000	1.53435	-1.79852	0.00000
1.46	0.00000	1.53207	-1.77448	0.00000
1.48	0.00000	1.52981	-1.75049	0.00000
1.50	0.00000	1.52758	-1.72654	0.00000
1.52	0.00000	1.52538	-1.70265	0.00000
1.54	0.00000	1.52321	-1.67881	0.00000
1.56	0.00000	1.52106	-1.65501	0.00000
1.58	0.00000	1.51894	-1.63126	0.00000
1.60	0.00000	1.51685	-1.60755	0.00000
1.62	0.00000	1.51478	-1.58388	0.00000
1.64	0.00000	1.51273	-1.56026	0.00000
1.66	0.00000	1.51072	-1.53668	0.00000
1.68	0.00000	1.50872	-1.51314	0.00000
1.70	0.00000	1.50675	-1.48964	0.00000
1.72	0.00000	1.50480	-1.46618	0.00000
1.74	0.00000	1.50288	-1.44276	0.00000
1.76	0.00000	1.50097	-1.41937	0.00000
1.78	0.00000	1.49909	-1.39603	0.00000
1.80	0.00000	1.49723	-1.37272	0.00000
1.82	0.00000	1.49539	-1.34944	0.00000
1.84	0.00000	1.49357	-1.32620	0.00000
1.86	0.00000	1.49178	-1.30299	0.00000
1.88	0.00000	1.49000	-1.27982	0.00000
1.90	0.00000	1.48824	-1.25668	0.00000
1.92	0.00000	1.48650	-1.23357	0.00000
1.94	0.00000	1.48478	-1.21049	0.00000
1.96	0.00000	1.48308	-1.18744	0.00000
1.98	0.00000	1.48139	-1.16442	0.00000
2.00	0.00000	1.47973	-1.14144	0.00000

TABLE 17:

This is the "upper" near saddle point for a double resonance medium with non-zero nu.

initial x = -0.05
initial y = 4.50 nu = 0.80

theta	x-value	y-value	Re phi	Im phi
1.02	0.00000	2.76888	-2.74130	0.00000
1.04	0.00000	2.76501	-2.69200	0.00000
1.06	0.00000	2.76088	-2.64578	0.00000
1.08	0.00000	2.75687	-2.59916	0.00000
1.10	0.00000	2.75291	-2.55273	0.00000
1.12	0.00000	2.74835	-2.51252	0.00000
1.14	0.00000	2.74525	-2.45929	0.00000
1.16	0.00000	2.74076	-2.41982	0.00000
1.18	0.00000	2.73772	-2.36724	0.00000
1.20	0.00000	2.73336	-2.32780	0.00000
1.22	0.00000	2.73040	-2.27554	0.00000
1.24	0.00000	2.72617	-2.23614	0.00000
1.26	0.00000	2.72329	-2.18419	0.00000
1.28	0.00000	2.71918	-2.14484	0.00000
1.30	0.00000	2.71637	-2.09319	0.00000
1.32	0.00000	2.71237	-2.05388	0.00000
1.34	0.00000	2.70964	-2.00252	0.00000
1.36	0.00000	2.70575	-1.96324	0.00000
1.38	0.00000	2.70237	-1.91933	0.00000
1.40	0.00000	2.69915	-1.87444	0.00000
1.42	0.00000	2.69599	-1.82939	0.00000
1.44	0.00000	2.69287	-1.78437	0.00000
1.46	0.00000	2.68980	-1.73941	0.00000
1.48	0.00000	2.68676	-1.69452	0.00000
1.50	0.00000	2.68377	-1.64970	0.00000
1.52	0.00000	2.68081	-1.60495	0.00000
1.54	0.00000	2.67788	-1.56026	0.00000
1.56	0.00000	2.67499	-1.51565	0.00000
1.58	0.00000	2.67214	-1.47109	0.00000
1.60	0.00000	2.66932	-1.42660	0.00000
1.62	0.00000	2.66653	-1.38218	0.00000
1.64	0.00000	2.66378	-1.33781	0.00000
1.66	0.00000	2.66106	-1.29350	0.00000
1.68	0.00000	2.65837	-1.24925	0.00000
1.70	0.00000	2.65572	-1.20505	0.00000
1.72	0.00000	2.65309	-1.16091	0.00000
1.74	0.00000	2.65049	-1.11683	0.00000
1.76	0.00000	2.64793	-1.07279	0.00000
1.78	0.00000	2.64539	-1.02882	0.00000
1.80	0.00000	2.64288	-0.98489	0.00000
1.82	0.00000	2.64040	-0.94101	0.00000
1.84	0.00000	2.63794	-0.89718	0.00000
1.86	0.00000	2.63551	-0.85340	0.00000
1.88	0.00000	2.63311	-0.80967	0.00000
1.90	0.00000	2.63074	-0.76598	0.00000
1.92	0.00000	2.62839	-0.72234	0.00000
1.94	0.00000	2.62606	-0.67874	0.00000
1.96	0.00000	2.62376	-0.63519	0.00000
1.98	0.00000	2.62149	-0.59168	0.00000
2.00	0.00000	2.61924	-0.54821	0.00000

TABLE 18:

This is the "lower" near saddle point for a double resonance medium.

initial x = 0.30
initial y = -3.00 nu = 0.00

theta	x-value	y-value	Re phi	Im phi
1.02	0.00000	-1.69011	1.11121	0.00000
1.04	0.00000	-1.59210	1.07849	0.00000
1.06	0.00000	-1.51521	1.04749	0.00000
1.08	0.00000	-1.45120	1.01788	0.00000
1.10	0.00000	-1.39752	0.98942	0.00000
1.12	0.00000	-1.34979	0.96198	0.00000
1.14	0.00000	-1.30809	0.93542	0.00000
1.16	0.00000	-1.26951	0.90967	0.00000
1.18	0.00000	-1.23428	0.88465	0.00000
1.20	0.00000	-1.20181	0.86031	0.00000
1.22	0.00000	-1.17166	0.83658	0.00000
1.24	0.00000	-1.14346	0.81344	0.00000
1.26	0.00000	-1.11755	0.79084	0.00000
1.28	0.00000	-1.09240	0.76876	0.00000
1.30	0.00000	-1.06854	0.74716	0.00000
1.32	0.00000	-1.04584	0.72603	0.00000
1.34	0.00000	-1.02416	0.70534	0.00000
1.36	0.00000	-1.00339	0.68507	0.00000
1.38	0.00000	-0.98344	0.66521	0.00000
1.40	0.00000	-0.96423	0.64574	0.00000
1.42	0.00000	-0.94570	0.62665	0.00000
1.44	0.00000	-0.92778	0.60792	0.00000
1.46	0.00000	-0.91042	0.58954	0.00000
1.48	0.00000	-0.89357	0.57150	0.00000
1.50	0.00000	-0.87719	0.55380	0.00000
1.52	0.00000	-0.86124	0.53642	0.00000
1.54	0.00000	-0.84569	0.51935	0.00000
1.56	0.00000	-0.83051	0.50259	0.00000
1.58	0.00000	-0.81566	0.48613	0.00000
1.60	0.00000	-0.80113	0.46996	0.00000
1.62	0.00000	-0.78689	0.45408	0.00000
1.64	0.00000	-0.77291	0.43849	0.00000
1.66	0.00000	-0.75919	0.42317	0.00000
1.68	0.00000	-0.74569	0.40812	0.00000
1.70	0.00000	-0.73241	0.39334	0.00000
1.72	0.00000	-0.71932	0.37882	0.00000
1.74	0.00000	-0.70642	0.36457	0.00000
1.76	0.00000	-0.69403	0.35057	0.00000
1.78	0.00000	-0.68142	0.33682	0.00000
1.80	0.00000	-0.66895	0.32332	0.00000
1.82	0.00000	-0.65661	0.31007	0.00000
1.84	0.00000	-0.64438	0.29707	0.00000
1.86	0.00000	-0.63226	0.28431	0.00000
1.88	0.00000	-0.62022	0.27179	0.00000
1.90	0.00000	-0.60827	0.25951	0.00000
1.92	0.00000	-0.59638	0.24747	0.00000
1.94	0.00000	-0.58455	0.23566	0.00000
1.96	0.00000	-0.57277	0.22410	0.00000
1.98	0.00000	-0.56101	0.21276	0.00000
2.00	0.00000	-0.54928	0.20166	0.00000

TABLE 19:

This the "lower" near saddle point for a double resonance medium wiht non-zero nu.

initial x = 0.02
initial y = -5.00 nu = 0.40

theta	x-value	y-value	Re phi	Im phi
1.02	0.00000	-1.86026	2.48008	0.00000
1.04	0.00000	-1.85638	2.45267	0.00000
1.06	0.00000	-1.85292	2.42305	0.00000
1.08	0.00000	-1.84956	2.39322	0.00000
1.10	0.00000	-1.84626	2.36345	0.00000
1.12	0.00000	-1.84301	2.33375	0.00000
1.14	0.00000	-1.83980	2.30414	0.00000
1.16	0.00000	-1.83665	2.27462	0.00000
1.18	0.00000	-1.83353	2.24518	0.00000
1.20	0.00000	-1.83047	2.21583	0.00000
1.22	0.00000	-1.82744	2.18655	0.00000
1.24	0.00000	-1.82446	2.15735	0.00000
1.26	0.00000	-1.82152	2.12822	0.00000
1.28	0.00000	-1.81862	2.09917	0.00000
1.30	0.00000	-1.81576	2.07019	0.00000
1.32	0.00000	-1.81294	2.04128	0.00000
1.34	0.00000	-1.81015	2.01244	0.00000
1.36	0.00000	-1.80740	1.98366	0.00000
1.38	0.00000	-1.80469	1.95495	0.00000
1.40	0.00000	-1.80202	1.92630	0.00000
1.42	0.00000	-1.79938	1.89772	0.00000
1.44	0.00000	-1.79677	1.86919	0.00000
1.46	0.00000	-1.79420	1.84073	0.00000
1.48	0.00000	-1.79166	1.81233	0.00000
1.50	0.00000	-1.78915	1.78398	0.00000
1.52	0.00000	-1.78668	1.75568	0.00000
1.54	0.00000	-1.78423	1.72745	0.00000
1.56	0.00000	-1.78182	1.69926	0.00000
1.58	0.00000	-1.77943	1.67113	0.00000
1.60	0.00000	-1.77707	1.64304	0.00000
1.62	0.00000	-1.77475	1.61501	0.00000
1.64	0.00000	-1.77245	1.58703	0.00000
1.66	0.00000	-1.77017	1.55909	0.00000
1.68	0.00000	-1.76793	1.53120	0.00000
1.70	0.00000	-1.76571	1.50336	0.00000
1.72	0.00000	-1.76351	1.47556	0.00000
1.74	0.00000	-1.76134	1.44781	0.00000
1.76	0.00000	-1.75920	1.42009	0.00000
1.78	0.00000	-1.75708	1.39242	0.00000
1.80	0.00000	-1.75498	1.36480	0.00000
1.82	0.00000	-1.75291	1.33721	0.00000
1.84	0.00000	-1.75086	1.30966	0.00000
1.86	0.00000	-1.74884	1.28215	0.00000
1.88	0.00000	-1.74683	1.25468	0.00000
1.90	0.00000	-1.74485	1.22725	0.00000
1.92	0.00000	-1.74289	1.19985	0.00000
1.94	0.00000	-1.74095	1.17249	0.00000
1.96	0.00000	-1.73903	1.14517	0.00000
1.98	0.00000	-1.73713	1.11788	0.00000
2.00	0.00000	-1.73525	1.09062	0.00000

TABLE 20:

This is the "lower near saddle point for a double resonance medium with non-zero nu.

initial x = 0.05
initial y = -4.00 nu = 0.80

theta	x-value	y-value	Re phi	Im phi
1.02	0.00000	-3.03531	2.90616	0.00000
1.04	0.00000	-3.03123	2.85079	0.00000
1.06	0.00000	-3.02679	2.80034	0.00000
1.08	0.00000	-3.02252	2.74885	0.00000
1.10	0.00000	-3.01829	2.69774	0.00000
1.12	0.00000	-3.01413	2.64669	0.00000
1.14	0.00000	-3.01002	2.59576	0.00000
1.16	0.00000	-3.00598	2.54494	0.00000
1.18	0.00000	-3.00134	2.50130	0.00000
1.20	0.00000	-2.99818	2.44232	0.00000
1.22	0.00000	-2.99358	2.39964	0.00000
1.24	0.00000	-2.99046	2.34158	0.00000
1.26	0.00000	-2.98600	2.29888	0.00000
1.28	0.00000	-2.98297	2.24112	0.00000
1.30	0.00000	-2.97863	2.19845	0.00000
1.32	0.00000	-2.97568	2.14102	0.00000
1.34	0.00000	-2.97145	2.09837	0.00000
1.36	0.00000	-2.96858	2.04127	0.00000
1.38	0.00000	-2.96447	1.99863	0.00000
1.40	0.00000	-2.96167	1.94184	0.00000
1.42	0.00000	-2.95766	1.89922	0.00000
1.44	0.00000	-2.95494	1.84273	0.00000
1.46	0.00000	-2.95104	1.80011	0.00000
1.48	0.00000	-2.94764	1.75234	0.00000
1.50	0.00000	-2.94517	1.69443	0.00000
1.52	0.00000	-2.94141	1.65196	0.00000
1.54	0.00000	-2.93814	1.60429	0.00000
1.56	0.00000	-2.93502	1.55543	0.00000
1.58	0.00000	-2.93196	1.50636	0.00000
1.60	0.00000	-2.92895	1.45729	0.00000
1.62	0.00000	-2.92597	1.40827	0.00000
1.64	0.00000	-2.92303	1.35931	0.00000
1.66	0.00000	-2.92013	1.31041	0.00000
1.68	0.00000	-2.91725	1.26158	0.00000
1.70	0.00000	-2.91441	1.21281	0.00000
1.72	0.00000	-2.91161	1.16410	0.00000
1.74	0.00000	-2.90883	1.11545	0.00000
1.76	0.00000	-2.90609	1.06686	0.00000
1.78	0.00000	-2.90337	1.01832	0.00000
1.80	0.00000	-2.90069	0.96984	0.00000
1.82	0.00000	-2.89804	0.92141	0.00000
1.84	0.00000	-2.89541	0.87304	0.00000
1.86	0.00000	-2.89282	0.82472	0.00000
1.88	0.00000	-2.89025	0.77645	0.00000
1.90	0.00000	-2.88771	0.72823	0.00000
1.92	0.00000	-2.88520	0.68006	0.00000
1.94	0.00000	-2.88271	0.63194	0.00000
1.96	0.00000	-2.88026	0.58387	0.00000
1.98	0.00000	-2.87782	0.53584	0.00000
2.00	0.00000	-2.87541	0.48786	0.00000

D FORTRAN Programs

The following programs are programs which we wrote to (1) calculate the locations of the saddle points for a single resonance medium, (2) calculate the real part of the phase function for a double resonance medium and draw it graphically versus x and y, and (3) calculate the locations of the saddle points for a double resonance medium.

```
Program to calculate the saddle point positions for a single
resonance medium.

      real x,y,j,tht,f,g,fx,fy,w0,del,b,ul,wl,u0
      real d1,d2,d3,d4,d5,d6,gx,gy,x1,y1,dx,dy,v0
      real v1,v2,a1,a2,a3,c1,c2,e1,e2,e3,e4,i,t
      real aa,cc,nn,ss,xx,yy,n,l,jo

      open(2,file='farsad',status='new')
      open(4,file='farinit',status='old')

      w0=4
      del=0.28
      b=20
      wl=(w0**2)+b

      do 100 n=1,4
      read(4,*)x,y

      write(2,5)x
      write(2,7)y
      write(2,*)

5     format(9x,'initial x =',f6.2)
7     format(9x,'initial y =',f6.2)

      write(2,10)
10    format(8x,'theta',4x,'x-value',6x,'y-value',10x,
     1       'Re phi',5x,'Im phi')

      do 90 i=0.02,1,0.02

      kount=0
      kount1=0

      tht=1+i

20    kount=1+kount
      kount1=1+kount1

c     This if-then is to help the program converge in the
c     area around the point where the saddle points coalesce.

      if (tht.gt.1.499.and.tht.lt.1.502.and.abs(x).lt.
     1      0.0001) then
      x=0.0005
      y=-0.18
      endif

      ul=x**2-y**2-w0**2-b-2*del*y
      u0=ul+b

      v0=x*(del+2*y)
      v1=x*(del+y)
      v2=x**2-y**2-y*del
```

```
      a1=v2*u0+2*v0*v1
      a2=v0*u0-2*v1*v2
      a3=u0**2+4*v1**2

      c1=u1+(b*a1/a3)
      c2=2*v1+(b*a2/a3)

      F=c1**2-c2**2-(tht**2)*(u1*u0-4*v1**2)
      G=c1*c2-(tht**2)*v1*(u0+u1)

      d1=2*x*u0+2*v2*x+2*v1*(del+2*y)+2*v0*(del+y)
      d2=4*u0*x+8*v1*(del+y)
      d3=u0*(del+2*y)+2*v0*x-4*x*v1-2*v2*(del+y)

      e1=2*x+(b*(d1*a3-a1*d2)/a3**2)
      e2=2*(del+y)+(b*(d3*a3-a2*d2)/a3**2)

      Fx=c1*e1-c2*e2-(tht**2)*(u0*x+u1*x-4*v1*(del+y))
      Gx=c2*e1+c1*e2-(tht**2)*((del+y)*(u0+u1)+v1*4*x)

      d4=-u0*(2*y+del)-2*v2*(y+del)+4*x*v1+2*x*v0
      d5=-4*u0*(y+del)+8*v1*x
      d6=2*x*u0-2*v0*(y+del)-2*x*v2+2*v1*(2*y+del)

      e3=-(2*(y+del))+(b*((d4*a3)-(a1*d5))/a3**2)
      e4=(2*x)+(b*((d6*a3)-(a2*d5))/a3**2)

      Fy=(e3*c1)-(e4*c2)+((tht**2)*((y+del)*(u0+u1)+4*v1*x))
      Gy=(c2*e3)+(c1*e4)-((tht**2)*(x*(u0+u1)-4*v1*(y+del))

      J=Fx*Gy-Fy*Gx

      Dx=(Fy*G-F*Gy)/J
      Dy=(F*Gx-Fx*G)/J

          if (abs(x).lt.1E-35) then
           dx=0
           x=0
          endif

      x1=Dx+x
      y1=Dy+y

c     This sequence calculates the value of the real and
c     imaginary parts of the phase function at the saddle
c     point that we calculate.

      aa= b*(b-2*u0)
      cc=u0**2+(4*(v1**2))
      nn=sqrt(sqrt(1+(aa/cc)))
      ss=atan((2*b*v1)/(cc-b*u0))

      XX=-(y)*(nn*cos(ss/2)-tht)-(x)*(nn*sin(ss/2))
      YY=(x)*(nn*cos(ss/2)-tht)-(y)*nn*sin(ss/2)
```

```
              if (x.eq.0) then
                if (abs(dy/y1).lt.0.0001) then
                  write (2,30)tht,x,(y1+y)/2,xx,yy
                  x=x1
                  y=y1
                  go to 90
                endif
              else

          if (abs(dx/x1).lt.0.0001.and.abs(dy/y1).lt.0.0001) then
            write(2,30)tht,(x1+x)/2,(y1+y)/2,xx,yy
            x=x1
            y=y1
            go to 90
          end if
              endif

30        format(6x,f6.2,2x,f12.7,1x,f12.7,5x,f10.6,1x,f10.6)

c         I have taken 1000 to be the upper limit on the number
c         of iterations the program should perform before giving
c         up hope of getting convergence.

          if (kount.gt.1000) then
            goto 90
          endif

c         This is my trick to speed convergence when the program
c         begins to alternate between two values.

              if (kount1.eq.40) then
              x=(x+x1)/2
              y=(y+y1)/2
              kount1=0
              else

          x=x1
          y=y1

              endif

          go to 20

90        continue

          write(2,*)
          write(2,*)

100       continue

          close(4)
          close(2)

110       stop
          end
```

```
c       This program calculates the value of the real part of
c       the phase function for a double resonance medium with
c       nu, the local field correction factor included.

        dimension x(201),y(201),z(201,201)

        real th,w0,del0,del2,b0,b2,nu,a,a0,a2,c,c0,c2,aa,cc
        real s1,s2,t1,t2,i,j,l,k,w2,psi,alp,bet
        real z1,z2,zz,w,nup,div

        w0=1
        w2=7
        del0=0.2
        del2=0.56

c       The values for the deltas are actually twice those
c       oughstun and shen use, but, I leave off a two in my
c       derivation necessitating that my deltas are multiplied
c       by two.

        b0=5
        b2=20

c       nu=0
        th=1.25

        call begplt(1,'dubl.tek',' ')

        do 101 nup=0,0.7,0.1
        div=10

c       The following will give me graphs at values for nu
c       from 0 to 0.2 on a scale from -10 to 10 in x and y
c       and two sets of graphs for nu from 0.2 to 0.6 on a
c       scale from -5 to 5 in x and y - a total of 13 graphs.

              if (nup.gt.0.2) then
                if (nup.gt.0.8) then
                   nu=nup-0.6
                   div=2*div
                else
                   nu=nup-0.1
                   div=2*div
                endif
              else
                nu=nup
              endif

        do 25 i=1,201
           x(i)=(i-101)/div
           y(i)=(i-101)/div
25      continue

        do 35 j=1,201
        do 30 l=1,201
```

```
      a0=w0**2-x(j)**2+y(l)**2+del0*y(l)
      a2=w2**2-x(j)**2+y(l)**2+del2*y(l)

      c0=2*x(j)*y(l)+del0*x(j)
      c2=2*x(j)*y(l)+del2*x(j)

      aa=b0*a2+b2*a0
      cc=b0*c2+b2*c0

      alp=a0*a2-c0*c2
      bet=a2*c0+a0*c2

      t1=aa*(bet-(nu*cc))-cc*(alp-(nu*aa))
      t2=((alp-(nu*aa))*(alp+aa*(1-nu)))+((bet-(nu*cc))*
     +     (bet+cc*(1-nu)))
      psi=atan(t1/t2)

      s1=(alp-(nu*aa))**2+(bet-(nu*cc))**2
      s2=sqrt(t1**2+t2**2)
      zz=sqrt(s2/s1)

      z(j,l)=y(l)*th-x(j)*zz*sin(psi/2)-y(l)*zz*cos(psi/2)

c     This truncates the peaks so that we can get a view of
c     the rest of the plane - they go to infinity anyway

            if (z(j,l).gt.10) then
            z(j,l)=10
            endif
            if (z(j,l).lt.-10) then
            z(j,l)=-10
            endif

30    continue
35    continue

c     The if-then here gives me "reverse" viewing on the same
c     graphs.

      if (nup.gt.0.8) then
       call def3d(-150.0,60.0,0.0,0.0,0.0,0.0,0.0,0.0,0.0,0,0,0,
     +            0,0,0,0)
      else
       call def3d(-30.0,60.0,0.0,0.0,0.0,0.0,0.0,0.0,0.0,0,0,0,
     +            0,0,0,0)
      endif
      call plot3d(x,y,z,201,-201,-201,-3,-3,'x',1,'y',1,
     +           'z',1,' ',1)

101   continue

      call endplt

110   stop
      end
```

```
Program to calculate the location of the saddle points for a
double resonance medium.

      real x,y,j,tht,f,g,fx,fy,w0,del,b,gx,gy,a0,a2,c0,c2,
     a0y,a2y,c0x,c2x
      real pr,pi,qr,qi,prx,pix,qrx,qix,pry,piy,qry,qiy,prp,
     pip,qrp,qip
      real prpx,prpy,pipx,pipy,qrpx,qrpy,qipx,qipy,r1,r2,
     r3,r4,r5,r6
      real s1,s2,s3,s4,s5,s6,al,be,alx,aly,bex,bey,rel,re2,
     im1,im2,relx
      real rely,re2x,re2y,im1x,im1y,im1y1,rely1,relx1,im1x1,
     aax,aay,ccx
      real ccy,dx,dy,i,k,l,pip1,pip2,nu,im2x,im2y,g0,g2
      real aa,cc,nn,ss,xx,yy,eks,t1,t2,sol,so2,psi

      open(2,file='tworesad.dat',status='new')
      open(4,file='twoinit',status='old')

      w0=1
      w2=7
      g0=0.2
      g2=0.56
      b0=5
      b2=20

      nu=0.35

c     The following makes a "grid" of points in the plane in
c     order to find all the solution points to our equations for
c     a given nu.  Once this is done we then have a good idea
c     what initial points to put into our initial file which
c     will thereafter be read by the program.

c     do 110 k=0,40
c     do 105 l=-15,15

c     The following is used after we have an idea where to
c     find various saddle points.

      do 100 n=1,4
      read(4,*)x,y

      write(2,5)x,g0/2
      write(2,7)y,nu
      write(2,*)

5     format(7x,'initial x =',f6.2)
7     format(7x,'initial y =',f6.2,2x,'   nu=',f5.2)

      write(2,10)
10    format(6x,'theta',4x,'x-value',4x,'y-value',8x,'Re phi')

      do 90 i=0.02,1,0.02
```

```
      kount=0
      kount1=0

      th=1+i

20    kount=1+kount
      kount1=1+kount1

      a0=w0**2-x**2+y**2+g0*y
      c0=2*x*y+g0*x
      a2=w2**2-x**2+y**2+g2*y
      c2=2*x*y+g2*x

      c0x=2*y+g0
      c2x=2*y+g2

      a0y=2*y+g0
      a2y=2*y+g2

      aa=b0*a2+b2*a0
      cc=b0*c2+b2*c0

      a1=a0*a2-c0*c2
      be=a2*c0+a0*c2

      pr=a1+(1-nu)*aa
      pi=-be-(1-nu)*cc

      qr=a1-nu*aa
      qi=-be+nu*cc

      prp=-2*x*(a0+a2+(1-nu)*(b0+b2))-2*y*(c0+c2)-c0*g2-c2*g0
      pip1=2*x*(c0+c2)-2*y*(a0+a2)-a0*g2-a2*g0
      pip2=-(1-nu)*(b0*(2*y+g2)+b2*(2*y+g0))
      pip=pip1+pip2

      qrp=-2*x*(a0+a2-nu*(b0+b2))-2*y*(c0+c2)-c0*g2-c2*g0
      qip=2*x*(c0+c2)-2*y*(a0+a2)-a0*g2-a2*g0+nu*(b0*(2*y+g2)
     +          +b2*(2*y+g0))

      rel=(x*qr+y*qi)/(2*(qr**2+qi**2))
      iml=(y*qr-x*qi)/(2*(qr**2+qi**2))

      re2=prp*qr-pip*qi-pr*qrp+pi*qip
      im2=pip*qr+prp*qi-pi*qrp-pr*qip

      F=(pr+rel*re2-iml*im2)**2-(pi+iml*re2+im2*rel)**2
     -     -(th**2)*(pr*qr-pi*qi)
      G=2*(pr+rel*re2-iml*im2)*(pi+iml*re2+im2*rel)
     -     -(th**2)*(pi*qr+pr*qi)

      alx=-2*x*(a0+a2)-c0x*c2-c2x*c0
      aly=-2*x*(c0+c2)+a0y*a2+a2y*a0
      bex=-2*x*(c0+c2)+c0x*a2+c2x*a0
      bey=2*x*(a0+a2)+a2y*c0+a0y*c2
```

```
aax=-2*x*(b0+b2)
aay=b0*a2y+b2*a0y
ccx=b0*c2x+b2*c0x
ccy=2*x*(b0+b2)

prx=alx+(1-nu)*aax
pix=-bex-(1-nu)*ccx
pry=aly+(1-nu)*aay
piy=-bey-(1-nu)*ccy

qrx=alx-nu*aax
qix=-bex+nu*ccx
qry=aly-nu*aay
qiy=-bey+nu*ccy

prpx=-2*(a0+a2)+8*x**2-2*(1-nu)*(b0+b2)-2*y*(c0x+c2x)
        -c0x*g2-c2x*g0
pipx=2*(c0+c2)+2*x*(c0x+c2x)+8*x*y+2*x*(g0+g2)
prpy=-2*x*(a0y+a2y)-2*(c0+c2)-8*x*y-2*x*(g0+g2)
pipy=8*x**2-2*(a0+a2)-2*y*(a0y+a2y)-a0y*g2-a2y*g0
        -2*(1-nu)*(b0+b2)

qrpx=-2*(a0+a2)+8*x**2-2*(-nu)*(b0+b2)-2*y*(c0x+c2x)
        -c0x*g2-c2x*g0
qipx=2*(c0+c2)+2*x*(c0x+c2x)+8*x*y+2*x*(g0+g2)
qrpy=-2*x*(a0y+a2y)-2*(c0+c2)-8*x*y-2*x*(g0+g2)
qipy=8*x**2-2*(a0+a2)-2*y*(a0y+a2y)-a0y*g2-a2y*g0
        -2*(-nu)*(b0+b2)

relxl=(qr+x*qrx+y*qix)*(qr**2+qi**2)
          -(x*qr+y*qi)*(2*qr*qrx+2*qi*qix)
relx=relxl/((2*(qr**2+qi**2)**2))

imlxl=(y*qrx-qi-x*qix)*(qr**2+qi**2)
        -(y*qr-x*qi)*(2*qr*qrx+2*qi*qix)
imlx=imlxl/(2*(qr**2+qi**2)**2)

re2x=prpx*qr+prp*qrx-pipx*qi-pip*qix-prx*qrp-pr*qrpx
      +pix*qip+pi*qipx
im2x=pipx*qr+pip*qrx+prpx*pi+prp*qix-pix*qrp-pi*qrpx
      -prx*pip-pr*qipx

r1=(pr+rel*re2-iml*im2)
r2=(prx+relx*re2+rel*re2x-imlx*im2-iml*im2x)
r3=(pi+iml*re2+im2*rel)
r4=(pix+imlx*re2+iml*re2x+im2x*rel+im2*relx)
r5=th**2*(prx*qr+pr*qrx-pix*qi-pi*qix)
r6=th**2*(pix*qr+pi*qrx+prx*qi+pr*qix)

relyl=(qi+x*qry+y*qiy)*(qr**2+qi**2)
        -(x*qr+y*qi)*(2*qr*qry+2*qi*qiy)
rely=relyl/(2*(qr**2+qi**2)**2)

imlyl=(y*qry+qr-x*qiy)*(qr**2+qi**2)
        -(y*qr-x*qi)*(2*qr*qry+2*qi*qiy)
imly=imlyl/(2*(qr**2+qi**2)**2)
```

```
re2y=prpy*qr+prp*qry-pipy*qi-pip*qiy-pry*qrp-pr*qrpy
          +piy*qip+pi*qipy
im2y=pipy*qr+pip*qry+prpy*pi+prp*qiy-piy*qrp-pi*qrpy
          -pry*pip-pr*qipy

sl=(pr+rel*re2-iml*im2)
s2=(pry+rely*re2+rel*re2y-imly*im2-iml*im2y)
s3=(pi+iml*re2+im2*rel)
s4=(piy+imly*re2+iml*re2y+im2y*rel+im2*rely)
s5=th**2*(pry*qr+pr*qry-piy*qi-pi*qiy)
s6=th**2*(piy*qr+pi*qry+pry*qi+pr*qiy)


Fx=2*rl*r2-2*r3*r4-r5
Gx=2*(rl*r4+r2*r3)-r6

Fy=2*sl*s2-2*s3*s4-s5
Gy=2*(sl*s4+s2*s3)-s6

J=Fx*Gy-Fy*Gx

Dx=(Fy*G-F*Gy)/J
Dy=(F*Gx-Fx*G)/J

     if (abs(x).lt.1E-25) then
      dx=0
      x=0
     endif

xl=Dx+x
yl=Dy+y

tl=aa*(be-(nu*cc))-cc*(al-(nu*aa))
t2=((al-(nu*aa))*(al+aa*(1-nu)))+
            ((be-(nu*cc))*(be+cc*(1-nu)))
psi=atan(tl/t2)

sol=(al-(nu*aa))**2+(be-(nu*cc))**2
so2=sqrt(tl**2+t2**2)
eks=sqrt(so2/sol)

xx=y*th-x*eks*sin(psi/2)-y*eks*cos(psi/2)
yy=-x*th-y*eks*sin(psi/2)+x*eks*cos(psi/2)

         if (x.eq.0) then
           if (abs(dy/yl).lt.0.0001) then
             write (2,30)th,x,(yl+y)/2,xx,yy
             x=xl
             y=yl
             go to 90
           endif
         else

 if (abs(dx/xl).lt.0.0001.and.abs(dy/yl).lt.0.0001) then
   write(2,30)th,(xl+x)/2,(yl+y)/2,xx,yy
```

```
          x=x1
          y=y1
          go to 90
        end if
               endif

30      format(5x,f8.3,2x,f12.7,1x,f10.7,5x,f13.7,2x,f13.7)

        if (kount.gt.1000) then
          write(2,*)'          *'
          goto 90
        endif

            if (kount1.eq.100) then
            x=(x+x1)/2
            y=(y+y1)/2
            kount1=0
            else

        x=x1
        y=y1

            endif

        go to 20

90      continue

        write(2,*)
        write(2,*)

100     continue

c105    continue
c110    continue

        close(4)
        close(2)

120     stop
        end
```

E Annotated References

Aaviksoo, J., J. Lippmaa, and J.Kuhl, *Observability of optical precursors*, Journal of the Optical Society of America B 5,8,1631 (1988).

This paper is a theoretical consideration of the feasibility of experimental detection of precursors in the optical region. An experiment is also proposed which would separate the precursors from the main signal. We used this paper as a help in getting a physical understanding of precursors.

Arfken, George, *Mathematical Methods for Physicists*, 3rd ed, (Academic Press Inc., 1985).

We relied very heavily on chapters six and seven of this book for learning complex analysis and the method of steepest descent.

Born, M. and E. Wolf, *Principles of Optics*, 4th ed. (Pergamon, Oxford 1970), Appendix III.

This appendix dealt with the method of steepest descent and we used it as a reference for that method.

Brillouin, Léon, *Wave Propagation and Group Velocity*, (Academic Press, New York and London 1960).

This contained reprints of the original papers by Sommerfeld and Brillouin as well as some later papers by Brillouin. We used this fairly extensively as a reference to the original theory upon which Oughstun and Sherman improved.

Buerger, David J., *LATEX for Engineers and Scientists*, (McGraw Hill, New York 1990).

This proved to be an invaluable book in teaching us how to use Latex. This was perhaps only incidental to this thesis, but it still helped immensely.

Hecht, Eugene, *Optics*, 2nd ed, (Addison-Wesley, Reading MA 1987).

We used this book as an introduction to dispersion theory and relied on it in part for the derivation of the complex index of refraction as based on the Lorentz model of the atom.

Loudon, R, *The Propagation of electromagnetic energy through an absorbing dielectric*, Journal of Physics A. 3,233 (1970).

An improved derivation for the energy velocity is presented which the author claims offers a correction to Brillouin's analysis of the energy velocity. Oughstun uses this paper as his starting point for his analysis of the energy velocity. Since our concern was more with Oughstun's original paper, this issue, and hence the paper, was secondary to us.

Olver, F.W.J. *Why steepest descents?*, SIAM Review 12,2,228 (1970).

This is a rigorous analysis of the saddle-point method or method of steepest descent which includes a modified derivation, examples using the method, and a consideration of the bounds on the error involved in the approximation. The method presented here is the one used by Oughstun and Sherman and was for that reason important for us to understand.

Oughstun, Kurt E. and Shioupyn Shen, *Velocity of energy transport for a time-harmonic field in a multiple resonance Lorentz medium*, Journal of the Optical Society of America B 5,11,2395 (1988).

Loudon's treatment of the energy velocity is generalized to the case of a dispersive medium having several resonance frequencies. This was again secondary to our main interest, namely the shape of a pulse traveling in a Lorentz medium, so we read this article mainly out of curiosity, but did not use it explicitly.

Oughstun, Kurt E. and George C. Sherman, *Propagation of electromagnetic pulses in a linear dispersive medium with absorption (the Lorentz medium)*, Journal of the Optical Society of America B, 5,4,817 (1988).

This is the main paper we considered. Sommerfeld and Brillouin's theory of pulse propagation in a dispersive medium is reconsidered and improved using higher order approximations verified with modern computer techniques. The precursor fields for two specific pulses are calculated using the improved approximations and a modified interpretation is given to the signal velocity.

Oughstun, Kurt E. and George C. Sherman, *Uniform asymptotic description of electromagnetic pulse propagation in a linear dispersive medium with absorption (the Lorentz medium)*, Journal of the Optical Society of America B, 6,9,1394 (1989).

This paper is an extension and in part a correction to their 1988 paper which considered only the nonuniform expansion of the field and which therefore described a field that was not continuous under certain conditions.

Pleshko, Peter and Istvan Palocz, *Experimental observation of Sommerfeld and Brillouin precursors in the microwave domain*, Physical Review Letters 22,22,1201 (1969).

This paper reports the experimental verification of electromagnetic precursors. It includes a description of the experimental set up and pictures of the signals taken from an oscilloscope. We used this mostly as a help in gaining a physical understanding of precursors.

Reitz, John R., Frederick J. Milford, and Robert W. Christy, *The Foundations of Electromagnetic Theory*, (Addison-Wesley, Reading MA 1979).

We used this as an introduction to dispersion theory and relied in part on this for the derivation of the Lorentz model of the index of refraction.

Shen, Shioupyn and Kurt E. Oughstun, *Dispersive pulse propagation in a double-resonance Lorentz medium*, Journal of the Optical Society of America B 6,5,948 (1989).

This is another offshoot of the original paper and uses numerical analysis to calculate the medium response to a pulsed signal. An additional precursor is found for each additional resonance frequency beyond the first. We considered some of the work done here.

Smith, W. Allen, *Elementary Numerical Analysis*, Harper & Row, Publishers, Inc. 1979.

We used this book fairly exclusively in helping us discover an appropriate approximation technique which could be used to calculate the locations of the saddle points of the phase function. The derivation of Newton's method for two functions of two variables found in the section on the numerical calculation of the saddle points follows Smith's fairly closely.